Essays on Economic Geography, Development, and Climate Change

Author:
Bruno CONTE LEITE

Supervisors:
Hannes Felix MUELLER
Dávid Kristián NAGY

A Manuela e Maria Luiza,
que estão sempre comigo.

Acknowledgements

The work portrayed in these pages is a result of long and strenuous years of hard work. Throughout, I met and benefited from many people whose knowledge, experience, support, and friendship were decisive to have arrived at this very moment. This page is a small acknowledgment of my appreciation for them. Enumerating such an extensive list is nevertheless a hard task – I hereafter will be concise and apologize in advance in case I mistakingly leave someone out.

First and foremost, I thank Hannes Mueller and Dávid Nagy, whose invaluable support, encouragement, and patience have been pillars of the development of this thesis and myself as a research economist. They have been and remain a role model of a scholar and human being to me. I feel privileged to have had their shoulders to stand on.

I am also grateful to the faculty, staff, and colleagues of the UAB and the IDEA Ph.D. program. I am particularly thankful to André Groeger and Joan Llull – and especially to the latter. Joan has always been an example of a researcher and professor to me, and I will carry what I learned from him throughout my career. I must also thank Àngels López and Mercè Vicente for their tireless work to make IDEA such an outstanding research environment.

A special thanks go to the faculty and staff of the IAE, my workplace in the past 5 years, where I have always felt part of a big family. Working next to (and sharing a weekly *paella* with) such a nice crowd was remarkable. I will particularly miss the company of Angela Hernández, Carlota Manchón, Ana Rute Cardoso, and Ada Ferrer–i–Carbonell. I am especially grateful to the latter, Ada, for her advising and trust. Most of my teaching experience today is due to her trust in me for opportunities at the Barcelona GSE.

Navigating through the years of the Ph.D. would have been impossible without the company and care of my friends Anna Lopez, Hannes Mueller, Tommaso Santini, Luca Tomassetti, and Sarah Zoi. Besides, Lavinia Piemontese was the best office mate, co–author, job market coach, and friend I could have siding me. Finally, I am also very privileged to have had Fernanda Kokubu, my best friend since ever, next to me. Sharing joys (and eventually difficulties) in life and work did nothing but intensify our over–20 years friendship. Thanks for everything, Fefa.

Along the same lines, I thank Maripaz, Antonio, Pau, Ester, Joan, Marta, Juan, Nerea, Diego, Sara, Manuela, Antonio, Justo, Maite, Diego, and all the Ortiz Gómez family for welcoming me, having me as one of yours, and reminding me constantly that life is much more than work and ambition.

I am obviously thankful to my entire family – my mom, dad, siblings, grandparents, uncles, and aunties – whose endless love and care have been always the main fuel pushing me to achieve my goals, including handing this thesis in. Moreover, surviving the past years far from home would have been impossible without the close support of Alexandre, Amanda, Carla, and Adriana. I cannot wait to give you all a hug in person.

Finally, I will be forever grateful to my beloved and soon wife Teresa for her patience and support to overcome countless frustrations and endless nights of work. Her love and faith in me were the light in the darkest of the moments during this journey. I am extremely excited about the new journey we start together after this chapter of our life.

Thesis Outline

During the past decades, the connection between economic development and the global climate came to the center of attention. As temperatures increased, scholars and policymakers questioned increasingly more the sustainability of unconstrained economic growth. The complexity of the economy–weather relationship has been difficulting the design and implementation of coordinated worldwide mitigating policies. As a consequence, the predictions for potential impacts on the world economy and societies are not optimistic.

In this context, uncovering how the developing economies of the world are going to be affected is of the first order. Lacking sufficient economic, institutional, or technological capacity to fully hedge against the "climate change shock", these regions are at the center of the policy debate in terms of social and economic vulnerability. How these economies would adapt during the next decades, which could be the economic mechanisms behind such adjustments, and how large could potential welfare losses or gains be, are some of the key questions that arise when thinking of policies that could be put in place.

My doctoral thesis focuses on answering questions of this sort. Composed by three independent, self–contained chapters, it contributes to a literature at the intersection of economic development, economic geography, and trade. Methodologically, I rely upon either reduced–form causal inference or structural modeling – using the spatial trade theory for the latter – to build the ideal framework for answering the research question at hand. By combining it with real–world data, I provide well-founded and carefully quantified answers to the proposed questions. In the structural chapters, I take full advantage of the theoretical framework available by conducting counterfactual experiments that highlight the role and welfare implications of the economic mechanisms at play.

My thesis starts with Chapter 1, *"The Power of Markets: Impact of Desert Locust Invasions on Child Health"*. It provides reduced-form evidence of the importance of (access to) markets on the transmission of climate change–led agricultural shocks to human capital accumulation in low–income economies. Overall, it argues for the importance of addressing local market reactions to this type of agricultural shock when designing policy. It also conveys clear evidence of the vulnerability of agricultural, low–income economies, to short–term shocks induced by climate change. Hence, it motivates the subsequent chapters, in which I study the long–run economic reactions to and consequences of climate change.

In particular, in Chapter 2, *"Climate Change and Migration: the case of Africa"*, I study the potential economic costs and migration responses to climate change in the context of sub-Saharan Africa (SSA) during the next decades. For that, I develop a quantitative spatial framework that captures the role of trade networks and agricultural suitability on the distribution of population and GDP accounting for endogenous adjustments of crop choice and trade. I combine it with detailed geospatial data from SSA to simulate the impact of climate change using forecasts of agricultural productivity in 2080 from FAO.

My results suggest that climate change could lead to major migration flows within and across SSA countries, with substantial economic losses associated with it. Moreover, the capacity of adjusting the production mix across different sectors (crops and/or non–agricultural) or high access to markets partially mitigates the impacts of climate change in terms of population outflows. Finally, a policy experiment related to technology adoption in agriculture shows that the adoption of modern inputs in that sector could reverse considerably the negative impacts of climate change.

My thesis is concluded with Chapter 3, *"Local Sectoral Specialization in a Warming World"*, where I study the evolution of the geographical distribution of the world's economy and climate in a setup where both elements are endogenous to one another. In particular, I embed a mapping between the evolution of economic activity, carbon emissions, and global warming into a dynamic spatial general equilibrium model where spatial innovation drives the dynamics of the evolution of productivities and growth.

By simulating the evolution of the world economy for the next centuries, I find a much higher concentration of agricultural activity in northern latitudes (e.g. Siberia and Northern China) if compared to a scenario without

global warming. Moreover, in aggregate terms, climate change leads to different patterns of the evolution of sectoral–productivities, economic growth, and specialization into agriculture and urban sectors, in line with some of the results from Chapter 2. A policy experiment related to trade costs shows that higher frictions to trade reallocate production and factors close to the demand, by reducing the comparative advantage in more peripheral regions of the globe.

Overall, my doctoral thesis provides clear evidence of the spatial differences in the reactions to (and consequences of) climate change throughout the globe. It also argues firmly for the importance of trade as a key economic mechanism behind the transmission of this sort of shock to economic outcomes. In the present times of fast globalization, integration of markets, and expansion of trade networks, my thesis shows that bringing the most isolated markets closer to the global trade networks can have a key role in mitigating the future consequences of climate change.

Contents

List of Figures

List of Tables

Chapter 1

The Power of Markets: Impact of Locust Invasions on Child Health

Abstract

This paper investigates the consequences of a locust plague that occurred in Mali in 2004. We provide evidence of substantial crop market effects that explain the space-time pattern of the estimated impact of this plague. We argue first that the plague has affected households in Mali through two channels: first, a speculative price effect that kicked in during the plague itself, followed by a local crop failure effect. We find that, in terms of health setbacks, children exposed in utero only to the speculative price effect suffered as much as those exposed to the actual crop failure effect. Once we account for the impact on local crop prices, the estimated speculative effect vanishes, whereas the crop failure effect persists. Children born in isolated areas suffer more from the crop failure effect. Our results suggest that addressing local market reactions to this type of agricultural shocks is crucial for policy design.

1.1 Introduction

Climate change is receiving considerable attention both from the media and the academic community. One of its consequences is an increase in the likelihood and intensity of extreme weather conditions, which in turn can lead to severe agricultural shocks. Disruptions in agricultural production often lead to detrimental effects for many households in developing countries, with serious repercussions for young children. This amplifies the negative impact of such shocks since conditions experienced early in life have long-lasting effects on various socioeconomic outcomes. In particular, it is well established that harsh conditions experienced in utero can have detrimental and persistent effects on health throughout the whole life cycle (Lavy et al., 2016; Almond and Currie, 2011; Maccini and Yang, 2009; Stein et al., 1975). This concept, known as the fetal origins hypothesis, implies that it is harder to remedy bad fetal health later on in life.[1]

In this paper, we study the impact, on child health, of exposure to a specific type of agricultural shock that is indirectly linked to extreme weather conditions and climate change: the damage caused by desert locust plagues.[2] Locust swarm invasions are destructive events that recurrently put food supply in many developing countries at risk (Brader et al., 2006). They are caused by a specific species of grasshoppers that usually live, in their solitary phase, around the Sahara desert. Under favorable breeding conditions (excess rainfall), these grasshoppers go through a gregarization process with substantial changes in their behavior, morphology, and physiology. They become more voracious and can grow into huge swarms that travel to less arid areas to feed and reproduce causing devastating effects on agricultural production.

We study how early-life exposure to the most recent plague that occurred in Mali, between July and October 2004, led to detrimental effects on child health. While the impact of early life shocks on child health has been explored extensively in the literature, uncovering the channels through

---

[1]On the one hand, Almond and Currie (2011) provide an excellent review of the fetal hypothesis theory and its theoretical relation to later life outcomes. On the other hand, the empirical literature has successfully documented the impact of adverse in utero conditions on infant mortality (Kudamatsu et al., 2012; Dagnelie et al., 2018), child health (Akresh et al., 2011, 2012a; Bundervoet et al., 2009), adult health (Akresh et al., 2012b; Maccini and Yang, 2009), and adult socioeconomic outcomes such as literacy, educational attainment, income and labor market status among others (Almond et al., 2007; Alderman et al., 2006; Lavy et al., 2016).

[2]The direct consequence of extreme weather conditions and climate change on agricultural production is through crop failure due to droughts or floods.

which such shocks affect children is still a standing and relevant question. We make a step in this direction, arguing that agricultural shocks due to pest invasion, such as locust plagues, can affect households living in areas with a single harvest per year through two main channels. First, there is a *speculative price effect* that kicks in immediately during the growing season in which the plague is occurring, in anticipation of the upcoming harvest failure. At this point, households and markets are still relying on the harvest from the previous agricultural season. Yet, crop destruction by the pest in the ongoing season could lead to an anticipation of a future crop supply shock and drive up prices in local markets. Second, there is the actual *crop failure effect* that would constitute an income shock for farmers and a supply shock for markets after the harvest of affected crops. This effect should last at least until the following harvest.[3]

The key contribution of our paper concerns the fact that we are able to explore in detail these mechanisms, by making use of a minutely identified agricultural shock. Specifically, we rely on the exact timing and the precise location of locust swarm events to identify the temporal and spatial variation in the exposure of different cohorts of children to the 2004 locust plague in Mali. We also link this data to local agricultural crop price data from the Malian Agricultural Market Observatory (Observatoire du Marche Agricole - OMA) to tease out potential local market effects. We use geocoded household survey data with detailed information on the birth history and health outcomes of children from the Demographic and Health Surveys (DHS). Data on the timing and location of locust swarm invasions comes from the locust monitoring system run by the Food and Agriculture Organization (FAO) Desert Locust Information Service (DLIS).

Using a Difference-in-Differences identification strategy, we first show that children exposed in utero to the adverse effects of the locust plague suffer major health setbacks. They have, on average, a height-for-age Z-score 0.42 points lower than non-exposed children. This represents around 30% of the average height-for-age Z-score. Our estimates also suggest an increase in average stunting rate by more than 20%. We find no impact on cohorts of children exposed to the shock after birth.

We then study the timing of the estimated effect by quarter of birth. Our

---

[3]Locust plagues can also have a persistent effect if, for instance, the failed harvest in a given agricultural season affects the quality of seeds used for the next one. We found no evidence of such long-term effect.

results show that cohorts of children that were subject only to the *speculative price effect* in utero suffer as much as those exposed to the actual *crop failure effect*.[4] Using data on local crop prices, we show that the plague led to significant inflation of crop prices (average increase of 6 %) in affected areas, compared to non-affected areas, during growing season of 2004.[5] During this time window, local markets were still relying on the previous harvest that has not been affected by the plague. Therefore, the estimated price differences are argued to be caused by the speculation/anticipation of economic agents on a potential failure of the upcoming harvest. We find that, after controlling for local crop prices, the estimated health loss for children exposed only to the speculative price effect is dampened substantially and becomes insignificant. Conversely, we found no evidence of price inflation in locust affected areas during the *crop failure effect* period. The estimated impact for the children exposed to the crop failure effect remains stable after controlling for prices.

The extent to which local markets are isolated from other sources of agricultural supply also plays a crucial role in this context. In particular, we find that exposed children born in isolated areas, with limited access to crops from other areas, suffer more compared to those born in well-connected areas. This pattern is driven by the *crop failure effect*. We find that in utero exposure only to the *speculative price effect* does not lead to any stronger effect on children born in more isolated areas.

Our results are robust to specifications that include region-specific time trends, household and mother characteristics, climate shocks, and mother fixed effects. We also argue that they are less likely to be biased by potential migration, or pre-existing differences in trends between treated and non-treated areas. Results are also robust to restricting the analysis to male-female and rural-urban sub-samples.

The findings of this paper have relevant policy implications. In particular, we provide evidence of the existence of a strong *speculative price effect* that operates differently than the actual *crop failure effect* when agricultural shocks such as locust plagues occur. This calls therefore for different types of policy reactions. Fighting inflation and crop price speculation is crucial during

---

[4]We rule out the possibility that this effect is driven by exposure to the *crop failure effect* after birth.

[5]The agricultural season in Mali happens every year according to the following calendar: planting of seeds happens in May-June followed by the growing season from July to September and the harvest in October/November.

the growing season when the overall crop supply on markets is at its lowest level. Conversely, after the harvest period, policy action should focus on coping with the local crop failure shocks. Our findings also suggest that simple and diversified access to agricultural production from not affected areas can effectively mitigate this effect.

This paper belongs to two main strands of the economic literature. First, it contributes to the literature on the importance of early–life conditions (Lavy et al., 2016; Maluccio et al., 2009; Black et al., 2007; Behrman and Rosenzweig, 2004; Stein et al., 1975). A substantial part of it focused on identifying the effect on child health of exposure to weather shocks (Maccini and Yang, 2009), civil wars (Dagnelie et al., 2018; Valente, 2015) or adverse institutional setup (Kudamatsu, 2012). We complement this literature by investigating the impact of desert locust plagues on child health. One of the novelties of our analysis relies on the use of a shock characterized by a clear-cut spatial and temporal variation, i.e. geolocated locust swarm invasions. Moreover, this is the first paper, to the best of our knowledge, to shed light on the channels through which such pest invasion can affect households. In particular, we provide evidence of a clear distinction between the purely speculative price effect and the actual crop failure effect of the exposure to the swarm invasions. We also show that this shock has long-lasting health effects on children exposed in utero, but no effects after birth. Through several alternative specifications of our model, we show that the adverse effects are present for both male and female children. This contrasts with recent evidence in the literature on early life development, which generally finds larger adverse effects on females (Dagnelie et al., 2018; Lavy et al., 2016; Akbulut-Yuksel, 2017).

Second, this paper adds to the literature that studies the consequences of negative agricultural shocks caused by pest invasions. Baker et al. (2020) show that the boll weevil's pest invasion that affected US cotton production from 1892 to 1922 led to an increase in educational attainment due to reduced opportunity cost for schooling. Banerjee et al. (2010) show that the phylloxera invasion in 19th century France affected wine production and led to substantial effects on adult height for people born in affected areas in that period. De Vreyer et al. (2014) used locust plague invasion in 1987-1989 in Mali to show that it had a long term effect on educational attainment. We contribute to this literature by providing evidence on the channels through which pest invasion may affect household welfare in developing countries.

The remainder of this paper is organized as follows. Section 1.2 provides some background on the 2003-05 locust plague in Western Africa and its relation to food shortages and child health in Mali. Section 1.3 presents the data used for the empirical analysis. Section 1.4 discusses the channels through which locust invasions can affect the well-being of households. Section 1.5 presents the empirical strategy used and Section 1.6 shows the results obtained. Section 1.7 concludes.

1.2 Background

In this section we describe the context of our analysis. We first provide a general description of desert locusts, their habitat and their link to climatic conditions that can turn them into agricultural plagues. We then give some details of the locust plague that took place in the Sahel region in the mid 2000s, stressing on its consequences in Mali.

1.2.1 Desert Locust Plagues

Desert locusts are insects that live in the arid and hyper-arid zones of the Sahel region, northern Africa, Middle East, and Southeast Asia, as shown in Figure A.1. They pertain to the family of *grasshoppers* and normally inhabit desert zones, called *recession areas* (bounded by the black solid line in Figure A.1), in a solitary, harmless and integrated way with the local ecology. What makes them different from traditional grasshoppers is their capacity to mutate physically and change behavior under certain conditions. In particular, if specific areas called *breeding areas* (green and ocher areas in Figure A.1) experience periods of excessive rainfall, followed by periods of relatively mild temperatures, a process of fast reproduction takes place. The high density of locusts combined with a relative shortage of vegetation induce them to a *gregarious stage*: the locusts mutate physically and start behaving as a unique group, known as a *swarm*.

Upon gregarization, these groups become more and more voracious and reproduce faster. If needed, locust swarms will fly away to find a location with vegetation for feeding and appropriate conditions for reproducing. Within a few weeks after settling in a suitable new location, there can be a new generation of gregarious locusts. The increase in the size of the swarm can be remarkable: the incorporation of locusts from the new generation can

lead up to a ten-fold increase in the size of the swarm (FAO, 2004). If breeding conditions are favorable and there is no human intervention, the density of a swarm can become extremely high, exceeding a billion of insects.

Desert locusts swarms are very threatening because, while flying in search of new locations for feeding and reproducing, they end up following winds that move them away from the desert areas of the Sahara. Usually, the winds blow them towards the central Sahelian and tropical areas in the South or the Mediterranean regions in the North. These *invasion areas*, shown in Figure A.1 by the dashed red line, span over more than 50 countries and have a total surface of about 29 million square km (Herok et al., 1995). These zones are more densely populated and are used for agricultural production. Thus, crop yields and/or pasture vegetation can be partially or totally consumed by the swarms, potentially threatening the food supply of entire regions.[6] Moreover, the fact that the swarms can fly for very long distances, over hundreds of kilometers in a single day, implies that favorable conditions for gregarization in one place can create severe repercussions in relatively far away locations.

If climate conditions remain favorable for a long time within large geographic areas, the swarming, breeding, and migration behavior of locusts can create a regional plague, i.e. when locust swarms multiply exponentially in size and number, and spread over several countries. If so, food security in multiple countries can be under risk. Moreover, fighting the plague in these circumstances is extremely difficult and costly.

Fortunately, such events are not very recurrent nowadays – as seen in Figure A.2, there has been relatively less regional plague since 1970 compared to the previous period. This reduction is associated with active human preventive interventions (Cressman and Stefanski, 2016). The plagues that managed to take place since 1970, however, happened to be extremely severe. This is the case of the plague that occurred between 2003 and 2005, whose consequences we analyze in this paper.

1.2.2   The 2003-2005 Desert Locust Plague

The 2003-2005 desert locust plague started from optimal climate conditions in late 2003 which led to a massive plague throughout entire Western Africa

---

[6]A locust swarm can cover between less than one to several hundreds of square km, and each square km of the swarm has at least 40 million locusts. Each square km of swarm can consume daily the equivalent food consumption of 35,000 people (Symmons et al., 2001).

in 2004 (Ceccato et al., 2007), peaking in the third quarter of that year. Importantly, it developed from independent outbreaks that took place in different locations, taking the international prevention community by surprise (Cressman and Stefanski, 2016). It affected multiple countries, mostly in West Africa and North Africa, but also in central and eastern territories.

The 2003-2005 locust plague created a regional food crisis that involved more than eight million people in the whole Sahel region, implying a huge cost. On top of its direct cost (that includes the agricultural lands and the crops damaged), of which there is not a precise estimate, there was a substantial collateral cost of more than 400 million dollars needed to control the invasion (Brader et al., 2006). This loss does not include the indirect cost that the plague entailed, such as forgone investment for other national development activities or significant increases in food prices (Brader et al., 2006; FAO, 2005a).

1.2.3   The Case of Mali

Mali is a landlocked country in West Africa with a surface of about 1.2 million square km, spread in latitude across three different climate zones: the desert zone (Saharan), the transition zone (Sahel), and the tropical zone. As Figure A.1 depicts, a substantial part of its territory is a locust breeding area, which makes it very likely to experience (or be invaded by) locust swarm outbreaks.

This country is a relevant case study for our analysis for several reasons: first, as mentioned above, Mali is located in a very risky area in terms of the likelihood of experiencing locust plague invasions. Second, the pattern of the 2003-2005 swarm invasions was unevenly spread over its territory, allowing us to exploit this spatial variation together with variation in the timing of the plague in our empirical exercise. Third, this is a poor country that relies mostly on agriculture.[7]

Table A.1 provides an overview of Mali using standard aggregate data published by the World Bank. The country is classified as a low-income country, with a GDP per capita ranked 160th, with more than the 40% of its population below the poverty line. Malian population, of approximately 19 million individuals, is largely present in rural areas (about 60%). Mali is strongly dependent on agriculture, which accounts for about 40% of its GDP (in 2004

---

[7]The focus on Mali and not other similar countries is mainly due to data availability in the right time period.

this share was 30%). Its agricultural sector is largely composed of small-scale subsistence farming. As such, a large share of its population is vulnerable to agricultural hazards such as droughts and plagues.

Not surprisingly, Mali was among the countries that have been most damaged by the locust plague of 2003-2005. According to Brader et al. (2006), 1 million people were affected by this plague. Exact estimates of the agricultural losses are not available, but the existing evidence suggests that the plague had devastating effects. Brader et al. (2006) states that in Mali, the losses caused by the 2003-2005 plague have been evaluated at 90% of the expected cereal production in the affected areas. On top of this, around one-third of the pasture was also lost. By mid-2005, FAO (2005b) reported alarming increases in cereal prices and a deterioration of conditions for livestock production in the region. The poorest households suffered the most from this situation. The report states that, by mid–2005, "*access to main food staples [was] increasingly difficult for vulnerable households and pastoralists. Severe child malnutrition [was] increasing rapidly.*" (FAO, 2005b).

1.3   Data and Descriptive Statistics

In order to study how exposure to locust invasions in Mali impacted child health and the mechanisms behind it, we collect data from four different sources: (i) information on locust swarms are obtained from a rich database of worldwide locust monitoring, (ii) data on children anthropometrics is gathered from DHS, a widely used household survey, (iii) geographically disaggregated crop price data provided by the Malian Agricultural Markets' authority, finally (iv) climate data and other geographical characteristics at different levels of geographical disaggregation and sources complement these data.

1.3.1   Locust Swarm Data

We collect geographical and temporal incidence of locust swarms from the SWARMS database (Cressman, 1997). SWARMS contains historical geocoded information on many "locust parameters" including local breeding conditions, the incidence of adult locusts, hopper bands, swarms, and many others. For this application, we select information exclusively on locust swarms. Specifically, for each event related to the presence of a locust swarm, we collect the date and the geographic coordinates in which the event occurred.

The SWARMS system is held and maintained by the FAO Desert Locust Information Service (DLIS) Unit. This unit is monitoring, preventing and controlling locust incidence in the Sub Saharan Africa for over 60 years. For this, a national office in each Sub Saharan country conducts field activities. These activities include field incursions into areas prone to locust incidence and reproduction to search for (and code if found) locust bands and swarms. The coding is done in-field with a satellite-based technology; the information is automatically sent to the FAO-DLIS headquarters to be further cleaned if necessary. The data is complemented with information from local villages which self-report to field officers and/or the national DLIS office. The resulting data on the incidence of locust swarms spans from 1985 to 2016.

Figure A.3 shows the distribution of locust swarm incidence between 2000 and 2008 in Mali. Within this time window, most of the locust swarm related events occurred during the second half of 2004, and picked during the third quarter of this year. As discussed in details in Section 1.4, this period coincides with the growing season. Conversely, it can be noticed that nothing happened during the growing season of year 2003.[8] This means that, in Mali, the plague we study damaged the harvest of a single agricultural campaign, i.e. the one of 2004. In our main specification, we use all swarm events that happened in 2004.[9] Our results are robust to considering only those that occurred during the growing season of 2004.

Potential measurement error issues in the locust data are attenuated by the fact that during our period of study, the National Desert Locust Office in Mali has not faced any drastic changes or other difficulties that could affect its field operations.[10] The current political instability and terrorist threats in Mali started in 2012, long after our period of study.

---

[8] The locust started swarming in arid areas of the North after the end of the harvest period of 2003.

[9] Those events happened starting from June 2004 mostly in arid and desert areas in the North.

[10] This information was confirmed unofficially by an Information Officer at the DLIS office at FAO, Rome.

1.3.2   Children Anthropometrics Data

Information on child health in Mali is obtained from the Demographic and Health (DHS) Surveys. DHS surveys are being conducted in many developing countries since late 1990s with a standardized and nationally representative data collection methodology. The interviews target female individuals, aged from 15 to 49 years old. For a subsample of respondents' children (less than) 5 years old, anthropometric data such as height and weight are collected by trained surveyors. Importantly, children height are provided in Z-scores, i.e. the difference between the child's height and the mean height of the same-aged international reference population, adjusted by the standard deviation of the reference population.[11]

Moreover, DHS surveys provide GPS coordinates of where each household cluster is located.[12] These coordinates are published with a random noise for privacy reasons (set to up to 2 km for clusters located in urban areas, 5 km for those in rural areas, and 10 km for 1% of the latter). The locations of the clusters are drawn independently – thus differ – in each DHS wave. In order to have a geographical unit that is comparable across waves, we also collect the coordinates of the 0.5 x 0.5 decimal degrees PRIO-GRID cell (see Section 1.3.4) in which each enumeration area lays over.

In this analysis we use wave V and wave VI of DHS survey, whose interviews took place in 2006 and 2012/13 respectively. Therefore, children who were measured during the interviews covers all birth cohorts ranging from 2001 to 2013, which includes the plague period in the middle. In particular, children measured in the first wave are those whose cohort of birth can potentially be exposed to the plague early in life. Children from the second wave, instead, are too young to have been exposed to it. In our main specification, we use information on children born before the 2006 DHS data collection period. Data from the 2012 wave are used for robustness and placebo tests. To enrich the set of variables available, the data of each child is linked to other household characteristics.

---

[11]Unfortunately data on birth weight is of poor quality in the DHS surveys that we are using. Birth weight is reported for less than 30% of observations with a lot of bunching due to the fact that most respondents provide rough guesses from what they could recall.

[12]Empirical work using DHS data also call the clusters as enumeration areas or locations. We use the terminology of DHS cluster or enumeration area without distinction.

TABLE 1.1: Descriptive statistics

		Treatment	Control	Difference	Standard Error
Age of head of household (years)		41.66	41.70	-0.04	0.28
Head of household is female (percentage)		49.59	49.21	0.39	1.18
	Poor	35.82	41.53	-5.33***	1.16
Wealth of household (percentage by category)	Middle	21.28	20.89	0.39	0.96
	Rich	42.90	37.95	4.95***	1.15
Rural residence (percentage)		71.98	72.30	-0.32	1.06
Height (in centimeters)		162.70	161.12	1.11***	0.17
Education (years)		0.95	1.00	-0.05	0.06
Number of children 5 years old and under		2.30	2.29	0.02	0.01
Number of observations		12,118	2,091		

Source: DHS data, Mali waves 2006 and 2012. The table reports average values of each variable, computed for the treatment and the control groups. The former group consists of households located within a 30 kilometers from a locust swarm event. The third column reports the difference between the averages of treatment and control group for each variable. The fourth column reports the standard error of the difference. *** p<0.01, ** p<0.05, * p<0.1.

To have a broad picture of the socioeconomic conditions of our population of interest, Table 1.1 provides some descriptive statistics of the household and mothers characteristics. We distinguish between households located in areas exposed to the locust plague and the remaining ones.[13] Table 1.1 suggests that there are not remarkable differences between treated areas and non-treated ones. On average, surveyed households are headed by people in their early 40s and the gender distribution of head of household is even. More than the 70% of the surveyed households are located in rural areas. Concerning the distribution of wealth, compared to the control group, the treatment group has 5% less poor household and 5% more rich household. On average, mothers are slightly more than 160 cm tall, have a very low education level, i.e. only one year, and have more than two children aged 5 years or younger.

Figure 1.1, Panel A, depicts the spatial distribution of household clusters and locust swarms events in Mali. We can notice that the potentially treated clusters are mainly located in the eastern part of the country, where the most of the swarm events occurred. The remaining potentially treated clusters are located in the western and central regions of the country. This makes sense as these territories coincide with the breeding area depicted in Figure A.1 and the northern part of the country is part of the Sahara desert.

1.3.3 Crop Prices Data

We collect official data on crop prices from the Malian Agricultural Markets' authority, Observatoire du Marché Agricole (OMA prices henceforth). The

---

[13]An area is defined as exposed if it is located within 30 km from at least one locust swarm event during the plague.

FIGURE 1.1: Empirical context of the locust plague of 2004 in Mali – DHS clusters, locust swarms, markets, and integration to markets.

Panel A. DHS Clusters, Locust Swarms and Local Markets

Panel B. DHS Clusters by levels of isolation from main cities
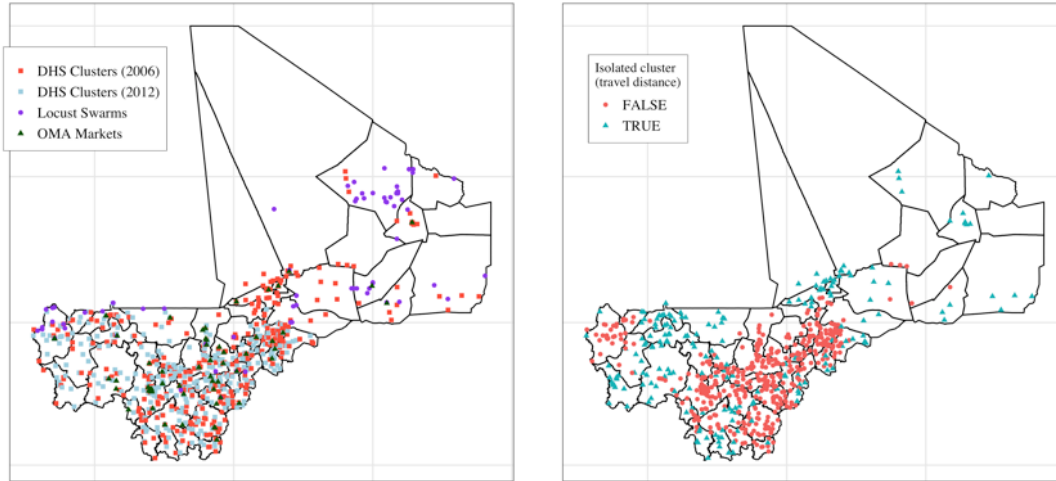
Source: DHS waves of Mali from 2006 and 2012, SWARMS–FAO database, OMA market prices' data, and GAM database. Panel A plots the location of the DHS clusters by wave, of the locust swarm events, and the OMA markets. Panel B distinguishes 2006 clusters in terms of their level of isolation according to the shortest travel time to the closest major town (households are defined as isolated (green triangles) if in the bottom quartile of the distribution of market access of each of the measures).

data provides the retail consumer prices, in national currency, of the 4 main cereal crops (maize, millet, sorghum and rice). Such data is gathered for 65 local markets in Mali from 2000 to 2015. These markets are depicted in Panel A of Figure 1.1 (green triangles). We link the market data to households by looking for the nearest OMA market located in the same PRIO-GRID cell where the DHS clusters lay on.

1.3.4 Additional Spatial Data

The georeferenced feature of the household and locust swarms datasets allows us to aggregate more information for our analysis. We add to the data described above geographical information from the PRIO-GRID dataset (Tollefsen et al., 2012). This is a geocoded dataset, whose statistical unit is spatial cells of 0.5×0.5 degrees, hereafter called PRIO-GRID cells. Moreover, we collect weather data from the Standardized Precipitation-Evapotranspiration Index (SPEI), a multiscalar drought index that considers the joint effects of precipitation, potential evaporation, and temperature (Vicente-Serrano et al., 2010). This allows us to take into account the fact that the impact of rainfall on the growing cycle of a plant depends on the extent to which water can be

retained by the soil.[14] This dataset is available at the 0.5×0.5 degrees, and so matched to the household coordinates.

We also collect data at finer levels of disaggregation that are linked to the DHS coordinates. We obtain data on access to transportation networks and, as a consequence, access to large cities and markets, from the Global Accessibility Map (GAM; Uchida and Nelson, 2010) project. This is a high resolution raster data which provides information on the travel time to the nearest 50,000 inhabitants town in 1km^2 geographical units, in the year of 2000. Panel B of Figure 1.1 shows, by distinguishing DHS clusters as non–/isolated, how they vary in terms of access to large cities and markets. There is substantial variation, even between clusters located relatively close to one another.

1.4 Effect of Locust Invasions on Child Health: Three Potential Channels

In this paper, we are interested in understanding how early life exposure to the 2004 desert locust plague could have affected child health using data from Mali. The mechanism that links the two elements is economic – as mentioned above, the plague of interest created a severe food crisis in Mali. We expect that to translate into a shock to the caloric intake at the household level, which in turn would hinder child development.

The relation between the timing of the exposure to the plague and food shortage is, however, not straight forward. The agricultural production has a cyclical nature, following a region–specific seasonal calendar. Crop damages caused by locust swarms in a period of time might not affect the food supply at that moment if markets are still relying on previous season's production. Therefore, to understand how the 2004 plague could have affected households in Mali, we first need to understand which harvest households and markets were relying on in each period.

Figure 1.2 shows the seasonal agricultural calendar in Mali (FEWS-NET, 2005). It starts with soil preparation between March and May followed by planting in May-June. The growing season happens between July and September; the harvest period is in October/November. Given that the 2003-2005

---

[14]See Appendix A.2 for a description of how we construct an index of local weather shocks using SPEI index.

FIGURE 1.2: Seasonal agricultural calendar in Mali.

Mar	Apr	May	Jun	Jul	Aug	Sept	Oct	Nov	Dec	Jan	Feb

Dry Season
Soil Prepration

Planting

Growing Period

Harvest

Dry Season
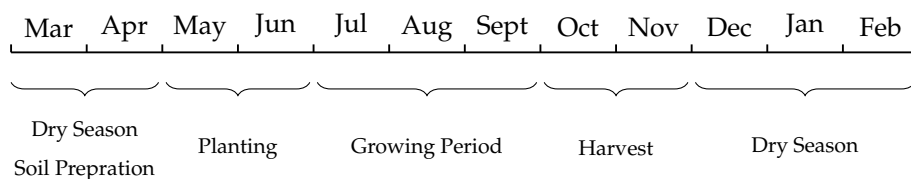
Source: FEWS-NET (2005). The timeline above documents the calendar starting in March of 2004 and ending on February 2005.

plague infested parts of Mali mostly during the third quarter of 2004 (see Figure A.3), the locust invasion has affected substantially the planting and the growing season of the 2004 agricultural season, scheduled to be harvested in October of that year. Therefore, food supply on local markets before October 2004 came from the harvest of the previous year, which, as shown in Figure A.3, has not have been affected by the plague. Given this, we identify three potential channels through which locust invasion could have affected households: (i) a speculative price effect, (ii) a local crop failure effect, and (iii) a potential long term effect on agricultural production.

1.4.1 Speculative Price Effect

Between July and October 2004, i.e., during the peak of the plague, households and markets were still relying on agricultural production from the previous season, harvested by the end of 2003. Hence, there was no threat to the food supply in this time window. However, there could have been a speculative price effect in anticipation of the imminent harvest failure in locust affected areas. The mere exposure to the plague could have led to severe inflation of local crop prices and harm households with limited resources, especially because the plague happened during the lean season.[15] In Section 1.6.5 we argue that this was indeed the case using market level crop price data. Specifically, we show that the plague led to significant inflation of crop prices in affected areas, compared to non-affected areas, during the growing season of 2004.

Therefore, it is possible that children that were in utero during the third quarter of 2004 were affected by this speculative price effect even though markets and households were still relying on harvests not affected by the plague. Consequently, cohorts belonging to the third quarter of 2004 were

---

[15]The lean season is a period of seasonal poverty in rural areas between planting and harvest periods when stocks of food are the lowest, there is no income and families often miss meals.

exposed only to the speculative effect. We use this information to disentangle the impact of the price effects, on child health, from other potential effects described below.

This speculative price effect is a negative shock for households that are net buyers of local crops in that period, but a positive income shock for those that are net sellers. Net sellers during the lean season in Mali are typically a small share of relatively rich households that buy local crops after each harvest and sell them throughout the year on the markets. This means that, in absence of any information on the economic activity of household members, the effect that we estimate is an average effect, which might be attenuated by the positive income effect from net sellers depending on their relative size. This attenuation effect might also occur in the actual crop failure effect described next.

1.4.2   Local Crop Failure Effect

The harvest that was directly affected by the locust swarms was gathered between October and November 2004. Households and local markets had to rely on this potentially bad harvest until the next one, gathered in October 2005. We can, therefore, expect that areas affected by locust invasions have been treated during all this period by the actual local crop supply shock. This agricultural production shock could have negatively affected all households that are net buyers of local crops through the increase in market prices. It could have also harmed farming households that had their fields invaded by the swarms (a direct income shock).[16]

Therefore, in terms of exposure of children, only the cohorts from the third quarter of 2005 onward were exposed exclusively to the crop failure effect. Children born between the fourth quarter of 2004 and the second quarter of 2005 were potentially exposed to both effects, as their 9-month pregnancy period overlaps with the third quarter of 2004, i.e., what we define as the speculative price effect period. We will exploit such distinction when separating the latter from the crop failure effect.

---

[16]Locust swarms can also affect livestock farmers through a decrease in the available pasture.

1.4.3 Potential Long Term Effect on Agricultural Production

The adverse effects of the plague should have disappeared after the harvest of November 2005, unless the crop failure in 2004 affected the quality of seeds used for the next harvest, or the income shock led to a depletion of productive assets (livestock, for instance). This would have led to a persistent effect, in the medium-run, on household food availability. We found no evidence suggesting that subsequent harvests suffered from the locust swarm invasions. First, there is no account of such effects from reports produced by agencies such as FAO. Moreover, we will show empirically in the next sections that there are no differences in health status between children conceived in the locust affected areas and children conceived in non-affected areas, after the harvest of 2005.

1.5 Empirical Strategy

We adopt a Difference-in-Differences approach to estimate the causal impact of locust invasions on child health. First, we define treatment and control groups at the enumeration area level, by setting as treated, clusters within 30 kilometers of a locust swarm event. Then, we exploit all the available variation in childhood exposure to treatment across enumeration areas and birth cohorts.

We estimate the following model:

$$ y_{i(h,t,e)} = \gamma T_{i(t,e)} + \mu_e + \beta_t + \theta_{hh} X_h + \theta_1 X^{(1)}_{i(h,t,e)} + \theta_2 X^{(2)}_{i(t,e)} + \epsilon_{i(h,t,e)}, \quad (1.1) $$

where i denotes a child belonging to cohort t (year-month), born in household h who lives in enumeration area e.[17] The dependent variable $y_{i(h,t,e)}$ measures height-for-age Z-score of child i in our main specification. The treatment variable is $T_{i(t,e)}$, a dummy that takes a value of one if child i belongs to an enumeration area in the treatment group and has been exposed in utero to the adverse effects of the plague, i.e. born between July 2004 and June 2006 in a locust affected area.[18]

---

[17]We omit from the notation, for neatness, the grid-cell g where enumeration area e lays over (see section 1.3.2). When estimating the model (1.1) with the two DHS waves, we replace the cluster fixed effects by grid cell fixed effects in order to compare geographical units consistent across waves. In that case, we add to (1.1) a dummy for treatment status at the cluster e level.

[18]This treatment dummy will be split below into different time bins to properly explore the timing and channels of this adverse shock.

We control for μ_e and β_t that are enumeration area and birth cohort fixed effects respectively. $X^{(1)}_{i(h,t,e)}$ and $X^{(2)}_{i(t,e)}$ are observable characteristics at individual level (gender, birth order among siblings, age gap with direct older and younger siblings, etc.) and enumeration area level (Standardized Precipitation-Evapotranspiration Index (SPEI) drought index), respectively. Finally, X_h is a vector that includes household–level controls, such as gender and age of household head, wealth index of household, education of the mother. Standard errors are clustered at 0.5 x 0.5 decimal degrees PRIO-GRID cell level (see section 1.3.2).

In the baseline specification of the model in equation 1.1, we control only for enumeration area fixed effects to account for permanent unobserved characteristics of the place of residence and cohort fixed effects to account for cohort–specific shocks, whereas the full version of the model includes controls for the relevant household and child characteristics.

Our coefficient of interest is γ, which measures the average difference in changes of height-for-age Z-scores of children born in locust infested areas and children born in non-infested areas, holding constant all the other relevant characteristics. The implicit assumption behind this identification strategy is that, after controlling for cohort and enumeration area fixed effects, household characteristics, and other relevant exogenous covariates, changes in height-for-age Z-scores would be similar across locust infested areas and non-infested areas in absence of the plague. Given that we control for cohort and enumeration area fixed effects, the coefficient γ does not represent the national impact of locust plague but the average effect with respect to local and cohort averages.

1.6 Empirical Results

1.6.1 Average Impact of Locust Plague on Child Health

Table 1.2 displays the point estimates of γ in Equation 1.1. Column (1) shows the estimated coefficient of the baseline specification of our model, in which we control only for location fixed effects and cohort fixed effects. As explained in Section 1.5, the treatment variable is a dummy equal to one for children born in locust affected areas between July 2004 (beginning of locust plague) and June 2006, i.e. the last cohort of children that relied on the

TABLE 1.2: Impact of locust plague on child health

Dependent variable	Height-age Z-score				Stunted	
	(1)	(2)	(3)	(4)	(5)	(6)
In utero treatment	-0.476***	-0.432***	-0.421***	-0.429***	0.074**	0.079***
	(0.112)	(0.115)	(0.112)	(0.092)	(0.031)	(0.023)
Observations	9,173	9,173	9,173	9,173	9,173	9,173
R-squared	0.200	0.220	0.239	0.245	0.183	0.189
Cohort FE	YES	YES	YES	YES	YES	YES
Location FE	YES	YES	YES	YES	YES	YES
Child characteristics	NO	YES	YES	YES	YES	YES
Family characteristics	N0	N0	YES	YES	YES	YES
Region specific time trend	N0	N0	N0	YES	N0	YES
Mean dependent variable	-1.425	-1.425	-1.425	-1.425	0.365	0.365

Source: SWARMS data base from FAO Desert Locust Information Service and household survey data from 2006 DHS wave in Mali. Full set of controls includes mother's height, education, gender and age of household head, household wealth index, SPEI index, birth order, time gap between conception and the previous and following pregnancies. Robust standard errors in parentheses are clustered at PRIO cell grid level. *** $p<0.01$, ** $p<0.05$, * $p<0.1$. The dependent variable in columns (1)-(4) is height for age z-score. Column (1) controls only for cohort and location fixed-effects. Column (2) and Column (3) include progressively child characteristics and family characteristics. Column (4) adds to the previous controls region-specific time trends. Columns (5) and (6) use a dummy equal to 1 if child is stunted (height-for-age Z-score<-2) as dependent variable.

2004-2005 agricultural campaign harvest while in utero.[19] The estimated impact is negative and statistically significant. The estimate is robust and remains significant after progressively adding controls for child characteristics in column (2) and family characteristics in column (3). Our main specification in column (3) suggests that exposed children have, on average, a Z-score 0.42 points below the one of non-exposed children. This represents approximately a 30% decrease in the average Z-score for the children in our sample. Column (5) shows an alternative way to quantify the magnitude of this effect. It shows that this plague increased stunting rates by 7.4 percentage points. This represents more than 20% of the average stunting rate in our sample.[20] The estimates of the impact of locust plague on height-for-age z-score and stunting rates are also robust to the inclusion of region-specific time trends (columns (4) and (6)). In Table A.4, we also show that this plague invasion did not have any detectable effect on neonatal mortality (death less than a month after birth) and infant mortality (death less than a year after birth).

---

[19]The youngest children used in this regression were born in March 2006.

[20]Stunting rate is defined as the share of children with height-for-age Z-score smaller than -2 standard deviations.

1.6.2   Robustness of the Average Effect

In validating the results presented above, we start by confirming that the estimated effect is not sensitive to the radius of 30 km used in our main specification. To this scope, we run several alternative specifications of our baseline model described in Equation 1.1 (Section 1.5); in each iteration, we change the definition of *treatment group*. In particular, in the first specification, an area is defined as *locust affected* if it is located at most 20 km from at least one swarm event during the 2004 plague. In the subsequent specifications, we add progressively 2 km to the threshold that defines what is a treatment area, up to 70 km. Figure A.4 plots the estimates of γ for each performed specification, together with their 95% confidence bands. It can be noticed that the adverse effect of locust invasions on child health is both negative and statistically significant for thresholds up to 40 km. After that, the estimates decrease towards zero and lose significance. This is consistent with the idea that locusts invasions are events that have adverse *local* effects.

In Table A.3 we present results of robustness checks performed on alternative empirical specifications and data samples. Column (1) shows robustness to very demanding mother fixed-effects specification where we are only relying on variation across siblings in exposure to the locust plague. The magnitude of the impact is smaller but remains significant. Columns (2), (3), (4) and (5) show the robustness of the main results presented in Table 1.2 when using, respectively, survey sample weights, spatial HAC standard errors, treatment at the municipality level, and including events that occurred beyond Mali country borders. Column (6) runs the main specification using data from both 2006 and 2012/2013 DHS waves and the estimated coefficient is still negative and significant. Column (7) uses both survey waves but restricts the sample to children born after the plague outbreak. This means that treated children belonging to the older cohorts and younger children are not treated.[21] To check that the estimated effect is not capturing any pre-existing time trends between treated and non-treated areas, we run a first placebo test in column (8). We use only data from the 2012/2013 survey and the placebo treatment is a dummy equals to 1 for children born in locust affected areas after 2010. The estimated coefficient is small, positive and not significant.[22]

---

[21] In our main specification in Table 1.2, treated children belong to younger cohorts and all the older children are not affected in utero by the plague.

[22] We discuss more evidence of absence of pre-existing trends in Section 1.6.4.

1.6.3 Impact of the Locust Plague on Child Health Across the Space

We have established that the 2004 locust plague in Mali led to major health setbacks for children exposed in utero. In this section, we explore whether and how the average impact on child health changes with the distance from the locust swarm events. To do so, we run an alternative specification of the model presented in column (3) of Table 1.2, in which we define as non-treated areas located at least 60 km away from any swarm event. We then split the treated areas into 6 groups using 10 km-wide intervals. Therefore, we have 6 treatment groups, the first one includes children belonging to households located at most 10 km away from the locust event, the second group includes child belonging to households located between 11 and 20 km away from the locust event, and so forth.

Results shown in Figure 1.3 suggest that the estimated effect is negative, significant, and fairly constant if the impacted child belongs to a household located within the first 30 km from the locust plague event. This means that the plague affected entire localities by impacting their local markets of reference, and not just those households or small communities that have experienced a bad harvest (or completely lost it) because of the invasion. The role of local markets is a key finding of our paper that we explore further in the next sections. The estimated coefficient fades out after 30 km, confirming the idea that locust invasions have local effects.

1.6.4 Timing of the Estimated Effect, Channels and Placebo Test

The fact that the 2004 locust invasion impacted Mali within a relatively narrow time window allows us to investigate the effect of such shock for different cohorts of children. Moreover, as discussed in Section 1.4, for each life-stage, we can differentiate between *speculative price effect* and *crop failure effect* as potential channels through which locust plagues affect child health. To do so, we estimate the impact of being born in a locust affected area for different birth cohorts during the different phases of the plague period.

Figure 1.4 depicts the estimated impact of being born in locust infested areas by quarter of birth between years 2003 and 2008, together with the 95%

FIGURE 1.3: Impact of the locust plague on child health across the space
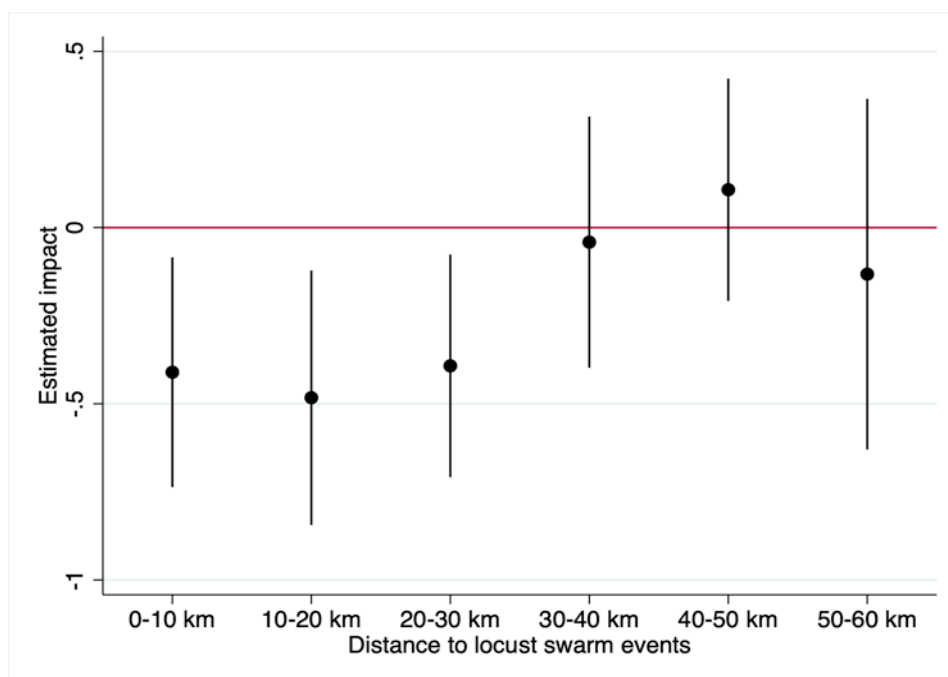
Source: SWARMS data base from FAO Desert Locust Information Service and household survey data from 2006 DHS wave in Mali. This figure depicts the estimated coefficient of locust invasion on height-for-age Z-scores splitting the treatment effect in the main specification into average effects by groups of 10 km rings around each location. Non-treated areas are those with no swarm event within a 60 km radius. The first coefficient plots the average effect for affected children with at least 1 swarm event within a 10 km radius. Each coefficient is plotted together with its 95% confidence bands.

confidence bands of each coefficient.[23] The dashed line represents the quarter when the locust plague started in Mali. This figure shows that children born in impacted areas before the plague, i.e., between the first quarter of 2003 and the second quarter of 2004 both included, have height-for-age Z-scores comparable to children belonging to the control group. This means that children already born when the plague hit did not suffer any effect perceptible in their height-for-age Z-scores.[24] It also confirms the hypothesis that the estimated impact that we documented in the previous section is not capturing pre-existing trend differences between treated and non-treated areas.

Moreover, between the third quarter of 2004 and the first quarter of 2006, there is a clear drop in our coefficient of interest, which becomes negative and statistically significant (estimates for quarters four of 2004 and one and two of 2005 are significant at 90% confidence level). This corroborates our finding

---

[23]The 2006 DHS survey data was collected between May and December so we restrict the analysis to children born before April 2006 to prevent survey timing biases from contaminating the estimated effect. The oldest cohorts with anthropometric measures from 2012-2013 survey were born in 2008.

[24]This justifies also our focus on in utero exposure in most of our analysis.

that all the cohorts of children that have been exposed in utero to the plague suffered substantial health setbacks.

Note that the estimated coefficient turns negative and significant for children born in July, August, or September 2004, i.e. the first three months of the locust invasion in Mali. According to the seasonal calendar reported in Figure 1.2, these children, during the onset of the plague, were still relying on the previous harvest that has not been affected by locust. Thus, this evidence suggests that the negative impact on their health status was driven by speculations on the agricultural campaign that was starting, which led to a sharp increase in prices of local food products. Note that this cohort was exposed also to the crop failure effect, but only after birth, and we find no effect of the plague after birth (see older cohorts of children in Figure 1.4). Yet, this negative effect could be explained by differences between the very first 2-3 months of life and the subsequent months in early childhood, which, to the best of our knowledge, has never been documented in the literature. Nevertheless, we rule out such alternative explanation in Section 1.6.5 by first showing evidence of a significant crop price increase during the third quarter of 2004 due to the plague. Later on, we show that when we control for local prices, the estimated effect for the impacted children born during this time window (i.e., exposed only to the speculative price effect) drops substantially and becomes insignificant.

Figure 1.4 shows negative coefficients also for children born between September 2004 and March 2006. These groups were relying on the harvest of the 2004-2005 season, i.e. the harvest that was directly damaged by locust swarms in treated areas. Therefore, these children were potentially subject to the crop failure effect due to the failed harvest while in utero. The negative and significant impact found for these cohorts supports this idea. Children born between October 2004 and June 2005 are potentially exposed in utero to both the *speculative price effect* and the *crop failure effect*. Those born after June 2005 are exposed only to the crop failure effect.

Finally, Figure 1.4 also depicts the estimated coefficients on younger cohorts, born after the plague ended, namely children born between January and December 2008. Those children were 4 to 5 years old at the time of the survey when they were measured so estimated coefficients are noisier and more volatile from quarter to quarter. In any case, there is no evidence of a

FIGURE 1.4: Estimated impact of the 2004 locust invasion in Mali
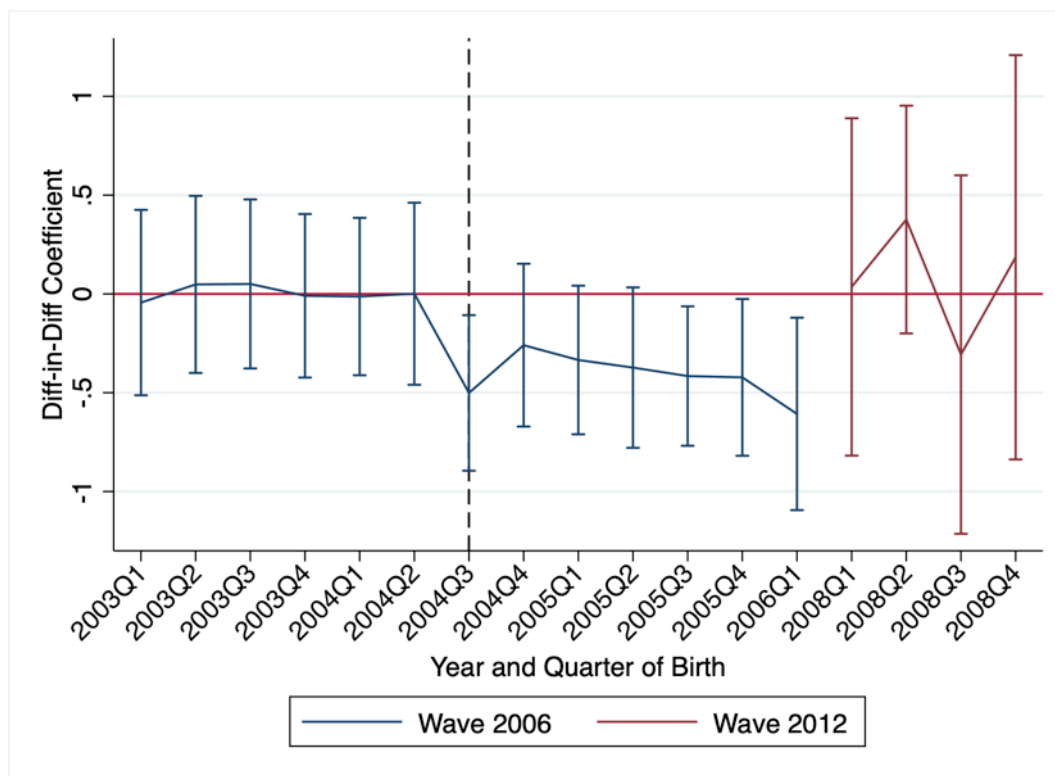
Source: SWARMS data base from FAO Desert Locust Information Service and DHS data, Mali waves 2006 and 2012. This figure depicts the estimated coefficient of locust invasion on height-for-age Z-scores for each quarter-year cohort born in locust invaded areas between January 2003 and December 2008. Each coefficient is plotted together with its 95% confidence bands. The blue colored coefficients are obtained using height-for-age Z-scores computed during the 2006 DHS survey, while the red ones are obtained using height-for-age Z-scores computed during the wave held in 2012. The black dashed vertical line shows the quarter of the onset of the locust plague in Mali.

clear trend and the estimated impact is oscillating around zero.[25] Given that the health status of children born in the locust affected areas (after the plague ended) is comparable to the health status of children born in non-affected areas, we can infer that the locust invasion did not have any perceptible long-lasting effects. The harvest gathered during the 2005-2006 season seems not to have been impacted by the damages which took place during the previous agricultural season.

1.6.5 The Power of Markets: Understanding their Role

We explore in detail the mechanisms through which the locust plague led to the estimated health setbacks. In Section 1.6.3 we have shown that the

---

[25]We show in column (8) of Table A.2 (Appendix A.3) a similar result in a placebo test where we consider older cohorts of children in the 2012 wave as not affected by the plague and younger cohorts of children as potentially affected by the plague.

plague's impact spreads over entire localities by affecting their local markets of reference. In this Section, we first take a closer look at what happened to the local crop prices when an area is hit by the plague (Subsection 1.6.5). Then, we examine impact of the plague on child health, accounting for price effects (Subsection 1.6.5). Finally, we study the importance of local crop market isolation on the impact of locust plagues on child health (Subsection 1.6.5).

Impact of Locust Plague on Crop Prices

We rely on a Difference-in-Differences approach, similar to Equation (1.1), to investigate how market prices evolved during the plague and among treated and non-treated locations. To keep our analysis consistent with the discussion in Section 1.6.4, we split the exposure to the plague into three distinct time windows: (i) the period in which children have been exposed, in utero, only to the speculative price effect, (ii) the period with both speculative and crop failure effects, and (iii) the period with crop failure effect only. In practice, we use OMA monthly crop prices from 2000 to 2015 as the dependent variable in the following specification:

$$\log(p_{m(c,t)}) = \theta_1 T_m \mathbb{1}(t \in 2004Q3) + \theta_2 T_m \mathbb{1}(t \in 2004Q4 \text{ to } 2005Q2) +$$
$$\theta_3 T_m \mathbb{1}(t \in 2005Q3 \text{ to } 2006Q1) + \beta X_{m(t)} + \mu_m + \delta_c + \xi_t + \epsilon_{m(c,t)}.$$
$$(1.2)$$

Variable $\log(p_{m(c,t)})$ stands for the prices (in logs) of crop c, in month-year period t, at market m. The treatment $T_{m(t)}$ is assigned to markets m in case a locust event is present within 30 km during the invasion of 2004. θ_1 is the main coefficient of interest: it measures the difference-in-differences impact of locust invasion on crop prices during the *speculative price effect* period (third quarter of 2004). Similarly, θ_2 and θ_3 quantify analogous estimates for the other exposure periods. We account for possible confounding factors by controlling for weather conditions (SPEI) in the 12 months previous to t in market m, $(X_{m(t)})$, and by adding market, crop and time fixed effects (μ_m, δ_c and ξ_t, respectively).

Table 1.3 presents the results. In Column (1), we report the estimates of θ_1, θ_2, and θ_3 not adding the set of weather controls, which is done in column (2). The results suggest that crop prices in locust affected markets were significantly higher, compared to non-affected areas, only during the *speculative price effect* period. The plague led to an increase of 6% on average

TABLE 1.3: Impact of locust plague on crop prices

	(log-) Crop prices (1)	(log-) Crop prices (2)	(log-) Crop prices (3)	(log-) Crop prices (4)
Speculative price effect (θ_1)	0.065***	0.065***	0.063***	0.061***
	(0.019)	(0.019)	(0.019)	(0.016)
Both effects (θ_2)	-0.004	-0.004	-0.005	- 0.001
	(0.007)	(0.007)	(0.007)	(0.006)
Crop failure effect (θ_3)	-0.008	-0.008	-0.009	-0.008
	(0.009)	(0.009)	(0.009)	(0.007)
Observations	48,503	48,503	48,503	48,503
R-squared	0.862	0.862	0.864	0.911
Market FE	YES	YES	YES	YES
Time FE	YES	YES	YES	NO
Crop FE	YES	YES	YES	NO
Weather controls	NO	YES	YES	YES
Market Time Trend	NO	NO	YES	NO
Crop-Time FE	NO	NO	NO	YES

Source: SWARMS data base from FAO Desert Locust Information Service and OMA crop prices at monthly level from 2000 to 2015. *** $p<0.01$, ** $p<0.05$, * $p<0.1$. Dependent variable is log crop price for maize, millet, sorghum and rice in local currency. Weather controls include SPEI index in the previous 6 months, separated in two distinct quarters. Columns (1) and (2) report the results of the estimation of Equation 1.2 respectively with and without weather controls. Columns (3) and (4) report the results of the estimation with weather controls, adding market-specific time trends and crop–time fixed effects, respectively.

prices during the third quarter of 2004. This result is robust to the addition of market–specific time trends and to the inclusion of more demanding fixed effects at crop–time level. These are reported in columns (3) and (4).[26]

Accounting for Prices in the Estimated Effect of Locust Plagues

We now use the three different exposure time windows previously presented, together with data on local prices, to further explore the different channels through which locust plagues impact child health. To do so, we build on our benchmark model of Equation (1.1) by splitting in utero exposure to the plague according to the aforementioned time windows: (i) the period in which children have been exposed, in utero, only to the speculative price effect, (ii) the period with both speculative and crop failure effects, and (iii) the period with crop failure effect only.

In column (1) of Table 1.4, we estimate the impact of the locust invasion on child health, allowing for a different impact for each of these 3 windows. Results show that the health setbacks implied by the locust invasion is statistically significant and similar in magnitude during the three types of exposure to the plague.[27]

---

[26]We find similar results when looking at the evolution of prices quarter by quarter around the year of the plague (see appendix Appendix A.5).

[27]This specification will be our main specification for everything that follows.

TABLE 1.4: Impact of locust plague on child health accounting for price effects

	Panel A			Panel B		
	(1)	(2)	(3)	(4)	(5)	(6)
Treatment with speculative price effect	-0.496***	-0.589**	-0.311	-0.492***	-0.716**	-0.415
	(0.168)	(0.268)	(0.261)	(0.176)	(0.276)	(0.259)
Treatment with both	-0.329**	-0.368	-0.339	-0.346***	-0.565***	-0.540**
	(0.144)	(0.271)	(0.286)	(0.127)	(0.205)	(0.211)
Treatment with crop failure effect	-0.489***	-0.496**	-0.495*	-0.494***	-0.749***	-0.767***
	(0.153)	(0.227)	(0.247)	(0.128)	(0.144)	(0.146)
Observations	9,173	2,910	2,910	9,173	2,910	2,910
R-squared	0.239	0.255	0.261	0.245	0.265	0.270
Cohort FE	YES	YES	YES	YES	YES	YES
Location FE	YES	YES	YES	YES	YES	YES
Child characteristics	YES	YES	YES	YES	YES	YES
Family characteristics	YES	YES	YES	YES	YES	YES
Region specific time trend	N0	N0	N0	YES	YES	YES
Mean dependent variable	-1.425	-1.273	-1.273	-1.425	-1.273	-1.273

Source: SWARMS data base from FAO Desert Locust Information Service and household survey data from 2006 DHS wave in Mali. Dependent variable is child height-age Z-score. Full set of controls includes mother's height, education, gender and age of household head, household wealth index, SPEI index, birth order, time gap between conception and the previous and following pregnancies. Robust standard errors in parentheses are clustered at PRIO cell grid level. *** $p<0.01$, ** $p<0.05$, * $p<0.1$. Column (1) uses the full sample. Column (2) restricts the sample to observations with price data without controlling for prices. Column (3) controls for prices. Column (4), (5) and (6) are equivalent to Columns (1), (2) and (3), respectively, but adding controls for region specific time trends.

We then run the same specification on the sub-sample of children for which we have market price data in column (2).[28] We get the same pattern in the estimated coefficients as in column (1), even on this restricted sub-sample that does not cover the entire country. In column (3), we control for average local prices during pregnancy to establish whether the negative effect of the plague due to the speculative price effect is explained by the increase of local prices in affected areas. Results show indeed a drop in estimated coefficient for children exposed only to the crop failure effect, but not for other children that have been exposed to the crop failure effect. Panel B of Table 1.4 shows that all the results in Panel A are robust to controlling for region-specific time trends.

Locust Plague and Level of Isolation of Local Markets

The evidence presented so far suggests that local markets play a key role on the timing of adverse impact of agricultural shocks such as locust plagues. The extent to which a given local market is trading crops with other markets

---

[28]As explained in Section 1.3, we observe local crop prices only for subset of areas in our study.

can also play a crucial role on the magnitude of the shock faced by house-holds. Local and minor agricultural shocks can be easily absorbed by well connected markets. Major shocks may however exacerbate the effect of food shortage at local level because crops are sold fast to a larger market (Burgess and Donaldson, 2010; Townsend, 1995).

Going back to the distinction between *speculative price effect* and *crop failure effect*, market openness can have very different consequences. On the one hand, well connected areas hit by the *crop failure effect* can rely on crop supply from non-affected areas in their network to mitigate the effects of the shock. Conversely, areas that are isolated and rely mostly on their own agricultural production may be more affected when hit by such shock. On the other hand, high level of trading may imply that local crops are sold fast, putting vulnerable households at higher risk. This may exacerbate the *speculative price effect* in rural areas with a single harvest per year.

In order to investigate how market openness affects the impact of locust plagues on child health, we use the travel time to the nearest major city to capture the level of isolation for different locations. For each household cluster coordinate from the DHS database, we get the minimum travel time to the nearest town of at least 50,000 inhabitants in 2000 from Uchida and Nelson (2010). This metric is derived from a global high-resolution (1 km^2 pixel) raster map of accessibility. It is the result of network analysis using a combination of several sources, most of them collected between 1990 and 2005. The original pixel value is the estimated travel time in minutes by land transportation from the pixel to the nearest major city.[29] The assumption behind the use of this metric is that large towns work as local trade hubs. Therefore, areas that are close to main cities have higher access to a well connected and diversified set of markets.

To investigate this issue, we build on the specification used in column (1) of Table 1.4, by including the interactions of our travel time metric with the three treatment variables. Results are presented in Table 1.5. Column (1) shows that children born in more isolated areas suffer stronger health setbacks when exposed in utero to the crop failure effect. This is not the case for children exposed only to the speculative price effect in utero. This pattern is robust to controlling for household wealth index in column (2).

---

[29]Empirically, we use standardized values of the travel time, inferring sample average and standard deviation of travel time from the sample of enumeration areas. The distribution of the DHS clusters by level of isolation (simplified as non-/isolated is shown in Figure 1.1, Panel B.

TABLE 1.5: Impact of locust plague on child health and level of isolation of local markets

Sample	All		Rural	Urban
	(1)	(2)	(3)	(4)
Treatment with speculative price effect	-0.461***	-0.458***	-0.469**	-0.568*
	(0.171)	(0.171)	(0.223)	(0.337)
Treatment with both	-0.268**	-0.270**	-0.261*	-0.291
	(0.135)	(0.135)	(0.142)	(0.213)
Treatment with crop failure effect	-0.402***	-0.395***	-0.438***	-0.267
	(0.139)	(0.139)	(0.148)	(0.259)
Treatment with speculative price effect × Travel time	-0.072	-0.068	-0.049	-0.282
	(0.087)	(0.085)	(0.081)	(0.334)
Treatment with both × Travel time	-0.129***	-0.128***	-0.130***	-0.126
	(0.014)	(0.015)	(0.019)	(0.099)
Treatment with crop failure effect × Travel time	-0.149***	-0.153***	-0.174***	0.107
	(0.024)	(0.025)	(0.028)	(0.296)
Observations	9,173	9,173	6,479	2,694
R-squared	0.239	0.240	0.240	0.209
Cohort FE	YES	YES	YES	YES
Location FE	YES	YES	YES	YES
Child characteristics	YES	YES	YES	YES
Family characteristics	YES	YES	YES	YES
Wealth Index	N0	YES	YES	YES
Mean dependent variable	-1.425	-1.425	-1.607	-0.986

Source: SWARMS data base from FAO Desert Locust Information Service and household survey data from 2006 DHS wave in Mali. *** $p<0.01$, ** $p<0.05$, * $p<0.1$. The dependent variable in all regression are the children's height-for-age Z-scores. Full set of controls includes mother's height, education, gender and age of household head, household wealth index, SPEI index, birth order, time gap between conception and the previous and following pregnancies. Travel time is the standardized travel time to the nearest city of more than 50,000 inhabitants.

This suggests that isolation itself plays a role and these results are not likely to be biased by the fact that more isolated households might be poorer, and thus more vulnerable, than better connected ones. Columns (3) and (4) split the sample into children born in rural and urban areas, respectively. The patterns followed by these two sub-samples are not different than those of columns (1) and (2). Our main interest here is in column (3) since there is more variation in the travel time metric within the sub-sample of children born in rural areas. This is mostly capturing the difference between rural areas that are in the outskirts of well-connected cities and those located in very remote areas. The sample of children born in urban areas is much smaller and by definition, they are in most cases, closer to main cities. To conclude, the fact that, in each specification, the interaction term between travel time and the speculative price effect treatment variable is small and not significant suggests that this effect is rather homogeneous across space, irrespective of how isolated local

markets are. This is not the case for the crop failure effect since it shows stronger effects as we move to more isolated areas.

1.6.6 Further Heterogeneous Effects: Migration and Gender

In this section, we discuss potential threats to identification due to migration, and how the main results of the paper vary by type of place of residence and gender. Investigating whether the estimated impact is driven by specific sub-groups of the population can be useful to further understand the channels through which this effect is operating. We run our main specification presented in column (1) of Table 1.4 on several sub-samples. Results are shown in Table 1.6.

First, we focus on migration. One plausible issue concerning our results is that anthropometric measures for children in our sample were measured few years after the plague took place. Some of these children may have migrated to other places of residence after the plague. This makes it impossible to attribute them to the right treatment group. If this is the case, our estimates might be subject to an attenuation bias. Moreover, a subgroup of those that have migrated across treatment areas might have been positively or negatively selected, leading to additional biases in the estimates. For instance, richer households may move out of the treated areas after the plague leading to an upward bias in the estimated coefficients.

We use information on the number of years of residence in the locations where each household has been surveyed and we run our main regression restricting the sample to those that lived at the same location for more than 2 years (before the plague since households were surveyed in 2006) in column (1) and those that have always lived there in column (2) of Table 1.6. Results are robust in both cases suggesting that our estimates are not affected by potential migration.

Furthermore, columns (3) and (4) display the results of the main regression estimated on urban and rural sub-samples. The results suggest that children living in both areas suffer major health setback.[30] The magnitude of the effect is similar for the speculative price effect, but lower in urban areas for the crop failure effect.

---

[30]Reduced sample size for the urban sample affects the precision of the estimates but the magnitudes are comparable to those in the rural sample. Table A.2 is equivalent to Table 1.6 when using a unique dummy variable for treatment.

TABLE 1.6: Heterogeneity: impact of locust plague on child health

	(1)	(2)	(3)	(4)	(5)	(6)
	Years of residence		Place of residence		Gender	
	2 + years	Always	Urban	Rural	Male	Female
Treatment with speculative price effect	-0.498***	-0.521**	-0.587	-0.505**	-0.837***	-0.296
	(0.170)	(0.220)	(0.356)	(0.208)	(0.268)	(0.350)
Treatment with both	-0.316**	-0.517***	-0.297	-0.344**	-0.496**	-0.149
	(0.151)	(0.174)	(0.153)	(0.168)	(0.209)	(0.176)
Treatment with crop failure effect	-0.463***	-0.485***	-0.287	-0.594***	-0.468**	-0.537***
	(0.152)	(0.183)	(0.159)	(0.169)	(0.186)	(0.204)
Observations	8,811	4,995	2,694	6,479	4,654	4,519
R-squared	0.241	0.268	0.209	0.238	0.269	0.300
Cohort FE	YES	YES	YES	YES	YES	YES
Location FE	YES	YES	YES	YES	YES	YES
Child characteristics	YES	YES	YES	YES	YES	YES
Family characteristics	YES	YES	YES	YES	YES	YES
Mean dependent variable	-1.431	-1.449	-0.986	-1.607	-1.484	-1.364

Source: SWARMS data base from FAO Desert Locust Information Service and household survey data from 2006 DHS wave in Mali. Dependent variable is height-for-age Z-score. Full set of controls includes mother's height, education, gender and age of household head, household wealth index, SPEI index, birth order, time gap between conception and the previous and following pregnancies. Robust standard errors in parentheses are clustered at PRIO Cell grid level. *** $p<0.01$, ** $p<0.05$, * $p<0.1$. Column (1) and (2) report the results of the baseline specification (column (3) of Table 1.2) restricting the sample to households that have reported living in the location where they were interview for at least 2 years, or since ever, respectively. Columns (3) and (4) split the sample between urban and rural. Column (5) restricts the sample to male children while Column (6) uses only female ones.

Finally, we explore the degree of heterogeneity of our results in terms of gender. Usually, the literature on in utero shocks finds a large negative bias against girls (Dagnelie et al., 2018; Valente, 2015) because female foetuses are more resilient and this may lead to a stronger selection effect for male children born alive. We find, instead, a negative impact of the plague on children of both genders on average. However, the estimates in column (5) and (6) of Table 1.6 show some differences depending on the timing of exposure to the shock. Boys seem to suffer significantly more from the speculative price effect while girls suffer slightly more from the crop failure effect. The latter result would be consistent with the potential in utero selection effect documented in the literature. All the children exposed in utero exclusively to the speculative price effect were in their last trimester of gestation. Adverse conditions at this stage, even if more harmful for boys, rarely leads to miscarriages. This may explain the stronger *speculative price effect* for boys.

1.7 Concluding Remarks

In this paper, we show that in utero exposure to desert locust plagues can lead to substantial health setbacks early in life. We estimate the causal impact of the plague that occurred in Mali in 2004 on the health status of children

located in territories invaded by locust swarms. We first find that children exposed in utero to the adverse effects of the locust plague have, on average, a height-for-age Z-score 0.42 points lower than non-exposed children. We show that the detrimental effects of locust invasions have broad repercussions that involve entire localities, by impacting their local crop markets.

We explore in detail the mechanisms that lead to these health setbacks. We show that there was a strong speculative price effect of the locust invasion that kicked in during the plague itself, and a local crop supply shock that lasted at least until the subsequent harvest. Cohorts of children that were subject only to the speculative price effect suffer as much as those exposed to the actual crop failure effect. After controlling for crop prices, the estimated negative impact that occurs during the speculative price effect period of the plague is dampened substantially and becomes insignificant. Conversely, the estimated impact for the children exposed only to the crop failure effect remains stable. A core empirical finding along this dimension is the role of access to markets: our results suggest that market openness dampens the adverse health effects of exposure to the plague.

This study has relevant implications from a policy perspective. In particular, our results suggest that it is important to address expectations during pest invasions that affect agricultural production. It is crucial to put efforts in two main directions: (i) prevent price speculations and inflation; (ii) provide safety nets to the most vulnerable households in order to dampen the consequences of these shocks on young children.

With the alarming climate change prospects, one can expect more frequent extreme weather conditions in the breeding areas of the desert locusts, which could lead to more plagues in the future. More recently, several ongoing locust invasions are affecting countries in the Horn of Africa, the Middle East, South Asia, and Latin America since 2019. As of April 2020, 23 countries in Africa and Asia, from Pakistan to Tanzania, have been affected (World Bank, 2020). This is a global outbreak that is threatening to reach the level of a plague. Preparing to limit the consequences of such locust invasions is thus necessary for policy makers that operate in the potential invasion areas.

Chapter 2

Climate Change and Migration: the case of Africa

Abstract

This paper provides a spatial general equilibrium model to quantify the impact of climate change on the economy and migration. The model can capture the role of trade networks and agricultural suitability on the distribution of population and GDP accounting for endogenous adjustments of crop choice and trade. I use detailed geospatial data from 42 countries in sub-Saharan Africa (SSA) to simulate the impact of climate using forecasts of agricultural productivity in 2080 from FAO–GAEZ. Climate change is estimated to displace 12 percent of the SSA population and reduce real GDP by 4 percent. The capacity of switching crops, urbanizing, or trading goods reduces the impact of climate change in terms of population outflows. Finally, the adoption of modern inputs in agriculture reverses considerably the negative impacts of climate change.

2.1 Introduction

One of the most concerning potential consequences of climate change is population displacement, recently coined as the *Great Climate Migration* (Lustgarten, 2020). Subsistence agricultural economies, like the sub-Saharan African (SSA henceforth) countries, lie at the center of this issue. These are highly agriculture–dependent economies, which are expected to be amid the fastest–growing zones, in terms of population, during the next decades (United Nations and Social Affairs, 2019). Understanding how these economies will adjust to a climate–changing world, in which crop yields will be different than today, is key to uncover where this growing population will be geographically reallocated.

Assessing which could be the decisions of economic agents when adapting to climate change is challenging, especially in an agricultural context like SSA. If facing changed agricultural yields, farmers could switch their production towards different crops, remaining however in the agricultural sector. Alternatively, these agents could switch to a non–agricultural sector, potentially moving geographically. Trade would have a crucial role in the extent to which a specialization into agricultural and non–agricultural sectors could take place. Therefore, understanding how these forces – production switching, trade, and migration – will respond to climate change is key to evaluate the effect of climate change on migration and the economy.

In this paper, I develop a quantitative spatial model that accounts for these forces and can be used to quantify how their response to climate change translates into population displacement and economic losses. The model is calibrated with a rich geographical dataset that I assemble, covering 42 countries of SSA. By simulating it for a future scenario of climate change in 2080, I find that about 12 percent of the SSA population could be displaced. The results are very heterogeneous across countries and subnational locations: the median country(location)–level population change is about -12 (-9) percent, while the 10th and 90th percentiles are -22 (-28) and 8 (3) percent, respectively. Moreover, a key finding is that urbanization, crop–switching, and access to trade are relevant margins along which the economy adjusts so to dampen the impact of climate change.

I begin my analysis by showing that the future changes in agricultural yields are expected to be spatially heterogeneous across locations and crops. As a consequence, they would consist of a shock to comparative advantages

in the agricultural sector. Informed by this empirical evidence, I develop a multi-sector Ricardian spatial trade model with partial labor mobility. The model's spatial units are 1°x1° grid–cells, where farmers and firms can produce goods of multiple agricultural sectors (crops) and a non-agricultural sector, respectively. Differences in total factor productivity and market access generate trade, shaping the spatial pattern of the sector–specialization. Relative sectoral prices determine consumers' expenditure shares, allowing for structural transformation. Migration frictions and other congestion forces counteract the agglomeration forces in the model.

The advantages of my framework are manifold. First, my general equilibrium approach considers the long–term adjustments of the economy along many dimensions as the climate changes. Second, the multi–sector feature of the model allows me to predict future sectoral expenditure shares in counterfactuals so that the results speak closely to the recent literature on urbanization and structural transformation in SSA. Third, my setup allows for the simulation of policy-relevant experiments, such as the adoption of modern inputs in agricultural production. Fourth, my quantification strategy requires only data on the distribution of the economic activity and population within countries, similar to Desmet et al. (2018). As such, it overcomes the main limitation in the migration literature, which is the need of observing within and cross-country bilateral migration flows.

In terms of empirics, I assemble a rich micro spatial (1°x1° degree) dataset on population, economic activity, transportation infrastructure, and agricultural production and suitability. The latter is a core element of this paper: climate change is modeled to impact the economy as a shock to the suitability for growing crops. In practice, I draw on the work of agronomists and climatologists from the GAEZ (IIASA and FAO, 2012) project, and use their estimates of crop-specific potential yields for several grain crops for recent, past, and future – under a climate change scenario – periods.[1] These potential yields are calculated based exclusively on natural characteristics (e.g. topographic and climatic), providing a measure of geographical natural advantages for each crop.[2] Importantly, as I focus on subsistence agriculture in

---

[1]To my knowledge, my paper is the first one to exploit the variation of the GAEZ estimates over time for past periods. Therefore, it contrasts with related research which uses the long–term averages (1960–1990) of the GAEZ estimates.

[2]Hereafter, I refer to the GAEZ potential yields as natural or fundamental productivities/advantages indistinctly.

FIGURE 2.1: FAO–GAEZ Agro-climatic yields of cassava in 2000 (left) and 2080 (right).
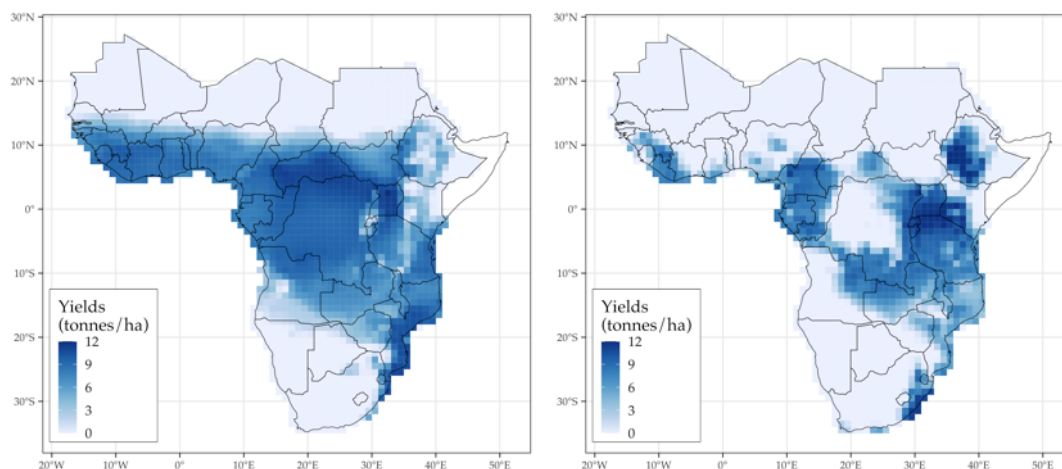
Notes: The two graphs above depict average potential yields of cassava, within 1°x1° grid cells, drawn from the GAEZ database for 2000 (left) and 2080 (right). The potential yields stand for the average production, in tonnes/hectares, that could be achieved in each cell (conditional on natural characteristics only). Somalia is not considered due to the unavailability of data from other sources. See Section 2.2 and Appendix B.2 for details.

SSA, I consider the main staple crops that are grown and consumed in the region: cassava, maize, millet, rice, sorghum, and wheat.[3]

A key insight obtained with the GAEZ forecasts is that agricultural suitability is not expected to change uniformly. Figure 2.1 illustrates this idea with the potential yields of cassava in SSA for 2000 and 2080. Several locations are expected to become much less productive as a consequence of climate change. Surprisingly perhaps, the opposite is expected for a handful of locations (e.g. in Ethiopia, Southern Kenya, and Northern Tanzania), contrasting with the idea of climate change as a negative–only shock to agriculture. The same pattern is observed for other crops, though differently in terms of spatial distribution. Therefore, the presented evidence suggests that the changes in the climate will be a heterogeneous shock to the spatial degree of comparative advantages within the agricultural sector.

The model is calibrated to fit the SSA economy in 2000. To do that, I first use the GAEZ yields for 2000 as the measure of the fundamental productivities in each agricultural sector (crops). Second, I use comprehensive

---

[3]These grain crops account for about 80% of the total production, in tonnes, of the main staple and cash crops (cassava, coffee, cotton, groundnut, maize, millet, palm oil, rice, sorghum, soybean, sugarcane, and wheat; see Table B.2) and for about 50% of the caloric intake in SSA (Porteous, 2019).

data on transportation infrastructure in SSA to build an optimal trade net–
work between all locations pairs of my empirical setup. The resulting bi–
lateral distances between location pairs are used to estimate trade frictions.
Third, I quantify the unobserved fundamentals and parameters: the sets of
fundamental productivities of the non–agricultural sector, location–specific
productivity shifters of all sectors, and amenities. This last step requires the
inversion of the spatial equilibrium so that the model achieves an exact fit
of the data in terms of GDP distribution, sectoral output, and population in
2000.

I validate my calibrated model with a backcasting exercise. In particular,
I simulate my calibrated model with crop suitabilities for 1975 and compare
its outcomes with observable data. The model achieves a very good fit when
predicting the grid cell–level changes in population between 2000 and 1975,
reassuring its capacity of providing similar numbers for future periods. As
an additional overidentification test, I find that the model identifies well the
degree of specialization in agriculture across countries.

My main counterfactual exercise consists of simulating a climate changed
SSA in 2080. I draw the estimates for agricultural productivities in 2080 for
that scenario[4,5] and simulate my model with these values, keeping all other
fundamentals unchanged. The results are striking: compared to a scenario
with no climate change, more than 300 million people could be displaced[6]
(about 12 percent of SSA's total population), and real GDP drops by about 4
percent. As previously mentioned, the results are very heterogeneous across
countries and locations.

Subsequently, I evaluate the mechanisms of the model at play by inves–
tigating the heterogeneity of my results. My findings suggest a decrease in
the non–agricultural employment, on aggregate, and heterogeneous changes
across countries. The median country experiences an increase in the non–
agricultural labor of 1 percent, and the 10th and 90th percentiles are -3 and

---

[4]The GAEZ estimates are available for different hypothetical scenarios for the future –
I pick the one that compares the closest to the standards, according to climatologists, for a
severe scenario: the Representative Concentration Pathway (RCP) 8.5 (see Appendix B.2.1).

[5]To account for the uncertainty around the estimates for the future climate, I test the
robustness of all results with respect to different climate models and/or RCP scenarios used
to generate the GAEZ data. That provides confidence intervals for the estimated results. See
Section 2.6.3 for details.

[6]Population displacement is defined as the difference between the model–implied pop–
ulation, at the grid–cell level, of two simulations: with and without climate change in 2080.
Grid–cells with positive (negative) values experience population inflows (outflows). See
Section 2.6.1 for a careful discussion.

5 percent, respectively. The mechanism driving this result is sectoral special-ization: while the most severely hit locations (and countries) specialize out of agriculture, the opposite takes place for the least hit locations. Indeed, the capacity of moving the production towards the non–agricultural sector mitigates the impacts of climate change in terms of population losses at the grid–cell level. Along the same lines, crop–switching and access to trade are likewise important. Among the locations severely hit by climate–change, those able to reshuffle their agricultural production mix, or better connected to markets, exhibit lower rates of population outflows.

Finally, I perform a policy experiment centered on technology adoption in agriculture. In particular, I simulate a climate changed SSA where farmers exogenously adopt more modern inputs in the production, such as animal traction, mechanization, usage of high yielding varieties, and fertilizers. In such a scenario, the estimated GDP losses of climate change are considerably reversed. However, population flows remain considerably large, mainly be-cause more productive inputs in agricultural production intensify the geo-graphical specialization between the non-/agricultural sectors.

This paper contributes to several strands of the economic literature. First, to a large set of reduced–form studies that establish a causal relationship between weather anomalies and migration,[7] especially in subsistence agri-cultural economies like SSA.[8] However, by mostly focusing on short term climate events for identification, this literature does not provide the means for assessing the resulting migration of the long–term changes entailed by climate change (Burzyński et al., 2019). I add to this literature by using a spa-tial general equilibrium approach to assess migration flows caused by the climate change shock to agriculture.

As such, I also contribute to the literature that investigates the relation-ship between population displacement and climate change with quantitative spatial models. Within this literature, Desmet et al. (2021) quantify the re-shaping of the world's economy and population upon coastal flooding with

---

[7]See Berlemann and Steinhardt (2017); Cattaneo et al. (2019) for the most recent surveys, and Baez et al. (2017); Gröger and Zylberberg (2016); Cai et al. (2016) for two examples of Latin America, Southeast Asia, and worldwide studies, respectively.

[8]The lack of technological adoption in SSA's agriculture is argued to be among the main causes of underdevelopment (Porteous, 2020; Sheahan and Barrett, 2017) and vulnerability with respect to weather shocks (FAO, 2015). Indeed, Barrios et al. (2006); Henderson et al. (2017) show that changes in the rainfall patterns during the past decades played a determi-nant – and causal – role in the high urbanization rates of SSA.

a one–sector spatial framework that embeds land losses in the spatial dynamics of the economy. Desmet and Rossi-Hansberg (2015); Conte et al. (2020); Nath (2020a) embed global warming into a spatial general equilibrium setup where temperature changes dynamically shape the evolution of sectoral productivities. Unlike these papers, I focus on the heterogeneous impact of climate change within the agricultural sector, allowing for within (switching crops) and across (agriculture–urban) sector adjustments. In my results, I show that the capacity for such an adaptation is a quantitatively relevant margin that mitigates the impact of the climate shock in terms of migration at the grid–cell level.

My paper is close to the work of Costinot et al. (2016a), who quantify future GDP losses due to climate change as a shock to agricultural suitability. I contribute to their work by allowing for labor mobility and quantifying the migration consequences of the climate shock in a spatial general equilibrium framework. As a consequence, my work also relates to Shayegh (2017); Burzyński et al. (2019, 2021), who study climate migration in an OLG model where migrations decisions respond to temperature and sea levels. My contribution is to explicitly model the geography of the economy and the impact of climate change throughout its locations, making migration (within and across countries) a key mechanism of the long–run structural adjustment of the economy to climate change.[9]

Importantly, my paper also adds to the current policy debate about potential climate migration. Policy circles have been stressing the concerns with climate refugees for several years (IPCC, 2007, 2012, 2018). More recently, several institutions have produced quantitative studies to guide policymakers in this matter. Worth noting are, among others, the World Banks' (Rigaud et al., 2018), and the Pulitzer Center's (Lustgarten, 2020) projects, which use the gravity–based spatial framework of Jones and O'Neill (2016) to estimate climate migrant flows. The closest result to the context of my paper is the estimate of about 100 million migrants by 2050 in SSA (Rigaud et al., 2018). I contribute to this debate by providing results with a richer quantitative

---

[9]Indirectly, I also add to a rich and growing modern spatial economics literature on developing contexts. A non–exhaustive list include Donaldson and Hornbeck (2016); Morten and Oliveira (2018); Donaldson (2018); Pellegrina and Sotelo (2021); Ducruet et al. (2021); Balboni (2019); Sotelo (2020) on the relevance of transportation infrastructure, Desmet et al. (2018) on the dynamic effects of the spatial diffusion of ideas, Nagy (2020); Allen and Donaldson (2020) on city location and historical dependence, Allen et al. (2019) on border walls, and Pellegrina (2020); Moneke (2020) on technology adoption.

framework. In particular, my model considers the interconnection of pro-
duction, trade, and residence decisions by agents within and across coun-
tries, accounts for the heterogeneity of the climate change shock within the
agricultural sector, and allows for the simulation of real–world policies.

Finally, I also contribute to the broader economics of climate change lit-
erature, based on the seminal work of William Nordhaus (1992, 2013, 2018,
2019). His DICE/ RICE integrated assessment model (IAM) became a stan-
dard tool to quantify the potential economic impacts of global warming by
endogenizing the global climate to economic activity. While not allowing
such relation,[10] my framework is capable of accounting for the economic con-
sequences of climate change as well as many other aspects not contemplated
in IAM studies, such as production, trade, and migration decisions.[11,12]

The remaining of the paper is organized as follows. Section 2.2 describes
the main sources of data used and Section 2.3 documents a number of empir-
ical facts that illustrate the potential impact of climate change on the agricul-
tural economy of SSA. Section 2.4 presents the theoretical framework. Sec-
tion 2.5 details how the model is brought to the data, and Section 2.6 the re-
sults of the climate change counterfactuals, policy experiments, and several
robustness checks. Section 2.7 concludes.

2.2 Data

This study builds upon several sources of geographical data. These are ag-
gregated at $1°\times1°$ degree grid cells (about 100 x 100 km at the equator), the
unit of observation for this study. The set of cells covering 42 countries of
SSA contains 2,032 cells. Below, I describe the collection and aggregation of
the main data sources; further details are documented in Appendix B.2.

GDP. I obtain data on GDP disaggregated in areas within countries from the
Global Gridded Geographically Based Economic Data v4 (G-Econ, Nordhaus
et al., 2006a). It consists of a dataset with *gross cell product*; i.e. gross product

---

[10]Africa contributes with about 3 percent of total CO_2 emissions as of 2015, which allows
me to assume climate change to be exogenous to economic activity in my framework.

[11]An exception is Benveniste et al. (2020a), who integrates cross–country migration within
an IAM.

[12]Other studies that exploit past weather changes to evaluate the economic impacts of
global warming are Burke et al. (2015); Burke and Emerick (2016); Dell et al. (2009, 2014);
Schlenker et al. (2005); Schlenker and Lobell (2010).

of grid cells of 1 square degree. The data spans from 1990 to 2005 in intervals of five years.

Population. Information on the distribution of the population is gathered from several sources. First, the G-Econ database provides the population count for the periods from 1990 to 2005. I complement it with gridded population of 1975 from the Global Human Settlement Project (GHSP, Florczyk et al., 2019). Finally, I collect projections for future population, at the country level, from United Nations and Social Affairs (2019) for the period of 2021 to 2100.

Agricultural suitability. I construct a time-varying, geographically disaggregated data set of crop–specific suitabilities from the Food and Agriculture Organization's Global Agro-Ecological Zones (GAEZ, IIASA and FAO, 2012) database. This data built with a state-of-the-art agronomic model that combines fine–grained data on geographic characteristics (e.g. soil, elevation, etc.) and yearly climatic conditions to produce several agricultural-related outputs disaggregated at the 5 arc-minutes (about 0.083 degrees) resolution from 1960 to 2000. Among these, I collect and aggregate estimates of agro-climatic potential yields for the 6 crops of interest for 1975 and 2000. These potential yields, measured in tonnes/hectares, refer to the yield that a certain cell would obtain if its surface was fully devoted to a specific crop. Moreover, the GAEZ database provides this data for a climate–changed world in 2080, which I also collect. The final data is a panel, at the cell-crop level, of agro-climatic yields for 1975, 2000, and 2080.

Agricultural production. Actual crop production is obtained from two sources of data. First, GAEZ provides actual values (tonnes) of production and harvested land (in hectares) for 2000. Moreover, FAOSTAT provides crop production, in current US$, at the country level for 2000–2010.

Transportation network. In order to build up a network connecting all grid cells of SSA, I first collect the African extract of the Global Roads Open Access Data Set (gROADS v1, CIESIN, 2013), which combines the best available public domain road data by country into a global roads coverage database. The date range for the road network representations is from the 1980s to 2010 depending on the country, as their data is gathered from different sources. In order to overcome potential missing roads in some particular country, and to capture links between locations not necessarily through roads, I explore the transportation friction surface from the Accessibility to Cities' project (Weiss

et al., 2018). This high–resolution surface (0.01 degrees resolution) provides the instantaneous cost of passing through a cell conditional on geographical features (e.g. type of terrain, steepness) as well as on infrastructure (whether the cell is on a road, railroad, river, etc.).

2.3 Motivating facts

This section documents two facts about the potential impacts of climate change in SSA. I show first that these effects are expected to be strong and heterogeneous. Second, I document that as such climate change could be determinant in the future organization of the SSA economy. Overall, they provide empirical support for my Ricardian approach when modelling how climate change could affect SSA.

Fact 1: Climate change is expected to bring substantial, and spatially heterogeneous, changes to agricultural suitability in SSA.

I use GAEZ estimates of agro-climatic potential yields for 2000 and 2080[13] to stress out how severe and heterogeneous the impact of climate change is expected to be. I define ΔA_i^k as the changes in the yields of crop k in location i between the two periods, and ΔA_i as the change in average crop yields in every location i.

Panel A of Figure 2.2 shows that the average climate change shock to agricultural yields is very heterogeneous. In terms of levels, several locations are estimated to become less suitable to agriculture, with average yields reducing by 50% or more. Impressively perhaps, a handfull of location are expected to become more suitable if compared to 2000, and the magnitude of such gains are likewise substantial. This finding goes against the general sense of climate change as a homogeneous negative shock to agriculture.

To illustrate how heterogeneous these effects are across crops, Panel B of Figure 2.2 documents the dispersion of the climate change effects at the location level (in standard deviations of A_i^k at the location i level). It can be observed that the changes in yields are not homogenous across crops so that the relative ranking of crop–suitabilities will be differently shifted. As

---

[13]The 2080 forecasts from GAEZ are calculated assuming a hypothetical scenario for the future evolution of the world climate. Appendix B.2.1 describes how I choose the scenario to draw my data from so that my numbers compare the closest possible to the standards from the climatologist community.

FIGURE 2.2: Expected impact of climate change to average crop yields (left) and standard deviation of crop–yield changes (right) in SSA between 2000 and 2080.

Panel A: Change in average suitability to agriculture.

Panel B: Standard deviation of changes in crop suitabilities at the location level.
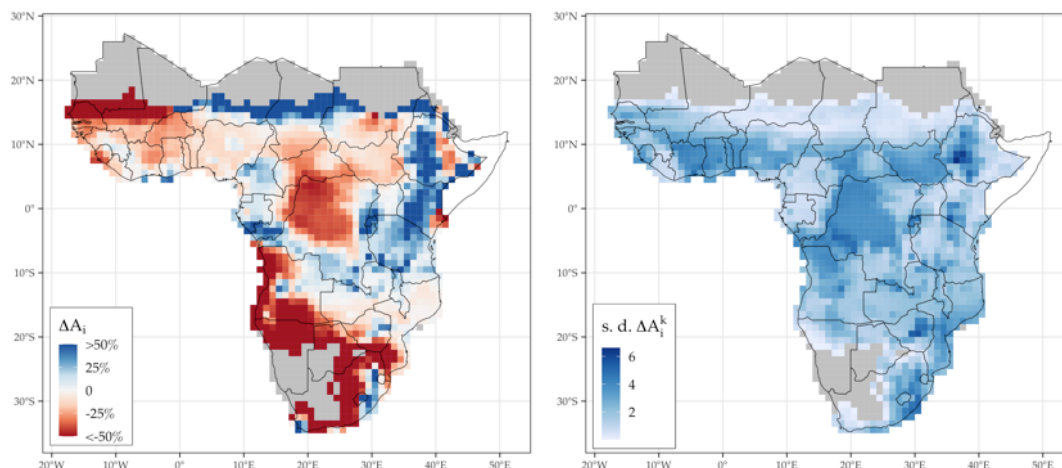
Notes: The potential yields stand for the production, in tonnes/hectares, attained within $1° \times 1°$ grid–cells conditional on natural characteristics. Panel A documents the estimated change (truncated for easiness of visualization) in average potential yields between 2000 and 2080. Panel B shows the standard deviation of the crop–level yield changes within locations. Grey areas stand for cells in with zero potential yields for all crops in both time periods. See Section 2.2 and Appendix B.2 for details.

such, climate change will consist of a shock to the geographical comparative advantage for each crop.

Therefore, several locations of SSA could potentially cope with the climate change shock in terms of agricultural loss by adjusting their crop choices. Alternatively, the economy could also reshuffle its factors to the non–agricultural sector. The degree of natural advantages on all sectors, interacted with market access, would determine the patterns of sector–specialization upon the climate change shock through comparative advantages.

The extent to which such Ricardian economic adjustments could take place in SSA depends on the strength of comparative advantages on shaping the agricultural production and trade in the continent. The next empirical fact provides evidence for such a mechanism holding in reality and emphasize the importance of embedding it into my theoretical framework.

Fact 2: Natural suitability to grow crops explains a large degree of crop-specialization and trade in SSA.

I next document how natural advantages for growing crops explain the spatial patterns of agricultural production and trade in SSA. To do that, I first

FIGURE 2.3: Comparative advantage and the organization of the SSA economy: relationship of crop yields with production and trade.

Panel A: Crop production (in tonnes).   *Panel B:* Bilateral crop trade (in US$).
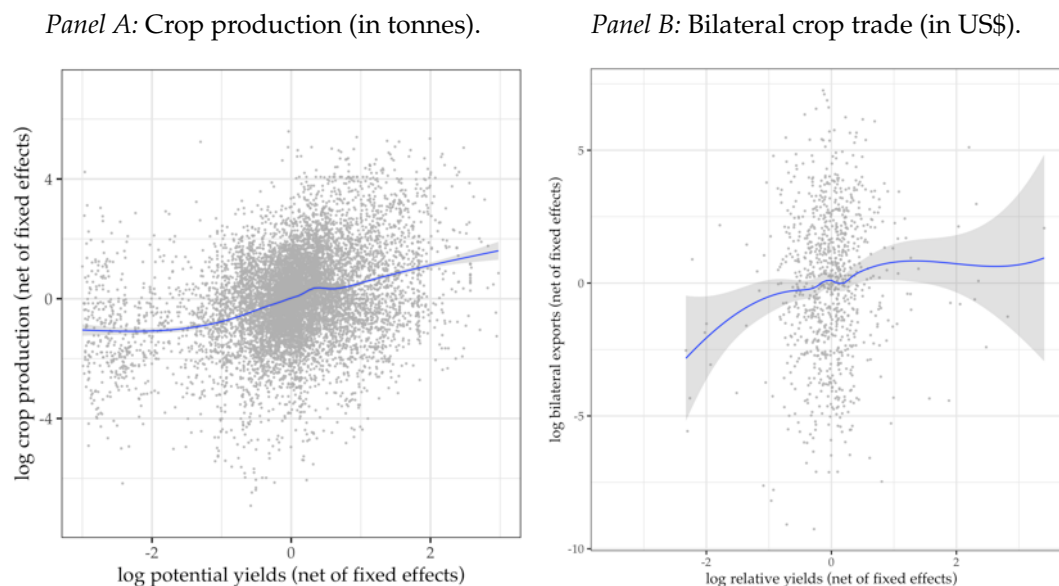
Notes: Panel A (B) plots the correlation between GAEZ potential yields and effective production (bilateral crop trade) at the location–crop (country–pair) level. The blue line stands for an estimated polynomial regression, and grey–shaded areas the 95% confidence bands. See Appendix B.4 for details.

match the yields data with effective production at the grid–cell level. Second, I average out the yields at the country level and match them with bilateral crop trade data from COMTRADE.[14]

Figure 2.3[15] how production and trade correlate with with the GAEZ yields. In particular, Panel A plots the crop production against the yields at the location–crop level. The raw data values are first net out of location and country–crop fixed effects, so that confounding factors at both levels are controlled for. There is a strong correlation between the natural advantages and effective production. Analogously, Panel B shows a strong correlation between bilateral crop exports and relative yields between countries. In this case, the raw data is net out of exporter, importer, and crop fixed effects, as well as of controls at the country–pair level. These two facts are statistical significant if estimated with fixed effects regressions (see Appendix B.4).

Overall, the data conveys a sound message: crop–specialization happens both across and within countries, and country trade flows reflect that. To generate this pattern, my general equilibrium model will take the perspective

---

[14]Refer to Appendix B.2.2 for details on the collection and aggregation of the trade data.

[15]Appendix B.4 provides the details of the econometric models that generate the graphs of Figure 2.3 and several robustness checks.

of subnational units that specialize in (and trade) crops based on comparative advantage.

2.4 Model

This section outlines a spatial model[16,17] that allows for a credible quantification of the general equilibrium impact of future climate change. The model provides a tractable framework to account for the role of several dimension of heterogeneity (fundamental productivities across many sectors, market access, factor productivities, among others) across geographical locations on the spatial distribution of the economic activity.

2.4.1 Environment

The economy is composed by N locations $i \in S = \{1, ..., N\}$ and populated by $\mathcal{L} = \sum_{i \in S} L_i$ workers who supply their labor inelastically. There are K sectors $k \in \mathcal{K} = \{1, ..., K\}$ in the economy: $K - 1$ agricultural sectors (crops) and a non-agricultural composite K sector. Locations (can) produce a locally differentiated variety of the goods of each of these sectors. Each location has a sector-specific fundamental productivity parameter $A_i^k \in \mathcal{A} = \{A_1^1, ..., A_N^K\}$ which drives the degree of comparative advantage between locations in each sector. Moreover, each location provides an amenity value $u_i \in \{u_i\}_{i \in S} \equiv \mathcal{U}$ for workers residing in it.

Goods and labor units are mobile in S, subject to frictions. As standard in the literature, $\mathcal{T} = \{\tau_{ij}\}_{i,j \in S}$ is the bilateral trade frictions' matrix; $\tau_{ij} = \tau_{ji} \geq 1$ stand for the amount of units of the good required to ship 1 unit from location i to j. Frictions in labor mobility are instead driven by an idiosyncratic taste shock to the choice of living in a certain location i. The dispersion of the distribution of these shocks drives the extent of frictions to labor mobility.

The *geography* of the economy is the set $\mathcal{G}(S) = \{\mathcal{L}, \mathcal{A}, \mathcal{U}, \mathcal{T}\}$: the spatial fundamentals that interact with the economic forces of the model and determine the distribution of the economic activity over S. In the following, I describe how the economic component is structured.

---

[16]Further details and derivations of the model are documented in the Appendix B.1.

[17]Appendix B.5 provides several extensions of the main model and discusses how their implementation would alter, qualitatively and quantitatively, the main predictions of the baseline framework.

Technology and Market Structure. In every location i, a representative firm produces goods of each sector k with labor as the unique input of the following linear production function

$$q_i^k = b_i^k A_i^k L_i^k, \tag{2.1}$$

where b_i^k stands for a location–sector efficiency parameter unrelated to the natural advantage of that location in producing goods of sector k (e.g. degree of technology adopted in the production). The output can be locally consumed or traded with other locations. Trade takes place in a perfectly competitive framework with full information, which implies no arbitrage in the trade between locations. Such market structure implies that the price of the sector k variety produced in i and shipped to (thus, consumed at) location j is

$$p_{ij}^k = (w_i / b_i^k A_i^k) \times \tau_{ij}, \tag{2.2}$$

where the first (second) subscript stands for the location of production (consumption/shipment). w_i stands for the wages in location i.

Preferences. Each location is populated by a continuum of heterogeneous workers. Their welfare is determined by a component related to the consumption of varieties and an amenity component. The latter is determined by their heterogeneous taste with respect to the location of living. Workers choose where to live and how much to consume so to maximize welfare; a v worker in location i has the following welfare function:[18]

$$W_i(v) = \left(\sum_{k \in \mathcal{K}} \left(C_i^k \right)^{\frac{\eta-1}{\eta}} \right)^{\frac{\eta}{\eta-1}} \times \varepsilon_i(v); \tag{2.3}$$

$\varepsilon_i(v)$ is the location taste shock the worker draws and $\eta > 1$ the elasticity of substitution between consumption of bundles of different sectors. C_i^k is the CES aggregate of the consumption of all varieties of goods from a sector k, defined as

$$C_i^k = \left(\sum_{j \in \mathcal{S}} \left(q_{ji}^k \right)^{\frac{\sigma-1}{\sigma}} \right)^{\frac{\sigma}{\sigma-1}}, \tag{2.4}$$

---

[18]I set preferences with a double-nested CES structure to allow for structural transformation. Differently from assuming preferences with a lower-tier CES and an upper-tier Cobb-Douglas aggregate, my set up allows for sector shares to be endogenous, rather than fixed and set by the Cobb-Douglas shares. Moreover, it provides an empirical advantage, as consumption shares do not need to be calibrated. Related literature usually does so with household consumption data, which might be unfeasible to obtain for all the countries my study is covering.

where q_{ji}^k is the per-capita quantity of the variety of sector k produced in j that is consumed in i and $\sigma > 1$ is the Armington CES.

Consumption choice. Each worker earns wage w_i, thus $\sum_{j \in S} \sum_{k \in \mathcal{K}} p_{ji}^k q_{ji}^k = w_i$ is the budget constraint for workers conditional on living in i. Welfare maximization with respect to consumption of varieties implies that the share of i's spending on j's variety of sector k is

$$\lambda_{ji}^k = \left(p_{ji}^k / P_i^k\right)^{1-\sigma}, \text{ where} \tag{2.5}$$

$$P_i^k = \left(\sum_{j \in S} \left(p_{ji}^k\right)^{1-\sigma}\right)^{\frac{1}{1-\sigma}} \tag{2.6}$$

is the Dixit-Stiglitz price index of sector k. An analogous result holds for the share of the expenditure on sector aggregates:

$$\mu_i^k = \left(P_i^k / P_i\right)^{1-\eta} \text{ and} \tag{2.7}$$

$$P_i = \left(\sum_{k \in \mathcal{K}} \left(P_i^k\right)^{1-\eta}\right)^{\frac{1}{1-\eta}} \tag{2.8}$$

are the share of location i's expenditure in goods from sector k and the overall price index in i, respectively. Thus, the equilibrium per capita demand for j variety of sector k goods in i is $q_{ji}^{k*} = \lambda_{ji}^k \mu_i^k w_i$. By inserting it in eq. (2.4), one finds that

$$\left(\sum_{k \in \mathcal{K}} \left(C_i^k\right)^{\frac{\eta-1}{\eta}}\right)^{\frac{\eta}{\eta-1}} = \frac{w_i}{P_i} \quad \forall i, \tag{2.9}$$

i.e. the per capita consumption in location i equals real wages. Moreover, the overall expenditure in i for goods produced in j, X_{ji}, is defined as

$$X_{ji} = \sum_{k \in \mathcal{K}} \lambda_{ji}^k \mu_i^k w_i L_i$$

$$= \sum_{k \in \mathcal{K}} (P_i^k / P_i)^{1-\eta} \left(\frac{w_j \tau_{ji}}{b_j^k A_j^k P_i^k}\right)^{1-\sigma} w_i L_i. \tag{2.10}$$

Bilateral expenditures take a gravity-like form: for a given sector k, it is decreasing with respect to marginal cost of shipping from j to i ($w_j \tau_{ji}/b_j^k A_j^k$). Besides, the (partial) elasticity of trade with respect to trade frictions τ_{ij} is driven by the CES parameter in the format of $1 - \sigma < 0$.

Location choice. Workers choose where to live so to maximize welfare. The

choice is subject to a location taste shock ε_j. Formally, a v worker chooses location j to solve

$$\max_j \quad W_j(v) = \frac{w_j}{P_j} \times \varepsilon_j(v). \tag{2.11}$$

Following Redding (2016), I assume that the taste shock is drawn independently (across workers and locations) from an extreme-value (Fréchet) distribution with shape parameter $\theta > 0$ and scale parameter $u_i L_i^{-\alpha}$. That is,

$$\varepsilon_i \sim G_i(z) = e^{-z^{-\theta} \times \left(u_i L_i^{-\alpha}\right)}. \tag{2.12}$$

The assumption above means that the workers' heterogeneity with respect to their location tastes (and the dispersion forces in the economy) is driven by the parameter θ. Higher values imply that agents are more homogeneous and that the economic components of welfare (real wages w_i/P_i) play a stronger role in the location decisions in Equation (2.11). In this case, there are weak dispersion forces in the economy. In contrast, lower values of θ imply more heterogeneous agents, who more likely draw higher values of taste shocks for every location. In this case, there are strong dispersion forces. The average of the preference draws are disciplined by $\left(u_i L_i^{-\alpha}\right)$; u_i stands for the fundamental amenity of location i and $\alpha > 0$ determines the extent to which population density diminishes the life quality in i.

The distributional assumption on the taste preference allows one to obtain closed-form solutions for the location choice of workers. As there is a continuum of workers in every location, the probability that a worker chooses to live in i is equivalent to the share of workers living in i in equilibrium. Following Eaton and Kortum (2002), one can show that the latter, defined as Π_i, is equivalent to

$$\Pi_i = \mathbb{P}\left(W_i(v) \geq \max\{W_j(v)\}_{j \neq i}\right) = \frac{(w_i/P_i)^\theta u_i L_i^{-\alpha}}{\sum_{j \in S} (w_j/P_j)^\theta u_j L_i^{-\alpha}}. \tag{2.13}$$

Therefore, the number of workers that will choose to live in i is

$$L_i = \Pi_i \times \mathcal{L}. \tag{2.14}$$

The result above is quite intuitive: locations with higher real wages (w_i/P_i) and/or life quality $\left(u_i L_i^{-\alpha}\right)$ will have, in equilibrium, a higher share of workers. The magnitude of it is partially driven by θ, which is the elasticity of the location choice with respect to real wages.

2.4.2 Spatial Equilibrium

Given the geography $\mathcal{G}(S)$ and the exogenous parameters $\{\theta, \eta, \sigma\}$, a spatial equilibrium is a vector of factor prices and labor allocations $\{w_i, L_i\}_{i \in S}$ such that eqs. (2.2), (2.6), (2.8), (2.10) and (2.14) hold, and markets for goods clear. Market clearing, formally, requires that total GDP in i equals total exports to *and* total imports from all locations $j \in S$, including itself, i.e.

$$w_i L_i = \sum_{j \in \mathcal{S}} X_{ij} = \sum_{j \in \mathcal{S}} X_{ji}. \tag{2.15}$$

This condition is equivalent trade balancing in all locations. Note that factor markets clearing is determined by eq. (2.14), as $\Sigma_i \Pi_i = 1$ in by construction. Moreover, by using eq. (2.10) on (2.15), one can characterize the spatial equilibrium with the system of $4 \times N$ equations and $4 \times N$ unkowns below:

$$w_i L_i = \sum_{j \in S} \sum_{k \in \mathcal{K}} (P_j^k / P_j)^{1-\eta} \left(\frac{w_i \tau_{ji}}{b_i^k A_i^k P_j^k} \right)^{1-\sigma} w_j L_j \qquad P_i^k = \left(\sum_{j \in S} (w_j \tau_{ji} / b_i^k A_j^k)^{1-\sigma} \right)^{\frac{1}{1-\sigma}}$$

$$(2.16) \hspace{5cm} (2.18)$$

$$L_i = \frac{(w_i / P_i)^\theta u_i L_i^{-\alpha}}{\sum_{j \in S} (w_j / P_j)^\theta u_j L_j^{-\alpha}} \mathcal{L} \qquad (2.17) \qquad P_i = \left(\sum_{k \in \mathcal{K}} \left(P_i^k \right)^{1-\eta} \right)^{\frac{1}{1-\eta}} \quad (2.19)$$

To solve this high-dimensional, non-linear system of equations, I apply an iterative algorithm whose intuition works as follows.[19] Given an initial guess for wages, I solve for prices and labor distribution. I then use the market clearing condition to solve for optimal wages conditional on its initial guess and the values calculated. I iterate this process until convergence.

Existence and Uniqueness. My model is not isomorphic to the general set up of Allen and Arkolakis (2014) and, as a consequence, the existence and uniqueness of the equilibrium cannot be guaranteed. The reason for that is the additional non-linearity introduced by the upper-level CES structure. I address that by solving my model for several parametric choices, starting from many different initial guesses. The equilibrium found is invariant across all cases.

---

[19] Appendix B.1.4 provides a detailed description of the algorithm.

2.4.3 Illustration of the spatial equilibrium

I illustrate how changes in the economy's fundamentals shape the distribution of the economic activity and population on the geography by representing it as a line with a discrete number of locations. I assume that locations are homogeneous with respect to amenity values ($u_i = u \; \forall i$) and sector productivities ($A_i^k = A^k \; \forall i, k$). Bilateral trade frictions are parametrized as

$$\tau_{ij} = e^{\tau \times |i-j|},$$

where $\tau = 0.05$. I set two sectors for the economy and assume that $A^2 > A^1$. I solve for equilibrium wages and labor allocations as described in Section 2.4.2; the distribution of L_i is plotted in Figure 2.4. In particular, Panel A shows that more central locations are those where most of the labor – thus economic activity – is allocated. The reason is that they are the most evenly distant from all other locations in the economy. Thus, shipping prices in these locations are lower due to the lower trade costs accrued in the trade with the other locations. There is more labor allocated to the second (more productive) sector; however, the economy also produces goods for the first sector as the love for varieties' feature of the CES demand creates demand for it.

Panel B describes how the spatial equilibrium changes by altering the geography of the economy. In particular, it shows the equilibrium allocation of workers when the right (left)-most locations as the most productive in the first (second) sector. The equilibrium allocation becomes skewed accordingly, showing that the model implicitly determines that the most productive regions are those in which the economic activity is going to be agglomerated in each sector.

2.5 Calibration and goodness of fit

I calibrate my model to match SSA in the year of 2000. To do so, I use a mix of calibration and parametrization methods to map the model above to observable features of the SSA economy. The goal is to calibrate the exogenous parameters $\{\sigma, \eta, \theta, \{b_i^k\}_{i,k}\}$ and the geography fundamentals $\{\mathcal{L}, \mathcal{A}, \mathcal{U}, \mathcal{T}\}$. Table 2.1 summarises the methods and sources used and Appendix B.1.5 the numerical algorithms used.

FIGURE 2.4: Equilibrium values for $\{L_i, L_i^1, L_i^2\}_{i \in S}$ in the spatial model represented on a line.
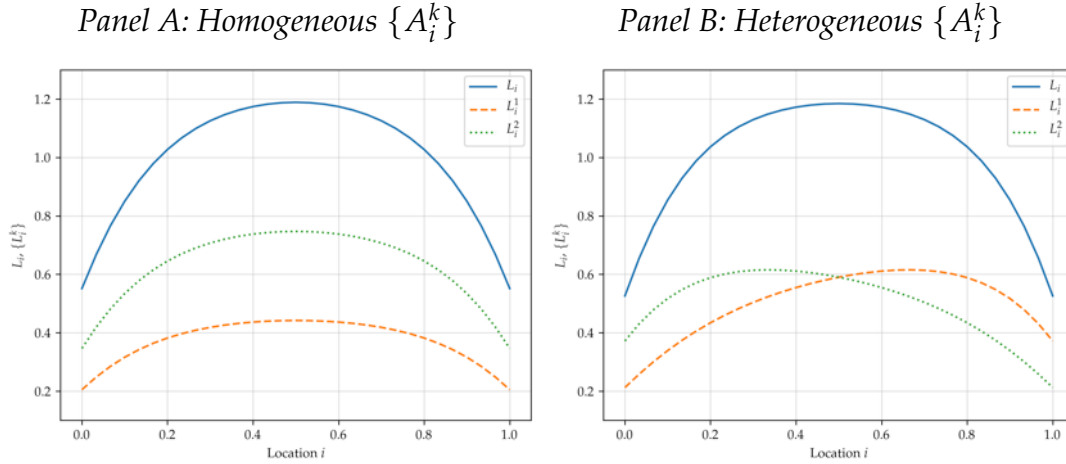
Panel A: Homogeneous $\{A_i^k\}$ *Panel B: Heterogeneous $\{A_i^k\}$*

Notes: Equilibrium labor allocations for a simplified version of the model as described in Section 2.4.3. Panel A describes the allocation of workers (total and sector specific) if sector productivities do not change across locations ($A_i^1 = A^1 < A^2 = A_i^2 \ \forall i$). Panel B plots how the sector specific labor demands change if the right (left) most locations are the most productive ones in the first (second) sector.

2.5.1 CES and Frèchet dispersion

The exogenous parameters $\{\sigma, \eta, \theta\}$ are drawn from related literature. The lower-tier CES is set as $\sigma = 5.4$ following Costinot et al. (2016a), who estimate it with similar data of mine at the same period, and for a geographical area comprising many SSA countries. The upper-tier CES is drawn from Sotelo (2020), i.e. $\eta = 2.5$. This value is estimated for the 1990's Peru, which is not a far-fetched approximation of the SSA economy in 2000. Finally, I set $\theta = 3.4$ following Monte et al. (2018) (the estimates for long term elasticities in development economies range between 2 and 4; see Morten and Oliveira (2018) for a discussion).

2.5.2 Transportation network and trade costs

Trade frictions between locations are assumed to be proportional to the travel distance that separates them. In particular, I follow related research in the literature (e.g. Pellegrina and Sotelo, 2021; Donaldson, 2018, among others) by assuming that the trade costs of shipping goods from i to j take the following parametric format:

$$\tau_{ij} = \text{distance}(i,j)^\delta \times \tau_{ij}^F, \tag{2.20}$$

where $\text{distance}(i,j)$ stands for the bilateral shortest distance between two

TABLE 2.1: Fundamentals, parameters, estimation methods and sources from the literature

Parameters	Description	Method	Reference
$\eta = 2.5$	Upper-tier CES	Literature	Sotelo (2020)
$\sigma = 5.4$	Lower-tier CES	Literature	Costinot et al. (2016a)
$\alpha = 0.32$	Congestion to pop. density	Literature	Desmet et al. (2018)
$\theta = 3.4$	Workers (inv.) heterogeneity	Literature	Monte et al. (2018), Morten and Oliveira (2018)

Parameters	Subset	Description	Data source / Moment matched
$\mathcal{L}$	–	SSA's population endowment	Population data
$\{b_i^k\}_{i \in S}$	–	Sectoral shifters	Matched to location–sector production data in US\$
$\mathcal{A}$	$\{A_i^k\}_{i \in S, k \neq K}$	Agricultural produc–tivities	GAEZ data
	$\{A_i^K\}_{i \in S}$	Non–agricultural pro–ductivities	Matched to GDP data in US\$
$\mathcal{U}$	–	Amenities	Matched to population data
$\mathcal{T}$	dist(i,j)	Bilateral travel distance	Transportation data
	$\delta = 0.3$	Distance elasticity of τ	Moneke (2020)
	$\tau_{ij}^F = 1.15$	Trade friction to foreign markets	Baum-Snow et al. (2020)

locations and $\tau_{ij}^F > 1$ for an additional trade friction in case the location pair refers to places in different countries (i.e. $\tau_{ij}^F = 1$ if i, j belong to the same country). To calculate the bilateral distances between all location pairs, I proceed as follows. I overlay the roads' network data from gROADS onto the Accessibility to Cities' friction surface and set the pixels over the roads' data to be "cheapest" ones to be passed through.[20] I then use a pathfinding algorithm to calculate the shortest routes and respective distances between all neighboring cells.[21] With these distances in hand, I use the Dijkstra algorithm to calculate the shortest distance between all location pairs. The final step involves using these distances to build $\mathcal{T}$ following eq. (2.20): I set $\delta = 0.3$

---

[20]The advantage of my "two-input" strategy is that it provides additional information for my pathfinding algorithm when looking for the route between two coordinates that are not over a road. In such a case, the path would "go" to a road through an optimal route (i.e. considering the local geography) and then "move" over the road. This approach provides a more realistic outcome than if assuming a linear path to the closest road.

[21]The coordinates of each cell are obtained from the longitude and latitude of the most populated settlement/city in each cell. See Appendix B.2 for more details and fig. B.6 for the results.

FIGURE 2.5: Estimated trade network for SSA – Western and Eastern Africa.
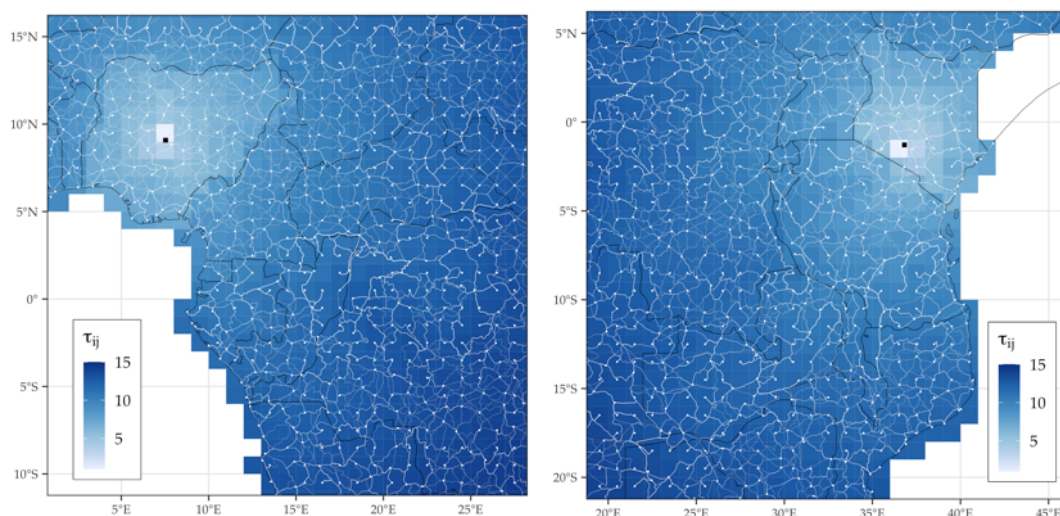
Notes: Estimated trade network for Western (left) and Eastern (right) Africa. The network is built by finding the shortest path between all neighboring cells over the road infrastructure with an optimal path algorithm. τ_{ij} stands for the estimated iceberg trade costs with respect to the capitals (black dots) of Nigeria (left) and Kenya (right). See Section 2.5.2 for details.

following Moneke (2020), and $\tau_{ij}^F = 1.15$ following Baum-Snow et al. (2020). The result of it is a 2,032 x 2,032 matrix of trade costs; Figure 2.5 illustrates a subsample of this matrix. It can be seen that the trade network is very complex and reflects well the existing transportation infrastructure within and across countries. Moreover, it shows that further and/or foreign locations are those whose trade with is subject to a higher degree of frictions.

2.5.3 Fundamental productivities and sectoral shifters

I build the set of natural advantages and efficiency productivity parameters by partially drawing it from observable data; the remaining parameters are obtained with a calibration technique. In particular, I use the agro-climatic yields from GAEZ as the fundamental productivities of the agricultural sectors, i.e. $\{A_i^k\}_{i \in S, k \neq K}$.[22] The rationale for using the GAEZ estimates is that they measure the potential yield a certain location would obtain should its area be fully employed to grow a certain crop. Therefore, as the yield variation across location-crops are driven by each location's natural characteristics (such as soil and climate), it provides a reasonable measure for the parameters I am interested in.

---

[22]To be consistent with the SSA context, I draw the agro–climate potential yields calculated for rainfed agriculture with low usage of modern inputs; see Appendix B.2.1 for details.

The remaining elements to be quantified is the set of non–crop productivities $\{A_i^K\}_{i \in S}$, as well as the sectoral shifters $\{b_i^k\}_{i,k}$. I back them out with a standard inversion of my model conditional on observed endogenous variables in 2000: I solve for $\{\{b_i^k\}_k, A_i^K\}_{i \in S}$ that makes the model to simultaneously match GDP and sectoral production, in US\$, in all locations. This step is done by inverting the spatial equilibrium with numerical methods, carefully explained in Appendix B.1.5. Importantly, since I am not able to separately identify b_i^K from A_i^K, what I estimate is their product, which suffices for simulating the model.

2.5.4 Fundamental amenities

With these fundamentals and parameters in hand, I can solve for prices in the economy (eqs. (2.18) and (2.19)) and then solve for $\{u_i\}_{i \in S}$ by matching the model-implied population with the observed one from the data. In practice, I take advantage of the fact that my identification of the fundamentals holds up to scale and invert Equation (2.17) to obtain a closed–form solution for $\{u_i\}_{i \in S}$ as follows:

$$L_i = \frac{(w_i/P_i)^\theta u_i L_i^{-\alpha}}{\sum\limits_{j \in S} (w_j/P_j)^\theta u_j L_j^{-\alpha}} \mathcal{L} \propto (w_i/P_i)^\theta u_i L_i^{-\alpha} \quad \rightarrow \quad u_i \propto \frac{L_i^{1+\alpha}}{(w_i/P_i)^\theta} \qquad (2.21)$$

2.5.5 Discussion of the inversion results

Figure 2.6 documents the results of the model inversion. First, wealthier locations are estimated to be particularly more productive in the non–agricultural sector. Moreover, densely populated locations with low income are estimated to have a higher value of amenities. Importantly, the amenities I back out could also be capturing cultural or institutional characteristics that trap individuals in some locations, like country borders to migration.

DR Congo and Ethiopia illustrate this feature. Being densely populated (but among the poorest countries in SSA) is rationalized by the model as a consequence of high amenities. However, it is also possible that barriers to entering nearby countries could be keeping individuals in those countries and not allowing them to move to somewhere else. Therefore, the amenities I back out must be interpreted as a combination of the fundamental amenities and these other aspects, which will be held constant in my counterfactuals.

FIGURE 2.6: Comparison between the results of the model inversion and observed endogenous variables.
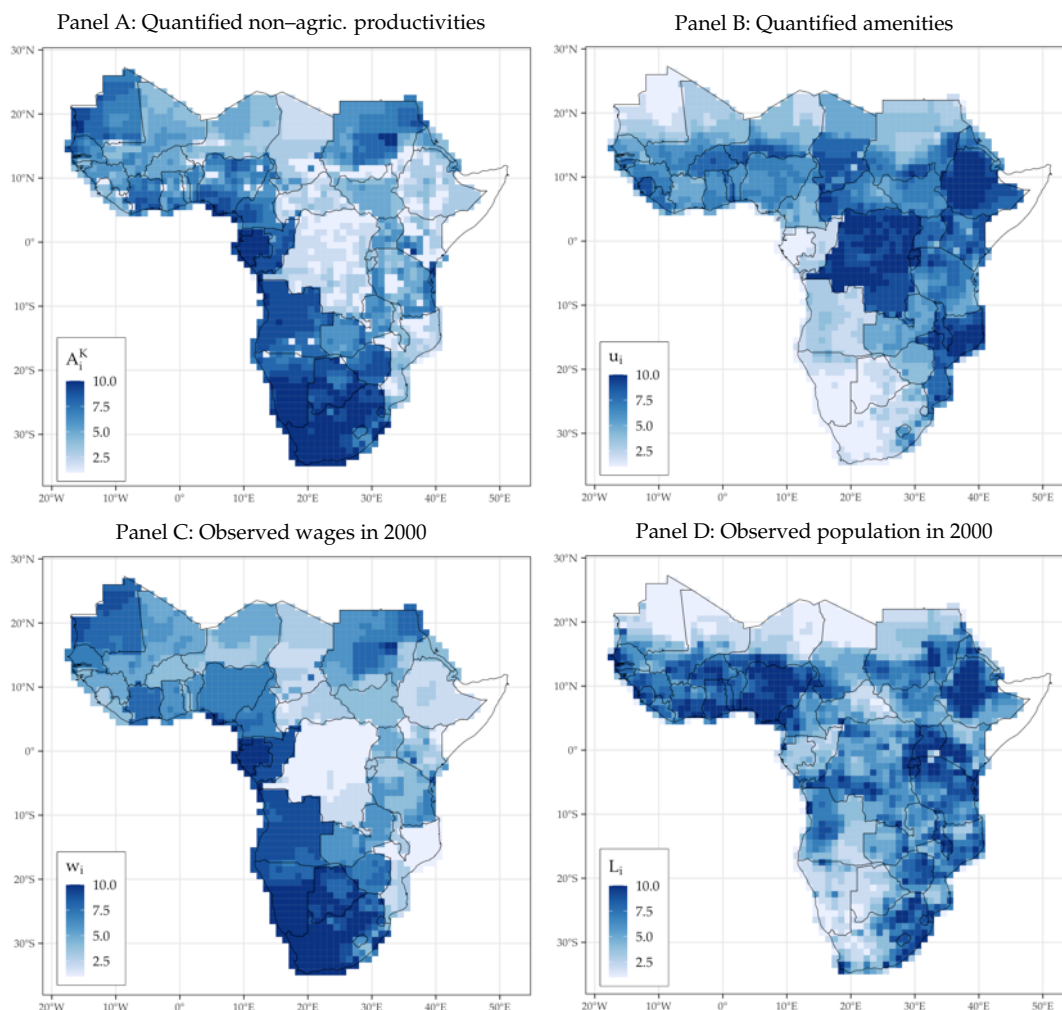
Panel A: Quantified non–agric. productivities   Panel B: Quantified amenities

Panel C: Observed wages in 2000   Panel D: Observed population in 2000

Notes: All results are shown in deciles, where 1 (10) stands for the bottom (top) decile of each sample. Each panel documents, respectively, the spatial distribution of the quantified non–agricultural productivities, quantified amenities, observed nominal wages and observed population.

In Appendix B.5.1, I provide an extension of the current model that separates amenities from migration borders. By quantifying them using country migration data, the distribution of the resulting amenities becomes much more sparse (see Figure B.9). The most amene locations cease to be the poorest ones, as the model rationalizes that individuals in those locations can be somehow trapped.

2.5.6 Model fit

Equipped with the calibrated model, I am able to test its capacity to replicate observed moments. I start with a backcasting exercise: I simulate the

FIGURE 2.7: Model goodness of fit with backcasting: population distribution in 1975.
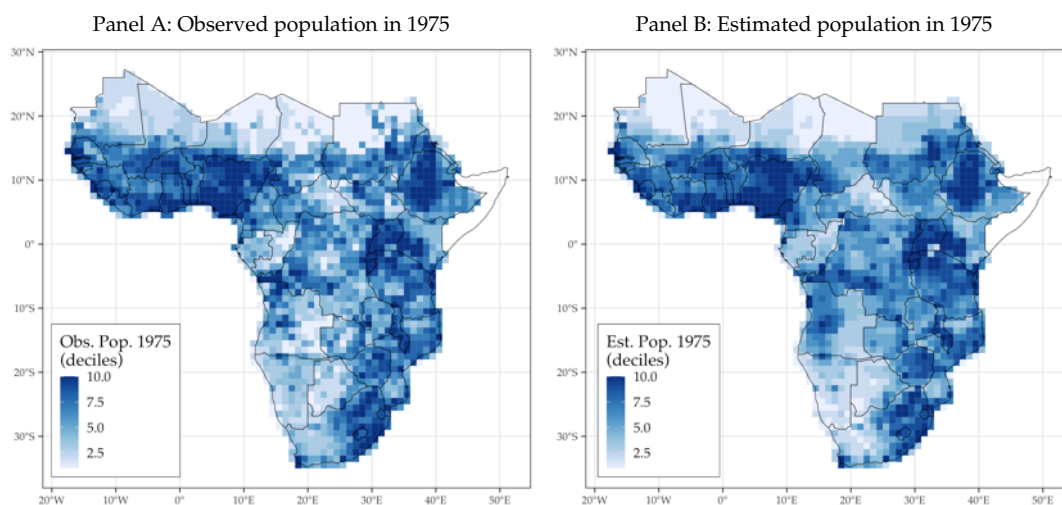
Notes: Panels A and B show the observed (from GHSP dataset) and model–implied population distribution in SSA for 1975, respectively. The values are shown in deciles; 1 (10) stands for the bottom (top) decile of each sample.

model after replacing the agricultural productivities and population endowments with their estimates for 1975. The result allows me to check whether my model replicates well the population distribution in SSA for that period. In addition to that, I check how well the model predicts the population displacement (differences) between 2000 and 1975 with respect to the observed values from the data, obtained from GHSP dataset.[23]

Figure 2.7 reports the results – the model is able to replicate closely the overall distribution of the population of 1975 within and across countries. Moreover, Panel A of Figure 2.8 documents the changes in the population counts between 1975 and 2000 are very well explained by the model (slope/R^2 of an OLS regression of 0.83/0.92).

Importantly, the only change used in this exercise is on the agricultural suitabilities between the two periods. According to the GAEZ estimates, between 2000 and 1975 there have been already a substantial degree of changes in agricultural suitability – about 75% of the locations of my empirical setup experienced a decrease in average crop yields. Therefore, the fact that such changes can explain well the changes in population between periods in my model reassures its capacity of providing reliable numbers for the future.

---

[23] As the data source for the population in 1975 (GHSP) comes from a different source than the data used in the calibration (G–Econ), I check their compatibility with the correlation of population in 2000 (available in both datasets) at the grid–cell and country level; see fig. B.3.

FIGURE 2.8: Model goodness of fit: backcasting results for differences in population and labor shares in agriculture for 2000.
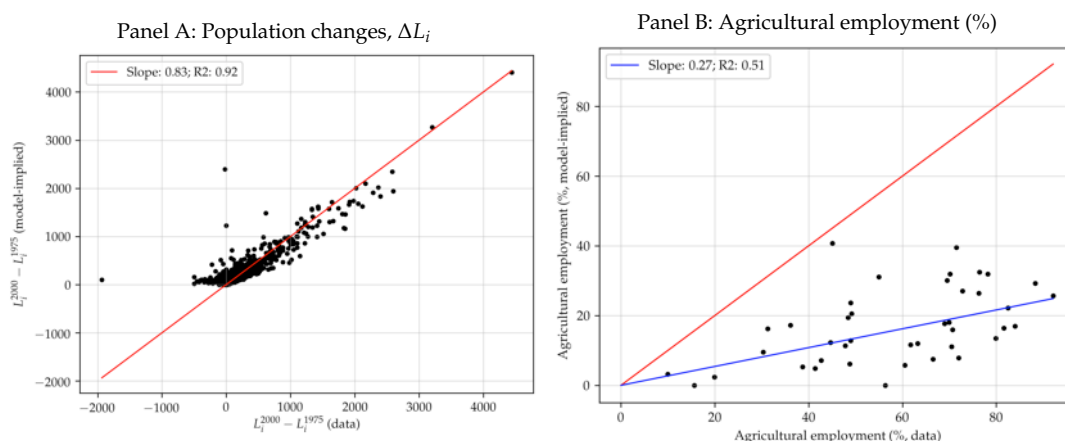
Notes: Panel A and B document the fit (observed versus model–implied) of the model for the changes in population (in thousands) between then and 2000, and 1975 and the country–level labor shares, respectively.

As an additional overidentification test, I check the model's capacity to replicate sectoral employment shares. I focus on comparing the model implied agricultural shares (i.e. all crops) at the country level. I gather the agricultural share of employment in 2000 from the World Bank and compare with the shares generated by the model; Panel B of Figure 2.8 displays the results. The model does a good job when identifying the rank of countries with respect to agricultural employment shares, though underestimating their levels. On aggregate, the model predicts 20% of employment in agriculture compared to 58% in the data. This discrepency can be explained by the fact that I am only modeling a small fraction of the value generated by agricultural production.

2.6 Climate Change and Migration: The 2080 Forecast

I use my calibrated model to quantify potential climate migration with a series of counterfactual exercises. The benchmark counterfactual consists of solving for the spatial distribution of the economic activity and population in 2080 after replacing the natural agricultural productivities with their estimates for 2080. The goal of this exercise is to quantify population reallocation with respect to a counterfactual SSA in 2080 in the absence of climate change.

Subsequently, I explore in detail the role that urbanization, crop–switching,

and trade have in the resulting outcomes, and then perform a number of policy experiments to understand how technology adoption in agriculture may alter the estimated impact of climate change. I end by checking the robustness of my results to the degree of frictions in the economy, as well as to the climate model and climate change scenario underlying the data GAEZ data.

2.6.1 Benchmark counterfactual

I solve my model using the estimates of total population and natural agricultural productivities for 2080,[24] obtaining the spatial distribution of the economic activity and of the population. As forecasts point towards large population increases for 2080, a simple comparison with 2000's population in levels yields increases nearly everywhere. To address that, my metric for population displacement measures how the counterfactual population for 2080, L_i, compares with the model–implied distribution for 2080 without climate change, $\tilde{L}_i$. I define this metric ΔL_i, formally calculated in percentual changes as follows:

$$\Delta L_i = \left(L_i / \tilde{L}_i\right) - 1 \tag{2.22}$$

The results is shown graphically in Panel A of Figure 2.9. The first striking fact is the large number of locations – about 80% – whose population in 2080 are expected to be lower vis–à–vis a hypothetical scenario with no climate change. There is a large degree of heterogeneity, both within and across countries and locations. The median of the location–level population change is -9.3 percent, and the bottom and top deciles are -28 and 3 percent, respectively. Analogously, the median country experiences a -12 percent change in population, and the bottom and top deciles are of -22 and 8 percent change, respectively.

A comparison with Figure 2.3 (motivating fact 1) reveals a strong relationship between the intensity of climate change effects on productivities and the population movements. The fact that some locations, highly spatially clustered in Eastern Africa, are expected to become relatively more suitable to grow certain crops translates into higher specialization into agriculture inside my model. Such a pattern allows the SSA to adjust to climate

---

[24]When drawing the data for future periods, I choose the scenario that compares the closest to Representative Concentration Pathway (RCP) 8.5, a standard in the climatologist literature for a severe future (see Appendix B.2.1). I check the robustness of my results to less severe scenarios in Section 2.6.3.

FIGURE 2.9: Results of simulations of the SSA economy in a climate changed world in 2080.

Panel A: Population changes   Panel B: Changes in non-crop employment
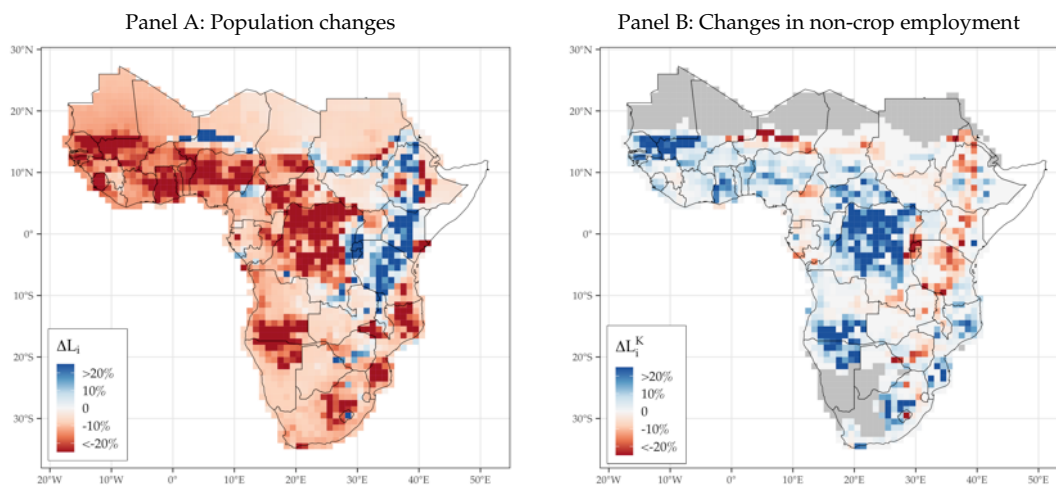
Notes: Results of counterfactual simulations for 2080 using agricultural productivity for 2080 estimated by GAEZ under a climate change scenario. Panels A shows the changes in the cells' population compared to a scenario had the population distribution remained the same as in 2000. Panel B documents the difference between the within country population shares of the two scenarios.

change such that the overall supply of grain crops is not substantially affected, which would not be the case should climate change entail only productivity losses.[25]

Indeed, in terms of structural transformation, the aggregate employment share in the agricultural sector increases by 6 percentual points. This effect is very heterogeneous within and across countries, as shown in Panel B of Figure 2.9. Some countries (e.g. Ethiopia, Kenya, or Tanzania) go through an uneven process of sector–specialization, where some locations specialize more in agriculture and others in the non–agricultural sector. Other countries instead specialize more homogeneously. As a result, at the country level, the median change in non–agricultural employment increases by 1 percent, and the bottom and top deciles changes are of -2.8 and 5 percent, respectively. [26]

Importantly, the results do not imply that all agricultural production would take place in Eastern Africa only. Indeed, it remains substantially spread out throughout SSA, and the most populated countries produce the highest bulk of grain production; see Figure B.4. Moreover, by comparing the least and most hit locations in terms of population loss, I find that they do not

---

[25]Indeed, if simulating a climate change scenario with suitability losses only, the magnitudes of the population displacements and agricultural production changes both decrease.

[26]Appendix B.5.2 provides an extension of the current model with frictions to sectoral switching (e.g. from crops to the non–agricultural sectors), which would discipline the intensity of the sectoral specialization across space observed in the benchmark results.

systematically differ in terms of fundamentals such as non–agricultural productivities, amenities, and market access. Such a fact, shown in Figure B.5, is very important to reject the hypothesis that the fundamentals that remain unchanged in my counterfactuals are the drivers of my results. Instead, a complex combination of several economic mechanisms and the climate change shock drives the population displacements, which I show next.

Heterogeneity of the results. I investigate how the economic mechanisms of my model interact with the estimated population displacements with a heterogeneity study. In particular, I focus on the locations expected to experience an outflow of people and investigate how, in the intensive margin, being able to urbanize, switch crops, and trade with other locations alters the observed climate change–migration relationship.

In order to do that, I estimate the relationship of several data moments and counterfactual outputs with a set of regressions. I begin with urbanization: I standardize the climate change–shock metric ΔA_i[27] and the estimated fundamental productivity in the non–agricultural sector, A_i^K, and use it to estimate the following regression:

$$\Delta L_i = \beta \times \Delta A_i \times A_i^K + \beta_1 \Delta A_i + \beta_2 A_i^K + \varepsilon_i, \qquad (2.23)$$

where ΔL_i stands for the estimated population displacement in cell i in percentual terms. Standard errors are clustered at the country level. The coefficient of interest, β, estimates how much ΔL_i, in a location where the climate change shock is one standard deviation large, changes if being one standard deviation more productive in the non–agricultural sector. Therefore, it is informative of the role that the advantages in the non–agricultural sector have on the adjustment of the severely hit locations in terms of population changes.

The results are documented in Table 2.2, column 1. It shows that, on average, a large urban sector protects against the migration effects of climate change. This is shown by the point estimate of β: conditional on suffering a climate change shock one standard deviation high, being one standard deviation more productive on the urban sector decreases the outflow of people

[27]The measure ΔA_i stands for the changes in the average potential yields due to climate change in cell i; see Section 2.3 for details. However, to make the econometric interpretations more intuitive in this application, I calculate it in losses, such that positive values stand for an estimated decrease in the average suitability between 2000 and 2080.

TABLE 2.2: Population displacement induced by climate change: sensitivity to advantages in the non–agricultural sector, crop switching and market access.

	(1)	(2)	(3)
CΔ Impact	−8.547***	−6.913***	−7.889***
	(0.948)	(1.233)	(1.260)
Non–agric. productivity	1.921**		
	(0.870)		
CΔ Impact × non–agric. productivity	2.638***		
	(0.929)		
Switch crops		6.412***	
		(1.414)	
CΔ Impact × switch crops		3.645*	
		(2.062)	
Market access			−0.574
			(0.453)
CΔ Impact × market access			1.136***
			(0.378)
Observations	1,784	1,784	1,784
R^2	0.315	0.265	0.244

Notes: The dependent variable in all specification are the estimated population outflows, in percentual points, as of Equation (2.22). Urban productivity stands for the estimated fundamental productivity in the non–agricultural sector, in standard deviations. Switch crops stands for a dummy for switching the main crop of the production portfolio in 2080 vis–à–vis the production mix of 2000. Market access refers to a standard measure of market access in standard deviations. Standard errors are clustered at the country level; *p<0.1; **p<0.05; ***p<0.01.

by 2.6 percentual points, one average. That stands for about one–fifth of the median estimated displacement of people in percentual points.

Next, I show that the ability to switch crops very strongly protects against climate change. To do that, I identify in the counterfactual results the locations that switch the main crop produced if compared to the 2000's portfolio. I replace that for A_i^K, as a dummy, in Equation (2.23), so that β has an analogous interpretation but with respect to effectively changing the production mix as a consequence of climate change. The results, shown in column 2 of Table 2.2, provide qualitatively similar results: by switching crops, locations hit by climate change have population outflows 3.6 percentual points lower.

To conclude, I focus on the role of acces to trade, and find that it is an insufficient insurance against climate change. To show that, I calculate the degree of market access of every location in 2000, using a standard measure from the trade literature (Donaldson and Hornbeck, 2016; Pellegrina, 2020),

and replace it in Equation (2.23) as before. Therefore, the coefficient of interest measures the average change in the population displacement in a location hit by climate change but with access to markets one standard deviation higher, which is estimated to be of about 1.2 percentage points (column 3).

Overall, these three exercises provide a sound message: the capacity of urbanizing, switching crops, or trading plays an important shock coping role among the locations severely hit by climate change. Therefore, they emphasize the importance of accounting for these mechanisms when understanding potential climate migration, and the limitation of quantitative frameworks that do not do so. Another novel feature of my framework is the feasibility of policy experiments, which I perform next.

2.6.2   Policy experiment – technology adoption in agriculture

An issue on which the policy debate and academic research center is the low level of modern input usage in agriculture in low–income countries.[28] I explore the most of the GAEZ database to investigate how my results, in terms of population displacement and aggregates, change should the degree of technological inputs used in agriculture increase during the next decades.

As the benchmark simulation resorts to the GAEZ data that assumes production at the lower technological frontier (subsistence level), I perform two additional experiments using the 2080' crop suitabilities that assume the usage of intermediate and high modern inputs in production.[29] Moreover, to isolate the effects of climate change under these two scenarios, I also simulate the SSA economy by 2080 in the absence of climate change but with these higher degrees of technology. Therefore, I can estimate the climate change effects on two hypothetical worlds – with and without modern inputs in agriculture.

---

[28]See Osborne (2005); Restuccia et al. (2008); Sheahan and Barrett (2017), or Dethier and Effenberger (2011); Brenton et al. (2014); FAO (2015) for related policy studies.

[29]The subsistence level assumes that production is based on the use of traditional cultivars, labor intensive techniques, and no application of nutrients, no use of chemicals for pest and disease control. The intermediate level assumes that production is based on improved varieties, on manual labor with hand tools and/or animal traction and some mechanization, and uses some fertilizer application and chemical pest, disease and weed control. The high technological level assumes production at the technological frontier, i.e. a farming system that is mainly market oriented and commercial production is a management objective. Production is based on improved high yielding varieties, is fully mechanized with low labor intensity and uses optimum applications of nutrients and chemical pest, disease and weed control.

TABLE 2.3: Aggregate and disaggregated results of the policy experiments with respect to technology adoption.

	(1)	(2)	(3)
	Benchmark results	Intermediate technology	High technology
Panel A: Aggregate results			
Population displaced	11.84%	22.16%	28.15%
Real GDP Change	-4.24%	1.77%	13.32%
Change in non–agric. employment	-6.43%	-8.8%	-9.69%
Panel B: Country–level results			
Pop. displaced, bottom decile	-21.81%	-44.26%	-56.28%
Pop. displaced, median	-11.53%	-23.15%	-30.33%
Pop. displaced, top decile	7.93%	18.59%	16.19%
Real GDP change, bottom decile	-17.8%	-46.56%	-60.07%
Real GDP change, median	-9.47%	-20.8%	-26.33%
Real GDP change, top decile	11.39%	40.51%	40.32%
Panel C: Cell–level results			
Pop. displaced, bottom decile	-28.45%	-45.36%	-53.82%
Pop. displaced, median	-9.38%	-19.3%	-25.24%
Pop. displaced, top decile	2.99%	1.02%	-2.14%
Real GDP change, bottom decile	-34.23%	-52.23%	-60.72%
Real GDP change, median	-8.69%	-17.91%	-23.32%
Real GDP change, top decile	9.06%	12.12%	11.43%

Notes: Panel A documents the aggregate results, in terms of population displacement, real GDP change, and changes in the non–agricultural labor shares, of the benchmark counterfactual (column 1) and of the policy experiments related to technology adoption in agriculture (columns 2 to 3). Panel B provides moments of the country–level changes of each of these simulations, and Panel C of the grid cell–level changes.

The results are documented in Table 2.3. Compared to the climate change effects in a low–input SSA (benchmark results, column 1), the usage of intermediate or high inputs reverse considerably the negative baseline setbacks. In particular, the real GDP losses are fully compensated in the intermediate case, and even become gains in the extreme scenario in which the entire SSA adopts high technology in agriculture in all sectors. While perhaps counterintuitive at first glance, such a result is driven by specialization. As shown in Figure 2.2, one of the results of climate change is that the more suitable locations for agriculture are more spatially clustered (especially in Eastern Africa). Therefore, the economy benefits of agglomerating the production around these locations (as average marginal production costs decrease). Indeed, SSA specializes even more in agriculture if adopting higher degrees of technology, which is seen in the changes in the labor shares and the amount of population displaced.

2.6.3 Robustness checks

I conclude my study with a sequence of robustness checks. I first focus on the sensitivity of my results, in terms of climate migrant flows and other aggregates, to the trade frictions and the heterogeneity of workers' location preferences (driven by the δ and θ parameters, respectively). I check how my outcomes change if increasing/decreasing these by 10%. However, to properly isolate the climate change effects under each scenario, I proceed as in Section 2.6.2 by simulating also a scenario with no climate change but subject to the new degrees of frictions. The difference between these two exercises is the counterfactual to be compared with the benchmark results.

The results are reported in Table 2.4, Panel A (and in Figure B.7 at the grid–cell level). Lower trade frictions reduce the shipping costs in the economy and generate stronger agglomeration forces. Thus, the economic activity is more reshuffled if compared to the benchmark exercise. The mechanism behind it are the higher incentives for sectoral specialization between locations benefited/damaged by climate change and, as a consequence, more population displaced. With lower trade costs, fewer locations can produce and supply agricultural goods to a wider market (thus the decrease in the agricultural employment). The results in terms of real GDP changes also reflect that: the frictionless the economy becomes, the lower the climate–induced real GDP losses. The opposite holds for the case of higher trade frictions.

In terms of the degree of heterogeneity on workers' location preferences (dispersion forces), I find that the climate migration flows monotonically increase the more heterogeneous agents become. The reason is that agents choose where to live based increasingly more on idiosyncratic reasons (i.e. in locations with higher amenities rather than locations with higher real income). However, a large subset of the high–amenity locations in SSA are among the regions benefited by climate change (mostly Eastern Africa). As a consequence, higher dispersion forces pushes even more individuals into that region (see Figure B.7), which increases even more the employment shares in the agriculture sectors (crops). Nevertheless, GDP losses become larger because the economy does not organize as well, in terms of sectoral specialization based on comparative advantages, as in the benchmark scenario (where workers put a higher weight on the "economic component" of the location choice). The opposite holds should dispersion forces get weaker (workers become more homogeneous).

TABLE 2.4: Robustness of the benchmark results with respect to trade frictions, dispersion forces (workers' heterogeneity), GCM models, and climate change scenarios.

	(1)	(2)	(3)
	Population displaced	Changes in real GDP	Changes in non–agricultural empl.
Benchmark results	11.84%	-4.24%	-6.43%
Panel A: Robustness to frictions			
Lower trade frictions	12.33%	-3.88%	-6.28%
Higher trade frictions	11.46%	-4.41%	-6.46%
Lower worker's heterogeneity	11.15%	-2.13%	-6%
Higher worker's heterogeneity	12.01%	-5.66%	-6.55%
Panel B: Robustness to different GCM			
CCCma	8.29%	-3.61%	-4.52%
CSIRO Mk2	9.52%	-3.98%	-5.26%
MPI ECHAM	9.69%	-2.96%	-4.29%
Panel C: Robustness to RCP 4.5 scenario			
Hadley CM3	7.50%	-3.79%	-4.71%
CCCma	6.16%	-2.13%	-4.37%
CSIRO Mk2	8.02%	-3.72%	-5.20%
MPI ECHAM	7.32%	-2.84%	-5.43%

Notes: Panel A documents the aggregate effects of climate change to different degrees of trade frictions and workers' heterogeneity (dispersion forces), driven by the parameters δ and θ, respectively. Panel B provides the results of the benchmark simulation using climate change data from GAEZ generated by different GCM models. Panel C reports the sensibility of the benchmark results to a less severe climate change scenario.

Finally, I verify the robustness of my results to changes in the climate models generating the agricultural suitability data. As extensively discussed by Costinot et al. (2016a), the GAEZ forecasts are produced with climatic General Circulation Models (GCM), which simulate the evolution of the global climate under an assumption of the evolution of the world's stock of carbon (climate change scenario). As mentioned in Appendix B.2.1, the GCM from which my data is drawn is the Hadley CM3 model for the RCP 8.5 scenario (a severe scenario in which carbon emissions increase throughout the 21st and 22nd centuries). I test the sensitivity of my results to other GCM, under the same scenario for climate change. The results, reported in Panel B of Table 2.4, are qualitatively very similar. The range of the climate–led displacement of population goes from 8 to 12 percent, roughly, which provides a "confidence interval" for the possible effects given the uncertainty around

the estimates for the future climate.[30]

Moreover, I check the sensitivity of my results to the severeness of the underlying climate change scenario, by using the forecasts for the RCP 4.5. scenario (which assumes that carbon emissions will peak by mid–century and decrease thereafter, due to developments in the implementation of climate–friendly technologies). I simulate my model with the suitability data for this scenario produced by all GCM models available; the results are documented in Panel C of Table 2.4. As expected, all aggregate effects are attenuated under such a scenario.

2.7   Final remarks

The main message of this paper is that understanding (and quantifying) climate migration in agricultural economies is not straightforward. The forecasts by climatologists are spatially heterogeneous along many dimensions – e.g. along the geography and types of crops. As a consequence, the reactions of economic agents when adapting to such a shock could be numerous and interconnected.

Using a multi-sector spatial trade quantitative framework, I model climate change as a spatially heterogeneous shock to agriculture crops. I draw on state–of–the–art climate data to measure how agricultural economies in SSA would be impacted. I find that the expected changes in agricultural productivity could lead to large population displacements, within and across countries, of about 12 percent of the SSA population. I also discover that the adoption of technology in agriculture could reverse dramatically the economic losses of climate change.

One of the main takeaways of my paper is the shock coping role of sectoral reallocations (structural transformation). In particular, the capacity of adjusting the production mix towards other sectors – within agriculture or to non–agricultural sectors – upon being hit by climate change is shown to weaken considerably the climate shock–outmigration link. Trade is also found to be key when allowing for such mechanism.

---

[30]The estimates for the Hadley CM3 model/RCP 8.5 (benchmark counterfactual) are the most extreme (in terms of suitability losses) between all GCM models. That is the reason for the larger magnitudes of the results in terms of population displacement, real GDP losses, and sectoral specialization.

However, some questions remain to be addressed. First, would exporting (cash) crops be as affected as staple crops and, if so, which impact would that have in the adaptation of SSA to future changes in the global weather? Which role would international (i.e. out of Africa) trade play in such a scenario? Moreover, how would frictions to sector switching – a fact in developing economies – alter the steady–state equilibrium of SSA? Finally, how would other aspects of climate change – e.g. coastal flooding, extreme weather events – interact with the agricultural suitability losses that I account for in this project? Expanding my setup along these dimensions is left for future research.

Chapter 3

Local Sectoral Specialization in a Warming World

Abstract

This paper quantitatively assesses the world's changing economic geography and sectoral specialization due to global warming. It proposes a two-sector dynamic spatial growth model that incorporates the relation between economic activity, carbon emissions, and temperature. The model is taken to the data at the $1°$ by $1°$ resolution for the entire world. Over a 200-year horizon, rising temperatures consistent with emissions under Representative Concentration Pathway 8.5 push people and economic activity northwards to Siberia, Canada, and Scandinavia. Compared to a world without climate change, clusters of agricultural specialization shift from Central Africa, Brazil, and India's Ganges Valley, to Central Asia, parts of China and northern Canada. Equatorial latitudes that lose agriculture specialize more in non-agriculture but, due to their persistently low productivity, lose population. By the year 2200, predicted losses in real GDP and utility are 6% and 15%, respectively. Higher trade costs make adaptation through changes in sectoral specialization more costly, leading to less geographic concentration in agriculture and larger climate-induced migration.

3.1 Introduction

Global warming will change the comparative advantage of regions across the world. Areas that today have ideal temperatures for agricultural production, such as parts of India, Africa, and South America, will become too hot for agriculture and will adapt by switching to other sectors. Of course, their ability to shift specialization as an adaptation mechanism depends on their productivity in other sectors, such as manufacturing and services, as well as on their ability to trade with other parts of the world. If adaptation through sectoral specialization is ineffective, regions will suffer and population will migrate elsewhere, to areas in the world where conditions are more hospitable.

Assessing the changing economic geography of a warming world therefore requires a high-resolution multi-sector dynamic spatial model that is able to evaluate the relative importance of trade and migration as adaptation mechanisms in different parts of the world. Migration and trade are costly, so incorporating realistic frictions to moving people and goods is paramount. Of course, while climate change affects the economy, the reverse is true as well. Hence, explicitly modeling the relation between economic activity, carbon emissions, and temperature is essential too.

Starting with the spatial dynamic model of the world economy of Desmet et al. (2018), we introduce three changes to make it amenable to assessing the spatial and sectoral impact of global warming. A first change extends the theory to multiple sectors.[1]

A second change allows sectoral productivity to depend on temperature. Because certain sectors, such as agriculture, are more sensitive to rising temperatures, than other sectors, such as manufacturing and services, and because different locations start off with different temperature levels, a shock to temperature translates into a local shock to comparative advantage. As such, changing specialization patterns constitute a relevant margin of adjustment to climate change. A third, and last, change follows standard integrated assessment models by explicitly introducing the feedback from the economy

---

[1] We take preferences to be Cobb-Douglas across sectors. While this implies constant expenditure shares, we still find a declining agricultural employment share because of the climate-induced relocation of agriculture toward land-abundant areas. In many models of long-run development and structural transformation, the falling agricultural employment share is generated by either nonhomothetic preferences or an elasticity of substitution between agriculture and other sectors of less than one (e.g., Uy et al., 2013; Herrendorf et al., 2014; Świecki, 2017).

to the climate. Production requires energy use, which leads to emissions. Through the carbon cycle, emissions affect the atmospheric stock of carbon, translating into rising temperatures.

In any quantitative assessment of global warming, using high-quality data is essential. We use data on population, total output, agricultural output, and temperature at the 1° by 1° resolution for the entire world. Although the model allows for any number of sectors, we focus on just two: agriculture and a sector that combines all others, which we refer to as non-agriculture. Our baseline exercise calibrates to an increase in the carbon stock and in global temperature consistent with the predictions under Representative Concentration Pathway (RCP) 8.5 (van Vuuren et al., 2011; IPCC, 2020). This is a high-emissions pathway based on fossil-fuel-intensive economic growth, leading to a 1200 GTC increase in the stock of carbon and a 3.7°C global temperature increase by the end of the 21st century. One important element in our calibration is how sensitive local temperatures are to a rise in global temperature. For example, it is well known that the poles are warming faster than the rest of the world. Due to, among others, the albedo effect and poleward energy transport, in some polar regions a one-degree increase in global temperature translates into a more than three-degree increase in local temperature. To estimate location-specific parameters that map changes in global temperature into changes in local temperature, we use predicted local and global temperatures between 2000 and 2100 from the Intergovernmental Panel on Climate Change (IPCC). Another key element in our calibration is how sensitive agricultural and non-agricultural productivities are to temperature. For agriculture, we base ourselves on established estimates of the relation between temperature and crop yields from the agronomy literature, whereas for non-agriculture we use the model-predicted estimates of non-agricultural productivity to estimate its relation to temperature.

After calibrating the model, we simulate the model forward for 200 years. The baseline simulation assumes that frictions to moving people and moving goods remain unchanged at current levels. Our main results can be summarized as follows. First, while in the next 200 years many of the world's densest and richest regions continue to be dense and rich, climate change does have an impact. In terms of population, Scandinavia, northern Canada and Siberia gain, whereas the Arabian peninsula, northern India, North Africa, Brazil and Central America lose. In terms of income per capita, patterns are similar, though losses are more widespread, essentially spanning all latitudes

comprised between southern Africa and southern Europe. One exception are coastal areas that display greater resilience.

Second, when considering sectoral specialization, agriculture becomes spatially more concentrated. While this move toward greater geographic concentration happens independently of climate change, rising temperatures affect where the increased concentration occurs. In the absence of climate change, clusters of agricultural specialization can be found in South America, sub-Saharan Africa, and India's Ganges Valley. With rising temperature, these clusters shift to Central Asia, China, and Canada. In contrast to what one might hope, most of the regions that lose agriculture do not become thriving non-agricultural powerhouses. This is especially true in developing countries that start off with low-tech manufacturing and services.

Third, in the aggregate, by the year 2200 global warming leads to a 6% decrease in income per capita and a 15% decrease in utility. The larger drop in utility is related to climate change pushing people northward to areas with worse amenities, such as Siberia or northern Canada. How do the different sectors perform in the aggregate? Although agriculture is more sensitive to climate change than non-agriculture, we find that rising temperatures increase productivity growth in agriculture and decrease productivity growth in non-agriculture. Warmer temperatures push agriculture to regions, such as Central Asia, that initially suffered from a large temperature penalty. With global warming, these regions benefit from relatively high agricultural productivity.

To explore the role of trade, we conduct a number of counterfactual exercises with higher and lower trade costs. We find that higher trade costs lead to greater climate-induced movements of people. This indicates that trade and migration are substitutes: higher trade costs limit the scope of locally adjusting to a climate shock by changing specialization. This makes adjusting through migration relatively more attractive. These larger spatial changes when trade is more costly are also present when analyzing real GDP per capita.

When considering patterns of specialization, higher trade costs limit the spatial concentration of agriculture. Because goods are sourced from locations that are closer by when trade is more costly, agriculture in the year 2200 is spatially more dispersed under high trade costs than under low trade costs. In the aggregate, by the year 2200 climate-induced losses in global income per capita are higher under low trade costs than under high trade costs,

though that difference is reversed by the year 2400. One might have expected that higher trade costs would lead to larger climate-induced losses throughout. After all, with higher trade costs, there is less scope to respond to the sector-specific effects of global warming by changing specialization. However, higher trade costs lead to a greater shift of population and economic activity to high-productivity places in the U.S., Europe, and Japan, that are relatively less affected by the growing temperatures.

Our paper is related to a growing literature aimed at quantifying the economic effects of climate change across the globe. Nordhaus (1993, 2008, 2010) pioneered the development of integrated assessment models that incorporate the main insights of climate science into economic growth models. Other examples of integrated assessment models that build on standard quantitative macro frameworks include Golosov et al. (2014) and Hassler et al. (2016). While many of these models have only one region, some allow for multiple regions, and are thus able to evaluate how climate change affects different regions differently. However, with only a handful of regions, they are unable to capture the rich spatial heterogeneity of the effects of climate change. In addition, these models do not include trade and migration in the economy's response to global warming.

In recent years a burgeoning literature has developed high-resolution spatial models: most are static (Allen and Arkolakis, 2014), and only a few are dynamic (Desmet and Rossi-Hansberg, 2014; Desmet et al., 2018; Caliendo et al., 2019).[2] Needless to say, in the context of global warming, dynamics are of the essence, because of the slow-moving nature of climate change. Some of these spatial dynamic models have already been applied to evaluate the economic impact of climate change. Desmet and Rossi-Hansberg (2015) assess the spatial dynamic effect of global warming in a two-sector model with one-dimensional space. While a one-dimensional model is a reasonable simplification – only a small fraction of the variance in temperature occurs within latitudes – it fails to capture relevant differences between, for example, coastal areas and more inland regions. Using a two-dimensional spatial growth model that captures the world's true geography, Desmet et al. (2021) carry out a quantitative assessment of rising sea levels. Another relevant paper is Balboni (2019) who analyzes the welfare effects of large coastal infrastructure investments in Vietnam in a dynamic spatial model that takes into account future inundation.

---

[2]See Redding and Rossi-Hansberg (2017) for a review of the quantitative spatial literature.

In a contemporaneous and related contribution, Alvarez and Rossi-Hansberg (2021) propose a similar dynamic spatial model to evaluate the geography of the economic costs of global warming. They add a number of features that we abstract from here. In particular they incorporate the effect of changes in temperature on amenities and fertility, and model the choice to use and produce clean and carbon based energy. Importantly, they limit their analysis to one aggregate sector. Hence, although richer in some dimensions, they cannot study the role of specialization as an adaptation mechanism to global warming, which is our central goal.

A key contribution of spatial dynamic models is the explicit treatment of trade and migration. Since climate change affects some locations more negatively than others, migration is an adaptation strategy. And because not all sectors are impacted in the same way, so is trade.[3] For example, **?** find that the loss in real GDP due to coastal flooding in the year 2200 drops from 4.5% to 0.11% when incorporating the dynamic response of migration. In a related paper, Burzyński et al. (2019) predict that climate change will induce the displacement of 200 to 300 million people over the course of the 21st century, though only 20% will involve cross-boarder migration. In another recent evaluation, Benveniste et al. (2020b) find substantially smaller numbers, estimating excess climate-induced cross-border migration flows in the year 2100 of 75,000. In our paper, we also focus on the importance of mobility, and highlight that trade and migration may be substitutes in their response to climate shocks.

A large part of the literature on climate change deals with policies aimed at mitigating global warming. In fact, many integrated assessment models seek to quantify the optimal carbon tax (Nordhaus, 2010; Golosov et al., 2014; Hassler et al., 2016, 2018). Other papers analyze the use of different policies to promote the transition to clean energy (Acemoglu et al., 2012, 2016). While we do not focus on mitigation and energy transition, our paper does feature endogenous innovation. As a result, energy use per unit of production declines over time. In their related framework, Alvarez and Rossi-Hansberg (2021) study carbon taxes, clean energy subsidies, and abatement policies.

---

[3]Without using a spatial dynamic framework, other relevant papers that have analyzed the effect of climate change on comparative advantage include Costinot et al. (2016b) and Conte (2020) who emphasize the importance of crop switching, as well as Nath (2020b), who shows that subsistence food requirements may keep more people employed in agriculture in some of the areas that are hardest hit by climate change.

The rest of the paper is organized as follows. Section 3.2 develops the model. Section 3.3 describes the data and quantification of the model. Section 3.4 reports the main findings and Section 3.5 concludes. Appendix C.1 includes details on how to solve and invert the model to obtain local amenities and productivities by sector.

3.2 Model

Our starting point is the high-resolution dynamic spatial model of the world economy with trade and migration frictions of Desmet et al. (2018). To assess the economic impact of climate change, we extend this model in three ways. First, we allow for multiple sectors. To be precise, the economy consists of I sectors, indexed by $i = 1, 2, ..., I$, with each sector producing a continuum of goods $\omega \in [0, 1]$. Agents' utility is CES across goods within each sector and Cobb–Douglas across sectors. Labor is freely mobile across sectors. Second, at each location, sectoral productivity levels depend on the location's temperature. Third, each sector uses energy to produce. Energy is freely tradable and is supplied by a resource extraction sector that operates under decreasing returns. Energy use contributes to CO_2 emissions, and hence to the atmospheric stock of carbon, which affects temperature at every location. As a result, economic activity depends on temperature, and temperature depends on economic activity. We now proceed to describing the model in further detail. Inevitably, part of the description draws on Desmet et al. (2018).

3.2.1 Model Setup

Endowments and preferences. The world economy occupies a two–dimensional surface S, where a location is defined as a point $r \in S$. Location r has land density $H(r)$, and there are $\bar{L}$ agents in the world economy, each supplying one unit of labor. An agent j who lives in location $r \in S$ in period t with a history of having resided in $\{r_0, ..., r_{t-1}\}$ enjoys utility

$$U_t^j(r_0, ..., r_{t-1}, r) = \bar{\chi} a_t(r) \prod_{i=1}^{I} \left[\int_0^1 c_{it}^\omega(r)^\rho \, d\omega \right]^{\frac{\chi_i}{\rho}} \varepsilon_t^j(r) \prod_{s=1}^{t} m(r_{s-1}, r_s)^{-1} \quad (3.1)$$

in period t, where $a_t(r)$ denotes local amenities, $c_{it}^\omega(r)$ is the consumption of variety ω of good i, $1/(1-\rho)$ is the elasticity of substitution between different varieties of the same good, χ_i is the share of good i in the agent's expenditure, $\varepsilon_t^j(r)$ is a location preference shock drawn from a Fréchet distribution

with shape parameter $1/\Omega$, $m(r_{s-1}, r_s)$ is the cost of moving from r_{s-1} in period $s-1$ to r_s in period s, and $\bar{\chi} = \prod_{i=1}^{I} \chi_i^{-\chi_i}$ is a constant that simplifies subsequent expressions. Agents discount future utility using the discount factor β.

Local amenities at location r suffer from congestion and take the form:

$$a_t(r) = \bar{a}(r) \left(\frac{\bar{L}_t(r)}{H(r)} \right)^{-\lambda}, \tag{3.2}$$

where $\bar{a}(r)$ denotes location r's fundamental amenity, and $(\bar{L}_t(r) / H(r))^{-\lambda}$ represents a dispersion or congestion force coming from local population density (i.e., local population $\bar{L}_t(r)$ divided by land). The greater the value of λ, the stronger the dispersion force. In addition to the effect of density on amenities, there is another dispersion force coming from the preference shocks: a higher value of Ω implies greater taste heterogeneity, and hence a stronger incentive to spatially disperse.

The cost of moving from r to s is the product of an origin-specific cost, $m_1(r)$, and a destination-specific cost, $m_2(s)$, so that $m(r,s) = m_1(r) m_2(s)$. Remaining in the same place is costless, and so $m(r,r) = m_1(r) m_2(r) = 1$. This implies that the cost of leaving a location is the inverse of the cost of entering that location, i.e., $m_2(r) = m_1(r)^{-1}$. As a result, the permanent utility flow cost paid by an immigrant who enters s is compensated by a permanent utility flow benefit of the same magnitude when leaving s. Migrants therefore only pay the flow utility moving cost while residing in the host location, making any decision to migrate reversible. This simplifies an agent's forward-looking migration decision to a static decision.

In addition to earning income from work, $w_t(r)$, an agent residing in r at time t gets a proportional share of local land rents, $R_t(r) H(r) / \bar{L}_t(r)$, as well as a proportional share of global profits from the resource extraction sector, $\Pi_t / \bar{L}$. Following Desmet et al. (2018), we can show that the number of people choosing to live in r in period t, $\bar{L}_t(r)$, is given by

$$\bar{L}_t(r) = \frac{u_t(r)^{1/\Omega} m_2(r)^{-1/\Omega}}{\int_S u_t(s)^{1/\Omega} m_2(s)^{-1/\Omega} ds} \bar{L}, \tag{3.3}$$

where

$$u_t(r) = a_t(r) \frac{w_t(r) + \Pi_t/\bar{L} + R_t(r) H(r) / \bar{L}_t(r)}{\prod_{i=1}^{I} P_{it}(r)^{\chi_i}} \tag{3.4}$$

and $P_{it}(r)$ denotes the ideal price index of sector i, defined as

$$P_{it}(r) = \left[\int_0^1 p_{it}^\omega(r)^{\frac{\rho}{\rho-1}} d\omega \right]^{\frac{\rho-1}{\rho}}, \tag{3.5}$$

where $p_{it}^\omega(r)$ is the price of variety ω at r.

Production of varieties. The representative firm producing variety ω in sector i in location r at time t faces the constant returns production function

$$q_{it}^\omega(r) = L_{\phi,it}^\omega(r)^{\gamma_i} z_{it}^\omega(r) L_{it}^\omega(r)^{\mu_i} E_{it}^\omega(r)^{\sigma_i} H_{it}^\omega(r)^{1-\gamma_i-\mu_i-\sigma_i}, \tag{3.6}$$

where $q_{it}^\omega(r)$ denotes the firm's output, $L_{\phi,it}^\omega(r)$ denotes the amount of labor hired by the firm to innovate, $L_{it}^\omega(r)$ is the amount of labor hired to produce, $E_{it}^\omega(r)$ is energy use, $H_{it}^\omega(r)$ is the use of land, and $z_{it}^\omega(r)$ is an idiosyncratic productivity shifter.

We assume that the idiosyncratic productivity shifter $z_{it}^\omega(r)$ is i.i.d. across varieties, locations and time, drawn from a Fréchet distribution with c.d.f.

$$Pr\left[z_{it}^\omega(r) \le z\right] = e^{-(Z_{it}(r)/z)^\theta}, \tag{3.7}$$

where $\theta > 0$. By the properties of the Fréchet distribution, $Z_{it}(r)$ is the average idiosyncratic productivity of varieties of good i in location r. This average productivity depends on fundamental productivity, temperature, and agglomeration economies,

$$Z_{it}(r) = \tau_{it}(r) g_i(T_t(r)) \left(\frac{\bar{L}_{it}(r)}{H_{it}(r)} \right)^{\alpha_i}, \tag{3.8}$$

where $\tau_{it}(r)$ denotes the fundamental productivity of good i in location r at time t, $g_i(\cdot)$ is a temperature discount factor on the productivity of good i, $T_t(r)$ denotes temperature in r at time t, and $(\bar{L}_{it}(r)/H_{it}(r))^\alpha$ represent agglomeration forces that depend on local density in sector i, defined as total sectoral employment $\bar{L}_{it}(r) = L_{\phi,it}(r) + L_{it}(r)$ divided by sectoral land use $H_{it}(r)$. The greater the exogenous parameter α_i, the stronger the agglomeration forces.

Across periods, a location's fundamental productivity in sector i evolves according to equation

$$\tau_{it}(r) = L_{\phi,i,t-1}(r)^{\gamma_i} \left[\int_S e^{-\aleph dist(r,s)} \tau_{i,t-1}(s) \, ds \right]^{1-\delta} \tau_{i,t-1}(r)^{\delta}, \qquad (3.9)$$

where $L_{\phi,i,t-1}(r)$ denotes the total amount of innovation labor hired in sector i at time $t-1$, and $dist(r,s)$ denotes the geographic distance between locations r and s. As such, a location's fundamental productivity in sector i depends on local past sectoral innovation, local past sectoral productivity, and the spatial diffusion of past sectoral productivity from all other locations. Spatial diffusion is essential to avoid excessive spatial concentration over time.

We assume that the sector-specific temperature discount factor is bell-shaped in temperature, so

$$g_i(T_t(r)) = \exp\left[-\frac{1}{2} \left(\frac{T_t(r) - g_i^{opt}}{g_i^{var}} \right)^2 \right], \qquad (3.10)$$

where g_i^{opt} denotes the optimal temperature in sector i, and g_i^{var} is a parameter that determines the variance of the bell-shaped relationship between temperature and productivity in sector i. Note that the discount factor equals one at the optimal temperature but is below one at any other temperature.

Firms are perfectly competitive. Taking all prices as given, a firm producing variety ω of good i chooses its inputs $L_{\phi,it}^{\omega}(r)$, $L_{it}^{\omega}(r)$, $E_{it}^{\omega}(r)$ and $H_{it}^{\omega}(r)$, subject to production function (3.6), to maximize its static profits

$$p_{it}^{\omega}(r,r) q_{it}^{\omega}(r) - w_t(r) \left[L_{\phi,it}^{\omega}(r) + L_{it}^{\omega}(r) \right] - e_t E_{it}^{\omega}(r) - R_t(r) H_{it}^{\omega}(r), \quad (3.11)$$

where e_t denotes the global price of energy and $p_{it}^{\omega}(r,r)$ is the price of variety ω of good i produced and sold in r. The reason why a firm maximizes its static profits is because we assume that land markets are competitive and that any local investment in innovation becomes available to all potential entrants next period. Then, all future gains from innovation will be reflected in the value of the fixed factor, namely, land. Because a firm understands that its investments in innovation will yield zero profits in the future, its dynamic profit maximization decision simplifies to a static profit maximization

decision.[4]

Let $\bar{L}_{it}^{\omega}(r)$ denote the total labor used by the firm, that is,

$$\bar{L}_{it}^{\omega}(r) = L_{\phi,it}^{\omega}(r) + L_{it}^{\omega}(r). \tag{3.12}$$

Integrating the first-order conditions of the firm's maximization problem across goods yields relationships between the sector-level use of factors and total sectoral employment, namely,

$$L_{\phi,it}(r) = \frac{\gamma_i}{\gamma_i + \mu_i}\bar{L}_{it}(r), \tag{3.13}$$

$$L_{it}(r) = \frac{\mu_i}{\gamma_i + \mu_i}\bar{L}_{it}(r), \tag{3.14}$$

$$E_{it}(r) = \frac{\sigma_i}{\gamma_i + \mu_i}\frac{w_t(r)}{e_t}\bar{L}_{it}(r), \tag{3.15}$$

$$H_{it}(r) = \frac{1 - \gamma_i - \mu_i - \sigma_i}{\gamma_i + \mu_i}\frac{w_t(r)}{R_t(r)}\bar{L}_{it}(r). \tag{3.16}$$

Rearranging (3.16) and summing across sectors relates total land rents to wages and sectoral employment levels,

$$R_t(r)H(r) = w_t(r)\sum_{i=1}^{I}\frac{1 - \gamma_i - \mu_i - \sigma_i}{\gamma_i + \mu_i}\bar{L}_{it}(r). \tag{3.17}$$

In each period we normalize all nominal variables by average world wages. Hence, only real variables can be meaningfully compared over time.

Production of energy. The world supply of energy is exogenously given by

$$E_t = e_t^{\varphi}, \tag{3.18}$$

where $\varphi \in (0,1)$.[5] We abstract from the costs of resource extraction, which implies that profits made in the resource extraction sector equal revenues.[6] Thus,

$$\Pi_t = e_t E_t = e_t^{1+\varphi}. \tag{3.19}$$

---

[4]See Desmet and Rossi-Hansberg (2014) and Desmet et al. (2018) for a more detailed description of this argument.

[5]In principle, we could allow for a supply intercept different from one. However, we can always measure energy in units such that this intercept equals one.

[6]See Alvarez and Rossi-Hansberg (2021) for an alternative formulation in which the cost of extraction depends on the cumulative amount of carbon used in the past.

Carbon cycle and the evolution of temperature. Emissions from production affect the carbon stock in the atmosphere, which in turn affects temperature. The carbon cycle determines the relation between emissions and the stock of carbon. We follow Desmet and Rossi-Hansberg (2015) in assuming a carbon cycle in the spirit of Nordhaus (2010), with the carbon stock gradually decaying over time. More specifically, the stock of carbon in period t, K_t, is given by

$$K_t = \varepsilon_1 K_{t-1} + \varepsilon_2 E_{t-1}, \tag{3.20}$$

where $\varepsilon_1 \leq 1$ determines how the carbon stock decays and ε_2 determines the relation between energy and carbon emissions. Note that if we were to set $\varepsilon_1 = 1$ and $K_0 = 0$, then the carbon stock is equal to cumulative emissions.[7] Global temperature T_t at time t then evolves with the carbon stock according to

$$T_t = T_{t-1} + \nu (K_t - K_{t-1}) \tag{3.21}$$

where $\nu > 0$.

The rise in temperature due to global warming is not expected to be homogeneous across space. We allow for a location-specific linear relation between changes in local temperatures and changes in global temperature as in Stocker et al. (2013). Hence,

$$T_t(r) = T_{t-1}(r) + (T_t - T_{t-1}) \, \xi(r), \tag{3.22}$$

where $\xi(r)$ are the location-specific down-scaling factors that map changes in global temperature into local temperatures.

3.2.2 Equilibrium

Prices and export shares. Perfect competition implies that the price of each variety is equal to the marginal cost of production,

$$p_{it}^{\omega}(r,r) = \frac{mc_{it}(r)}{z_{it}^{\omega}(r)}, \tag{3.23}$$

where

$$mc_{it}(r) = \gamma_i^{-\gamma_i} \mu_i^{-\mu_i} \sigma_i^{-\sigma_i} (1 - \gamma_i - \mu_i - \sigma_i)^{\gamma_i + \mu_i + \sigma_i - 1} \, w_t(r)^{\gamma_i + \mu_i} \, e_t^{\sigma_i} R_t(r)^{1 - \gamma_i - \mu_i - \sigma_i} . \tag{3.24}$$

---

[7]Work by Allen et al. (2009) and Matthews et al. (2009) suggests that this is a reasonable simplification.

Trade across locations is costly. Let $\varsigma(s,r)$ denote the iceberg shipping cost from r to s. Then, the price of a variety produced in r and sold in s is $p_{it}^{\omega}(s,r) = \varsigma(s,r) p_{it}^{\omega}(r,r)$.

Equation (3.23), the Fréchet distribution of idiosyncratic productivities, and the iceberg nature of shipping costs guarantee that prices in any location are also distributed Fréchet. Using the standard techniques of Eaton and Kortum (2002), we can write the spending of location s on sector-i varieties of location r relative to the total spending of location s on sector-i varieties as

$$\pi_{it}(s,r) = \frac{Z_{it}(r)^{\theta} [mc_{it}(r)\varsigma(s,r)]^{-\theta}}{\int_S Z_{it}(u)^{\theta} [mc_{it}(u)\varsigma(s,u)]^{-\theta} du}. \tag{3.25}$$

One can also obtain the price index of sector i at location s as

$$P_{it}(s) = \bar{p} \left[\int_S Z_{it}(r)^{\theta} [mc_{it}(r)\varsigma(s,r)]^{-\theta} dr \right]^{-\frac{1}{\theta}}, \tag{3.26}$$

where $\bar{p} = \Gamma(1 - \frac{\rho}{(1-\rho)\theta})^{-\frac{1-\rho}{\rho}}$. Using (3.8), (3.16) and (3.24) allows us to rewrite equation (3.26) as

$$P_{it}(s)^{-\theta} = \kappa_i e_t^{-\sigma_i\theta} \int_S \tau_{it}(r)^{\theta} g_i(T_t(r))^{\theta} w_t(r)^{-(\alpha_i+\gamma_i+\mu_i)\theta} R_t(r)^{(\alpha_i+\gamma_i+\mu_i+\sigma_i-1)\theta} \varsigma(s,r)^{-\theta} dr \tag{3.27}$$

where $\kappa_i = \bar{p}^{-\theta} \gamma_i^{\gamma_i\theta} \mu_i^{\mu_i\theta} \sigma_i^{\sigma_i\theta} (\gamma_i + \mu_i)^{\alpha_i\theta} (1 - \gamma_i - \mu_i - \sigma_i)^{(1-\alpha_i-\gamma_i-\mu_i-\sigma_i)\theta}$.

Market clearing. Market clearing in sector i implies that the revenue of firms producing varieties of good i at any location r, $\frac{1}{\gamma_i+\mu_i} w_t(r) \bar{L}_{it}(r)$, equals total spending on these varieties in the entire world, namely,

$$\frac{1}{\gamma_i+\mu_i} w_t(r) \bar{L}_{it}(r) = \chi_i \int_S \pi_{it}(s,r) \left[\left(w_t(s) + \frac{\Pi_t}{\bar{L}} \right) \bar{L}_t(s) + R_t(s) H(s) \right] ds$$

$$= \chi_i \kappa_i e_t^{-\sigma_i\theta} \tau_{it}(r)^{\theta} g_i(T_t(r))^{\theta} w_t(r)^{-(\alpha_i+\gamma_i+\mu_i)\theta} R_t(r)^{(\alpha_i+\gamma_i+\mu_i+\sigma_i-1)\theta} .$$

$$\int_S P_{it}(s)^{\theta} \left[\left(w_t(s) + \frac{\Pi_t}{\bar{L}} \right) \bar{L}_t(s) + R_t(s) H(s) \right] \varsigma(s,r)^{-\theta} ds. \tag{3.28}$$

Worldwide market clearing for energy implies that

$$e_t = \left[\sum_{i=1}^I \frac{\sigma_i}{\gamma_i+\mu_i} \int_S w_t(r) \bar{L}_{it}(r) dr \right]^{\frac{1}{1+\varphi}}, \tag{3.29}$$

and, therefore using equation (3.19),

$$\Pi_t = e_t E_t = e_t^{1+\varphi} = \sum_{i=1}^{I} \frac{\sigma_i}{\gamma_i + \mu_i} \int_S w_t(r) \bar{L}_{it}(r) \, dr. \tag{3.30}$$

Finally, competitive land and labor markets clear at each location, so equation (3.17) holds, and

$$\bar{L}_t(r) = \sum_i \bar{L}_{it}(r). \tag{3.31}$$

Dynamic competitive equilibrium. For a given period t and a given distribution of fundamental amenities $\bar{a}(r)$, productivity $\tau_{it}(r)$ and temperature $T_t(r)$, equations (3.2), (3.3), (3.4), (3.17), (3.19), (3.27), (3.28), and (3.31) pin down the world price of energy e_t, profits in the resource extraction sector Π_t, the distribution of population $\bar{L}_t(r)$, utility $u_t(r)$, amenities $a_t(r)$, land rents $R_t(r)$, and wages $w_t(r)$ across locations, as well as the distribution of price indices $P_{it}(s)$ and sectoral employment $\bar{L}_{it}(r)$ across sectors and locations. These conditions determine the period-t equilibrium. Equation (3.13) gives the amount of innovation labor hired in each sector and each location. This, together with (3.9), yields the distribution of fundamental productivities in period $t+1$, $\tau_{i,t+1}(r)$. To update the distribution of temperature in $t+1$, $T_{t+1}(r)$, we use equations (3.20) to (3.22).

3.3 Quantification

3.3.1 Preliminaries

From now onwards, we assume the economy has two sectors: agriculture (A) and non-agriculture (which we denote by M, for manufacturing but includes all sectors that are not part of agriculture, including services). Further assume that we observe the matrix of bilateral trade costs $\varsigma(r,s)$, as well as land $H(r)$, temperature $T_0(r)$, total population $\bar{L}_0(r)$, the value of total output

$$Y_0(r) = \frac{1}{\gamma_A + \mu_A} w_0(r) \bar{L}_{A0}(r) + \frac{1}{\gamma_M + \mu_M} w_0(r) \bar{L}_{M0}(r) \tag{3.32}$$

and the value of agricultural output

$$Y_{A0}(r) = \frac{1}{\gamma_A + \mu_A} w_0(r) \bar{L}_{A0}(r) \tag{3.33}$$

at every location r at time 0. As we show in Appendix C.1, we can then use the model to recover the unique initial distributions of fundamental agricultural productivity, $\tau_{A0}(r)$, fundamental non-agricultural productivity, $\tau_{M0}(r)$, and fundamental amenities relative to utility, $\bar{a}(r)/u_0(r)$, that rationalize the data. We back out fundamental amenities $\bar{a}(r)$ by using subjective well-being data to measure $u_0(r)$, and we set moving costs $m_2(r)$ so that local changes in population between the first two periods coincide with what we observe in the data.

Appendix C.1 also describes in detail the algorithm to compute an equilibrium of the model. The model can be solved forward, using only current data, for as many periods as needed.

3.3.2 Data and Calibration

We discretize the world into 64,800 $1° \times 1°$ cells. At that level of spatial resolution, our quantification requires initial distributions of population, $\bar{L}_0(r)$, total output, $Y_0(r)$, agricultural output, $Y_{A0}(r)$, temperature, $T_0(r)$, as well as the distribution of land, $H(r)$. We also need estimates for bilateral transport costs, $\varsigma(r,s)$. Period 0 is taken to be the year 2000. Data on population, total output and land by grid-cell come from the G-Econ 4.0 database of Nordhaus et al. (2006b). These data cover the entire globe, with the exception of a few countries: Afghanistan, Iraq, Libya, North Korea, Somalia, Turkmenistan and Zimbabwe. Estimates on bilateral transport costs come from Desmet et al. (2018). The data on agricultural output and temperature require some more explanation.

Agricultural output and temperature. To estimate the initial distribution of agricultural output across grid-cells, we proceed in two steps. First, using high-resolution data on total crop production from GAEZ's Actual Yield and Production dataset, we compute grid-level agricultural production in year 2000 (IIASA and FAO, 2012). Second, we apply a country-specific conversion rate to local crop production so that its sum at the country level as a share of total output coincides with the share of value added that comes from agriculture, forestry, and fishing, as obtained from the World Bank Development Indicators. This is necessary because the GAEZ data do not include all

FIGURE 3.1: Agricultural Production in 2000
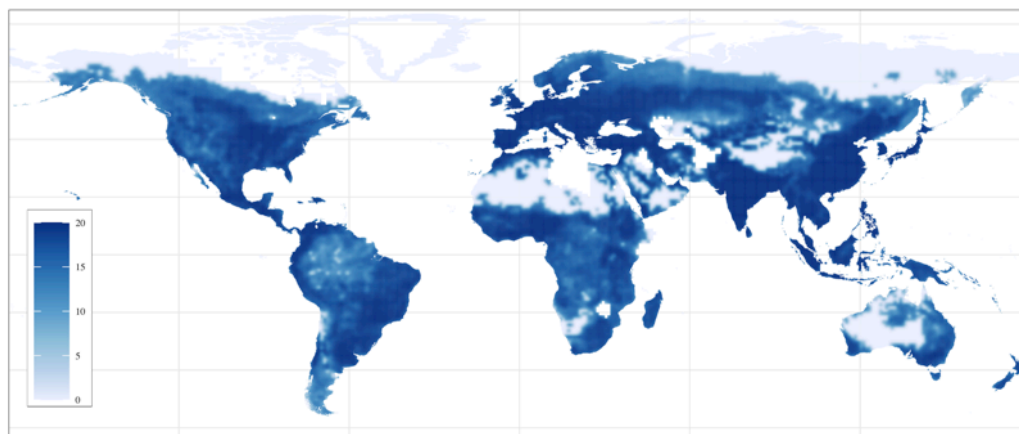
Note: Figure displays the log of agricultural output (US$ million, PPP).

agricultural activities. Figure 3.1 depicts the estimated distribution of agricultural output across the globe in year 2000.[8] Agriculture is widespread across the globe. Regions with particularly high agricultural output include the U.S. Midwest, Europe, northern India, and eastern China.

For the initial temperature distribution at the $1° \times 1°$ resolution we rely on data on yearly average temperature from the IPCC AR5 Data Distribution Center (IPCC, 2020). The resolution of the IPCC is $1.25° \times 0.9°$. When no centroid of any of these grid-cells lies within one of our $1° \times 1°$ grid-cells, we assign the temperature of the closest cell. Figure 3.2 depicts the world map of temperature in the year 2000. Much of the variation is across latitudes, but there are important exceptions: the Tibetan plateau, the Andes and the Rocky Mountains, for example, all have lower temperatures than their latitude would predict.

Parameter values. Table 1 reports the parameter values we use. Many of them are taken from Desmet and Rossi-Hansberg (2015) and Desmet et al. (2018). Others are either calibrated to moments in the data or come from other papers. The innovation parameter in agriculture, γ_A, is set to match the growth rate in agricultural productivity between 1975 and 2000 in 30 countries as estimated by Duarte and Restuccia (2010). Similarly, the innovation

---

[8]Although the land area of $1° \times 1°$ grid cells varies across latitudes, the map projection we use is such that all these cells have the same area. Hence, we prefer to display output rather than output density. Otherwise, integrating density across projected grid cells would yield a misleading measure of output. Of course, when we calibrate the model we incorporate into the analysis the exact land mass of each cell.

FIGURE 3.2: Average Temperature in 2000 (°C)
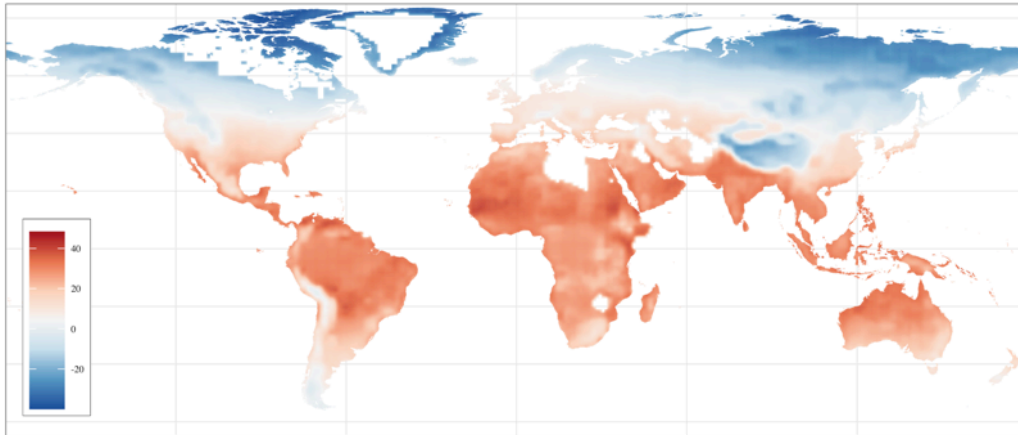
parameter in non-agriculture, γ_M, is set to match the manufacturing productivity growth rate in the same countries over the same time period. The value for the spatial decay of technology diffusion, $\aleph$, falls within the range of values estimated for a set of different technologies by Comin et al. (2012). Consistent with the predictions for Representative Concentration Pathway (RCP) 8.5, we calibrate the carbon cycle parameter ε_2 to obtain a 1200 GTC increase in the stock of carbon by 2100, and we set the parameter ν to obtain a 3.7°C global temperature increase by the end of the 21st century. Before discussing the parameter values pertaining to the sensitivity of agricultural productivity and non-agricultural productivity to temperature, we need the initial distributions of temperature-adjusted productivity in both sectors, denoted by $\hat{\tau}_{i0}(r) = \tau_{i0}(r)g_i(T_t(r)), i \in \{A, M\}$.

Solving for initial distributions. Using the initial distributions of land, total population, total output and agricultural output, as well as estimates of trade costs and the parameter values in Table 3.1, we follow the procedure outlined in Appendix C.1 to back out the distributions of the initial temperature-adjusted productivities in agriculture and non-agriculture, $\hat{\tau}_{i0}(r)$. Determining the distributions of the initial fundamental productivities $\tau_{i0}(r)$ will require estimates of the temperature discounts $g_i(T_t(r))$, an issue we turn to below.

As outlined in Desmet et al. (2018), we then use data on subjective well-being from the Human Development Report to back out the distribution of fundamental amenities. Location-specific moving costs are then set so that the model-predicted changes in population between 2000 and 2005 match

TABLE 3.1: Parameter Values

Parameter	Target/Comment
1. Preferences	
$\beta = 0.96$	Annual discount factor
$\rho = 0.75$	Elasticity of substitution of 4[1]
$\lambda = 0.32$	Relation between amenities and population[1]
$\Omega = 0.5$	Elasticity of migration flows with respect to income[1]
$\psi = 1.8$	Subjective well-being parameter[1]
$\chi_A = 0.051$	Data on agricultural and total output
$\chi_M = 0.949$	Data on agricultural and total output
2. Technology	
$\alpha_A = 0$	No agglomeration externality in agriculture
$\alpha_M = 0.01$	Agglomeration externality in non-agriculture[1]
$\theta = 6.5$	Trade elasticity[1]
$\mu_A = \mu_M = 0.6$	Labor share in agriculture and non-agriculture[2]
$\gamma_A = 0.001$	Growth rate of agricultural productivity[3]
$\gamma_M = 0.0002$	Growth rate of non-agricultural productivity[3]
$\sigma_A = 0.04$	Energy share in agriculture[2]
$\sigma_M = 0.07$	Energy share in non-agriculture[2]
$\delta = 0.993$	Technology diffusion[1]
$\aleph = 0.004$	Spatial decay of diffusion[4]
$\phi = 0.25$	Energy supply elasticity[2]
3. Temperature and carbon cycle	
$g_A^{opt} = 19.9°C$	Optimal temperature in agriculture[2]
$g_A^{var} = 7.28°C$	0.1% of world agricultural production at locations below discount factor 0.01
$g_M^{opt} = 10.5°C$	Relationship between non-agricultural productivity and temperature
$g_M^{var} = 11.0°C$	Relationship between non-agricultural productivity and temperature
$\varepsilon_1 = 0.9975$	Decay of carbon stock[2]
$\varepsilon_2 = 0.29$	1200 GTC increase in global carbon stock by 2100
$\nu = 0.0031$	3.7°C increase in global temperature by 2100

[1]Desmet et al. (2018), [2]Desmet and Rossi-Hansberg (2015), [3]Duarte and Restuccia (2010), [4]Comin et al. (2012). Further note that in Desmet et al. (2018) parameter α_M is set to 0.06. However, our notation is different: parameter α_M in the current paper is equal to α_M divided by θ in Desmet et al. (2018), so we set its value to 0.01.

those in G-Econ 4.0.[9]

---

[9]Agricultural output data indicates zero output in some cells of the world (particularly in deserts or polar regions). Given that our model and its inversion cannot handle zeros, we set the share of agricultural output in those regions to 10^{-12}. In a few cases the reported

FIGURE 3.3: Temperature Discount in Agriculture and Non-Agriculture

(a) Temperature discount

(b) Log non-agricultural producti-
vity and temperature
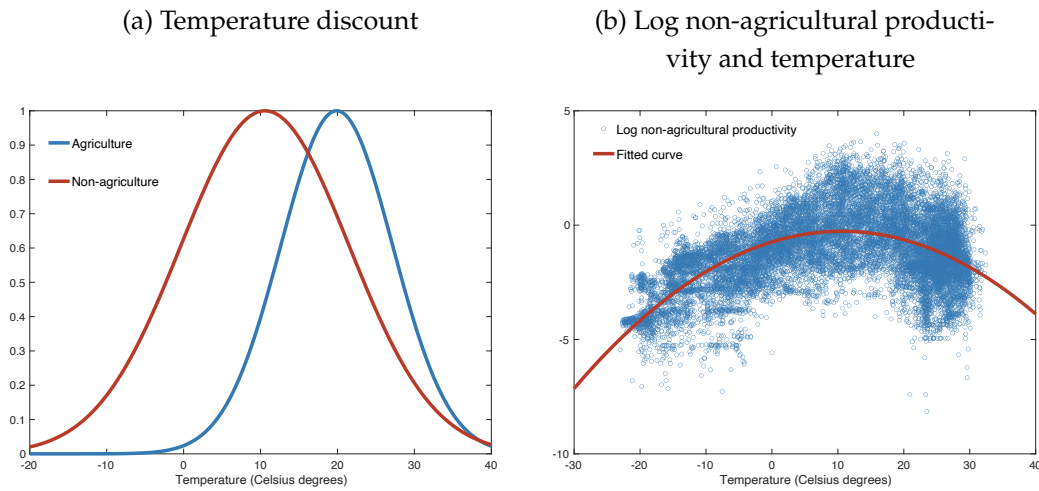
Sensitivity of agriculture and non-agriculture to temperature. To disentangle fundamental productivity from temperature-adjusted productivity, we use the sector-specific temperature discount factor (3.10). Parametrizing this bell-shaped discount function requires for each sector i estimates for the optimal temperature, g_i^{opt}, and for the variance of the relation between temperature and productivity, g_i^{var}.

For agriculture, Desmet and Rossi-Hansberg (2015) rely on agronomy studies to estimate an optimal growing-season temperature of 21.1°C. Because we use annual average temperature, we need to map growing-season temperature into yearly average temperature. To that effect, we regress annual average temperature on growing-season temperature across all grid-cells, and use the estimated mapping to obtain an optimal annual average temperature in agriculture, g_A^{opt}, of 19.9°C. We then set the variance parameter of the agricultural temperature discount so that only 0.1% of world agricultural production takes place in locations with a discount factor below 0.01. This yields $g_A^{var} = 7.28$°C. The estimated agricultural temperature discount is depicted in Figure 3.3 Panel (a).

For non-agriculture, we take a different approach. We calibrate the parameter values of the temperature discount to the observed relation between temperature and the model-generated non-agricultural productivity across

---

agricultural output we obtain from GAEZ and the World Bank yields agricultural cell output levels that are larger than the total output level reported by G-Econ. In those cases we set the non-agricultural output share to 10^{-12}.

all grid-cells.[10] To derive an estimating equation, we start by substituting the expression of the bell-shaped discount (3.10) into $\hat{\tau}_{M0}(r) = \tau_{M0}(r) g_M(T_0(r))$. This yields a relation between the temperature-adjusted and the fundamental productivity in non-agriculture given by

$$\log \hat{\tau}_{M0}(r) = \log \tau_{M0}(r) - \frac{1}{2} \left(\frac{T_0(r) - g_M^{opt}}{g_M^{var}} \right)^2.$$

Rearranging gives us the estimating equation

$$\log \hat{\tau}_{M0}(r) = \beta_0 + \beta_1 T_0(r) + \beta_2 T_0(r)^2 + v(r), \tag{3.34}$$

where $\beta_1 = g_M^{opt} / (g_M^{var})^2$ and $\beta_2 = -1/\left(2 (g_M^{var})^2\right)$. The identification assumption behind this estimation is that fundamental productivity $\tau_{M0}(r)$ is uncorrelated with temperature.[11] Using the model-generated values of $\hat{\tau}_{M0}(r)$, we run regression (3.34). The underlying data of this regression, displayed in Figure 3.3 Panel (b), strongly suggest that the relation between the log of non-agricultural productivity and temperature is indeed quadratic, with the most productive locations corresponding to those with moderate temperatures. From the estimates of β_1 and β_2, we can derive the two parameters of the bell-shaped temperature discount factor on non-agricultural productivity, $g_M^{opt} = 10.5°C$ and $g_M^{var} = 11°C$.

When comparing non-agriculture to agriculture, Figure 3.3 Panel (a) documents that its optimal temperature is lower and its sensitivity to temperature is smaller. These temperature discounts can be shown on a map. Panels (a) and (b) of Figure 3.4 depict the temperature discounts by location in the year 2000, $g_A(T_0(r))$ and $g_M(T_0(r))$. In agriculture relatively cold areas suffer the most: this explains the large discount on productivity in much of Canada and Russia. With the exception of some areas such as the Sahara desert, most regions closer to the Equator do not experience large productivity penalties. In non-agriculture, productivity does not suffer from much of a discount in

---

[10]For non-agriculture, there is less guidance from the literature. For a discussion of the few studies that exist, see Dell et al. (2014).

[11]This is plausible if temperature has had no effect on past investment decisions. Of course, if temperature has been an important determinant of the areas where humanity has concentrated and flourished, then the coefficients β_1 and β_2 are likely to include not just the direct effect of temperature on non-agricultural productivity, but also its indirect effect through cumulative past innovation. If so, we would be overstating the effect of temperature on non-agricultural productivity, because in our theory it is meant to only capture its direct effect.

FIGURE 3.4: Temperature Discount and Fundamental Productivity in 2000

(a) Temperature discount
in agriculture

(b) Temperature discount
in non-agriculture

(c) Fundamental productivity
in agriculture

(d) Fundamental productivity
in non-agriculture
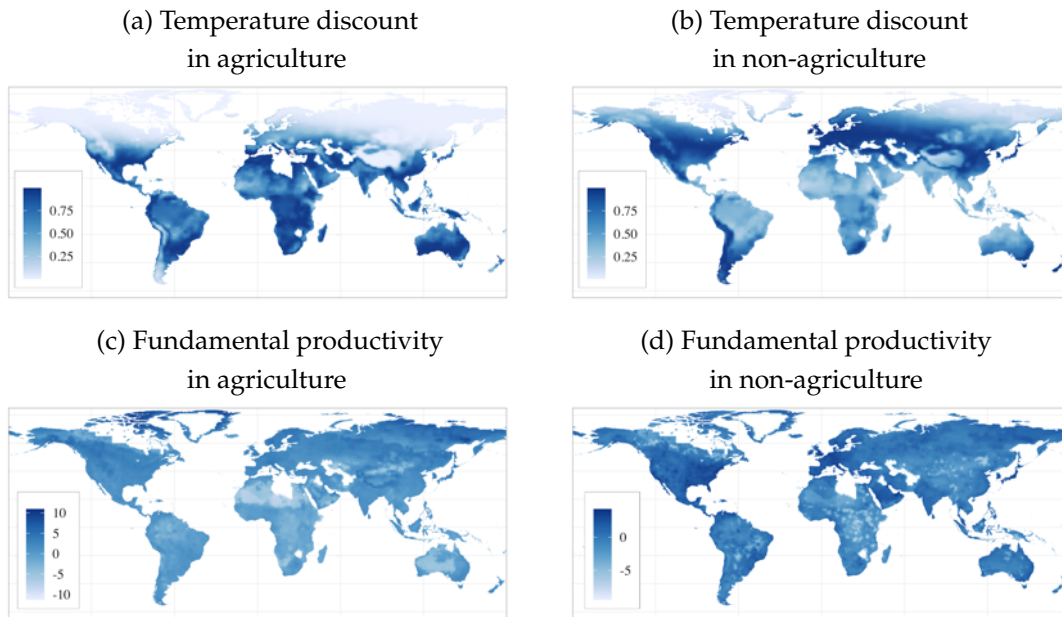
Note: Panel (a) depicts $g_A(T_0(r))$, Panel (b) depicts $g_M(T_0(r))$, Panel (c) depicts $\log(\tau_{A0}(r))$, and Panel (d) depicts $\log(\tau_{M0}(r))$.

large swaths of Canada and Russia, except in the northernmost areas. However, the lower optimal temperature in non-agriculture implies that warmer areas close to the Equator experience large productivity penalties.

Our estimates of the temperature discounts allow us to back out the initial distributions of fundamental productivity in agriculture and non–agriculture, displayed in Panels (c) and (d) of Figure 3.4. We see that large areas of China, Central Asia, and Canada have relatively high agricultural productivity, in spite of the important temperature discount they suffer. As global warming reduces the temperature penalty in northern latitudes, these regions stand to become some of the more productive in agriculture. Areas of high non-agricultural productivity tend to be spatially concentrated in the developed world, such as North America, western Europe, Japan, and southeastern Australia. Some areas in Brazil, Paraguay and Argentina, as well as parts of Central Africa, display markedly lower productivity in non-agriculture than neighboring regions. These are areas that heavily specialize in agriculture in the data, and so have limited experience in other sectors.

Model simulation. To simulate the model forward, we use the equilibrium allocation in period t to estimate fundamental productivities in period $t + 1$, and we use the carbon cycle, as well as the relation between the change in

FIGURE 3.5: Predicted Change in Temperature for 1°C Increase in Global Temperature
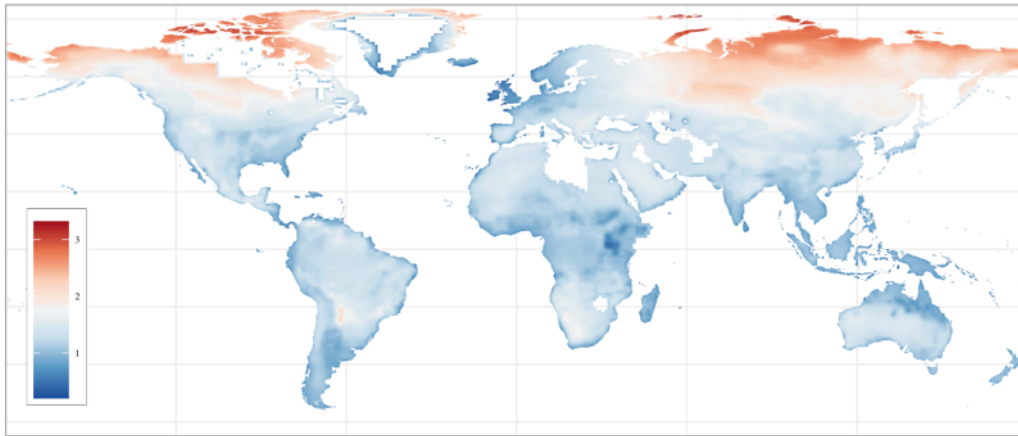
the carbon stock and the change in temperature in (3.22), to get estimates of temperature by location.

An important feature of global warming is that the rise in temperature is predicted to be heterogeneous across space. Polar latitudes are expected to experience higher-than-average increases in temperature, whereas coastal regions, including some islands such as Britain, are set to experience lower-than-average increases in temperature. To get estimates of the location-specific parameter $\xi(r)$ that measures the local increase in temperature for a one-degree global increase in temperature, we use twenty-year intervals of predicted local and global temperatures between 2000 and 2100 from the IPCC AR5 Data Distribution Center (IPCC, 2020) for RCP 8.5, and run the regression

$$T_t(r) - T_{t-1}(r) = \xi(r)\left(T_t - T_{t-1}\right) + v_t(r). \tag{3.35}$$

Figure 3.5 depicts the spatial distribution of $\xi(r)$. As can be seen, in some polar areas a one-degree increase in global temperature is predicted to translate into a more than three-degree increase in local temperatures.

With the distributions of fundamental productivities and temperatures in $t + 1$, we then solve for sectoral employment levels, wages and prices in $t + 1$. Using this algorithm we can compute the equilibrium allocation for as many periods as necessary.

3.4 Global Warming and Local Specialization

We now simulate our model forward for 200 years and analyze how global warming affects the world's economic geography. The effect of rising temperatures is location- and sector-specific. As a result, residents of particularly hard-hit locations may have an incentive to relocate, and local sectoral specialization may shift because of changing comparative advantage. Our goal is to document the spatial response of population, income per capita and specialization to global warming. We are also interested in the aggregate effects of climate change. Needless to say, the magnitude of spatial frictions affects the extent of these adjustments. In our baseline simulation we keep mobility frictions at their current levels. Given our interest in trade and specialization, we then explore the effects of higher or lower trade costs.

3.4.1 Current Spatial Frictions

Spatial distribution of population and output per capita. Figure 3.6 depicts the log difference of population in 2200 between the baseline with climate change and a counterfactual exercise with constant temperatures. Although the impact of climate change on population across the world is large and heterogeneous, with some regions doubling and others reducing by half their 2200 population, it does not dramatically affect the geography of the world's main population centers.[12] Many of today's densest regions, such as western Europe, India, and eastern China, continue to be densely populated two centuries from now, whether the world experiences climate change or not. There are some significant climate-induced shifts though. Northern latitudes gain in population density, at the expense of regions such as the Arabian peninsula, northern India, western Australia, northern Africa, Brazil and Central America. In the regions that lose population, inland areas tend to be more impacted by rising temperatures than coastal areas. This could reflect temperatures rising less in regions close to oceans; it could also reflect the greater resilience of coastal agglomerations due to their better connectivity to the rest of the world.

In terms of real output per capita, Figure 3.7 shows that over the next two centuries the more northern latitudes of Canada and Siberia improve their lot because of rising temperatures, whereas sub-Saharan Africa becomes worse

---

[12]Because the variation in population density in the world in 2000 and 2200 is as large as 15 log points, changes by 1 log point do not drastically alter the density map.

FIGURE 3.6: Effect of Climate Change on Predicted Population in 2200
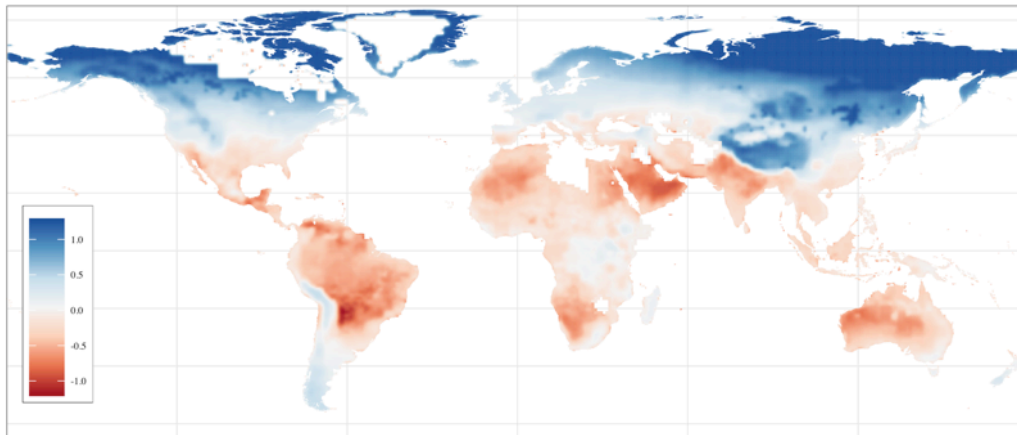
Note: Figure displays $\log(\bar{L}_{200}(r))$ under climate change minus $\log(\bar{L}_{200}(r))$ under no climate change.

off. The losses from climate change are more widespread in the case of real output per capita than in the case of population: almost all regions spanning the latitudes comprised between southern Africa to the south and the Mediterranean basin to the north lose output per capita. These more widespread losses are related to two factors. First, whereas the relocation of population is a zero-sum game, this is not the case with global output per capita. Second, the relocation of population is limited by mobility restrictions, implying that certain areas that suffer significant negative shocks to output per capita may lose relatively fewer people.

Sectoral specialization. What is the role of agriculture and non-agriculture in these geographic shifts? When considering agricultural output, Panels (a), (b) and (c) of Figure 3.8 show that over the next two centuries agriculture is predicted to experience increased geographic concentration. Climate change has a pronounced effect on where agriculture continues to be prominent. In the absence of rising temperatures, South America and sub-Saharan Africa maintain their importance, in addition to India, eastern China and eastern Europe. Today's developed world is predicted to specialize almost fully in non-agricultural sectors. With climate change, Canada emerges as a major agricultural producer, as do Russia and Central Asia. This comes at the expense of declining production in India, South America, and sub-Saharan Africa. The regions that gain from climate change are relatively cold areas with high fundamental productivity. Global warming reduces the temperature penalty they suffer, making them highly productive.

FIGURE 3.7: Effect of Climate Change on Real Output per Capita in 2200
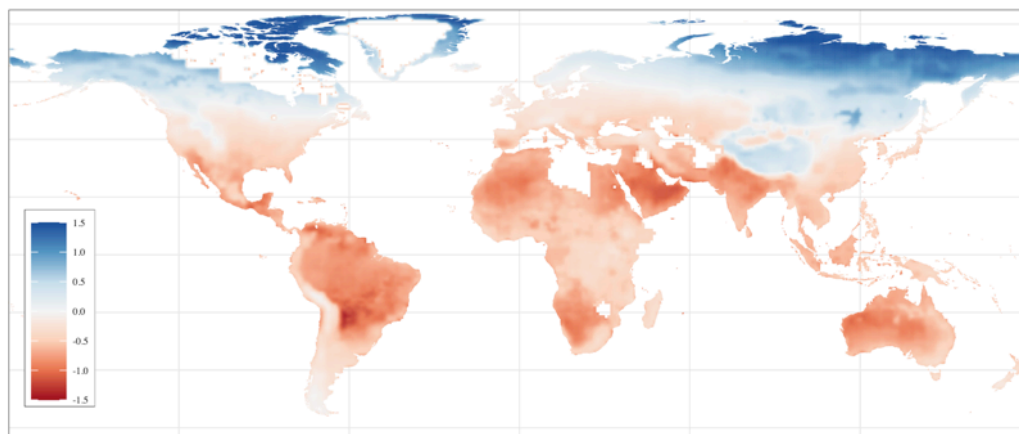
Note: Figure displays the log of real output per capita under climate change minus the log of real output per capita under no climate change in period 200.

With non-agriculture being less sensitive to rising temperatures than agriculture, we might have expected equatorial regions to become non- agricultural powerhouses. However, Figure 3.9 shows no evidence of this happening. Two reasons explain this. First, the optimal temperature for non-agriculture is lower than for agriculture, implying that any increase in temperature in equatorial regions leads to a loss in non-agricultural productivity. Second, their original productivity in non-agriculture is relatively low, and they are unable to catch up with more advanced economies.

When focusing on specialization patterns in terms of sectoral employment shares, Panels (a), (b) and (c) of Figure 3.10 confirm that the areas that specialize in agriculture become much more concentrated in space. While in the year 2000 we still have many locations with agricultural employment shares above 20% scattered around the globe, by the year 2200 areas of high agricultural specialization are limited to a few regions. In the absence of climate change, those regions are concentrated in South America, sub-Saharan Africa and India's Ganges Valley. With rising temperature, clusters of agricultural specialization shift to Central Asia, China and Canada.

Aggregate patterns. At the aggregate level, Panel (a) of Figure 3.11 shows that the growth rate of world real GDP per capita is predicted to increase from 2.2% annually in 2000 to 2.8% annually in 2200, further increasing to 3.0% by the year 2400.[13] Global warming leads to a loss in the level of world

---

[13]To sharpen the visualization of some of the very long-run trends, it is convenient to simulate the model for another 200 years, until the year 2400.

FIGURE 3.8: Agricultural Output
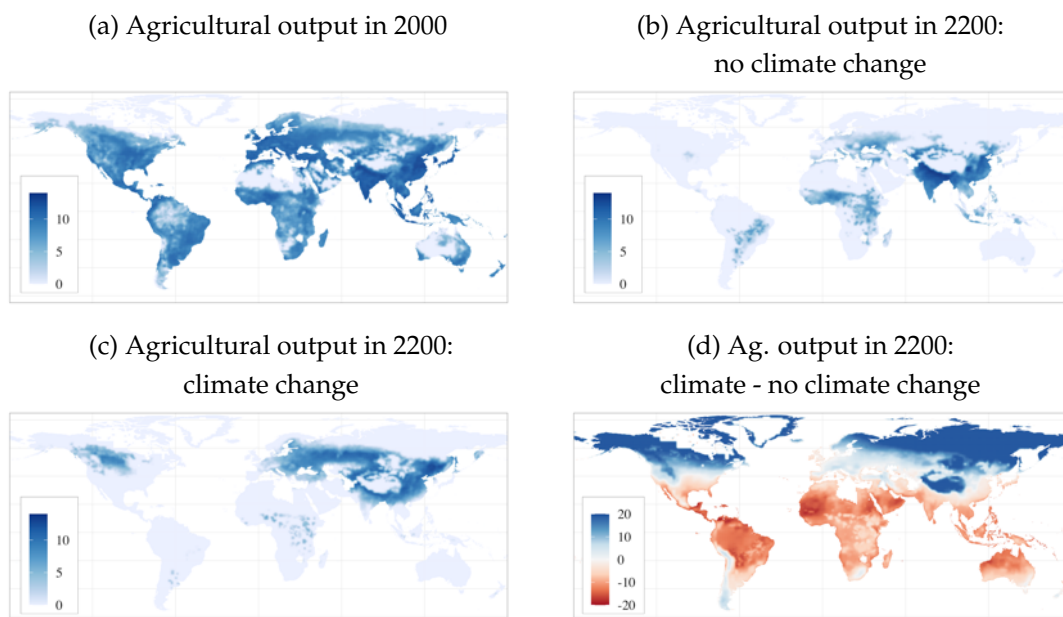
(a) Agricultural output in 2000

(b) Agricultural output in 2200:
no climate change

(c) Agricultural output in 2200:
climate change

(d) Ag. output in 2200:
climate - no climate change

Note: Panel (a) displays the log of agricultural output in period 1, Panel (b) displays the
log of agricultural output in period 200 under no climate change, Panel (c) displays the
log of agricultural output in period 200 under climate change, and Panel (d) displays
the log difference of agricultural output in period 200 with and without climate change.
In all panels agricultural output is normalized by average nominal wages in the world.

real GDP per capita of around 6% by the year 2200, increasing to around 9%
by the year 2400 (Panel (b)). In terms of world utility, Panel (a) shows that
its growth rate rises from 2.1% in 2000 to 2.7% in 2200 and 2.9% in 2400. The
losses due to global warming are greater than in the case of real GDP per
capita: more than 15% by 2200 and above 20% by 2400 (Panel (b)). To un-
derstand why losses from global warming are larger for utility than for real
income per capita, recall that utility takes into account amenities whereas
real GDP per capita does not. As global warming tends to benefit locations
at more polar latitudes which on average have worse amenities, rising tem-
peratures have a more negative effect on utility than on income per capita.[14]

Two other aggregate effects from global warming are worth mentioning.
First, Figure 3.12 Panel (a) shows that higher global temperatures lower the
growth rate of non-agricultural productivity, and increase the growth rate
of agricultural productivity. Given that agriculture is more sensitive to ris-
ing temperatures than non-agriculture, we might have expected the contrary.

---

[14]This effect would be mitigated if we allowed amenities to change with temperature as
in Alvarez and Rossi-Hansberg (2021).

FIGURE 3.9: Non-Agricultural Output
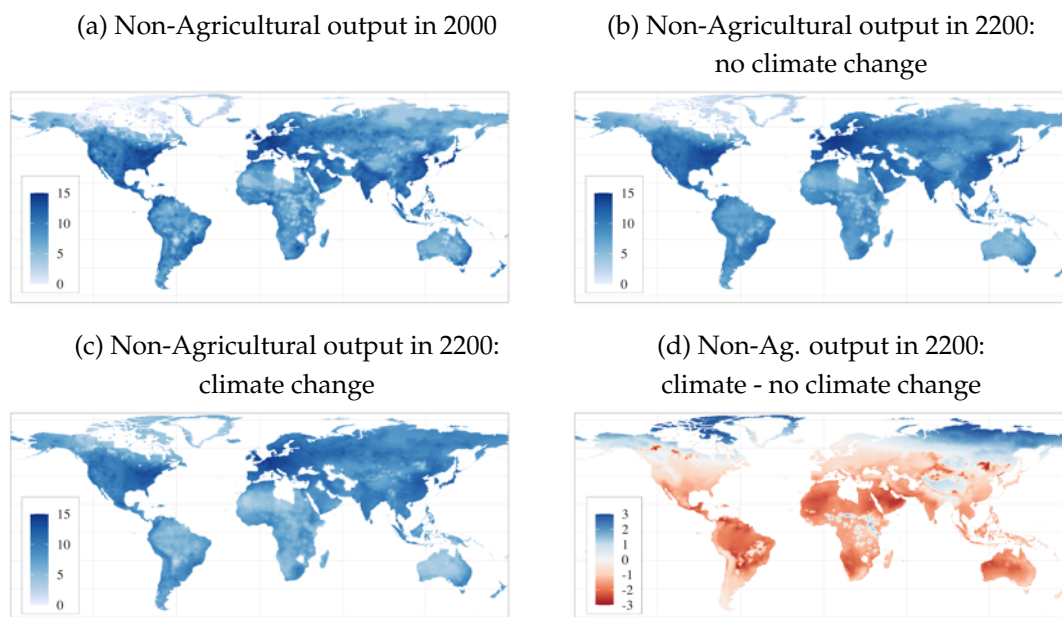
(a) Non-Agricultural output in 2000

(b) Non-Agricultural output in 2200:
no climate change

(c) Non-Agricultural output in 2200:
climate change

(d) Non-Ag. output in 2200:
climate - no climate change

Note: Panel (a) displays the log of non-agricultural output in period 1, Panel (b) displays the log of non-agricultural output in period 200 under no climate change, Panel (c) displays the log of non-agricultural output in period 200 under climate change, and Panel (d) displays the log difference of non-agricultural output in period 200 with and without climate change. In all panels agricultural output is normalized by average nominal wages in the world.

However, global warming shifts agriculture to areas with relatively high exogenous productivity. As an example, in a world without climate change, one of the regions with the highest agricultural employment share is northern India. Global warming shifts agricultural specialization to parts of Central Asia and Canada, which have higher fundamental agricultural productivity. Second, Figure 3.12 Panel (b) shows that climate change leads to lower agricultural employment. Given that our preferences are Cobb-Douglas in agriculture and non-agriculture, this is not a simple counterpart of the relative increase in agricultural productivity under climate change. Instead, it has to do with global warming pushing agriculture to regions where labor is relatively expensive. More specifically, Figure 3.8 shows that, with climate change, agricultural production moves to areas where land is abundant relative to labor (e.g. northern Canada, Russia, and Mongolia), so total agricultural employment falls. In contrast, without climate change, agriculture concentrates more in India, where labor is relatively abundant, so total agricultural employment increases.

FIGURE 3.10: Agricultural Specialization

(a) Agricultural specialization in 2000

(b) Ag. specialization in 2200: no climate change

(c) Ag. specialization in 2200: climate change

(d) Ag. spec. in 2200: climate - no climate change climate - no climate change
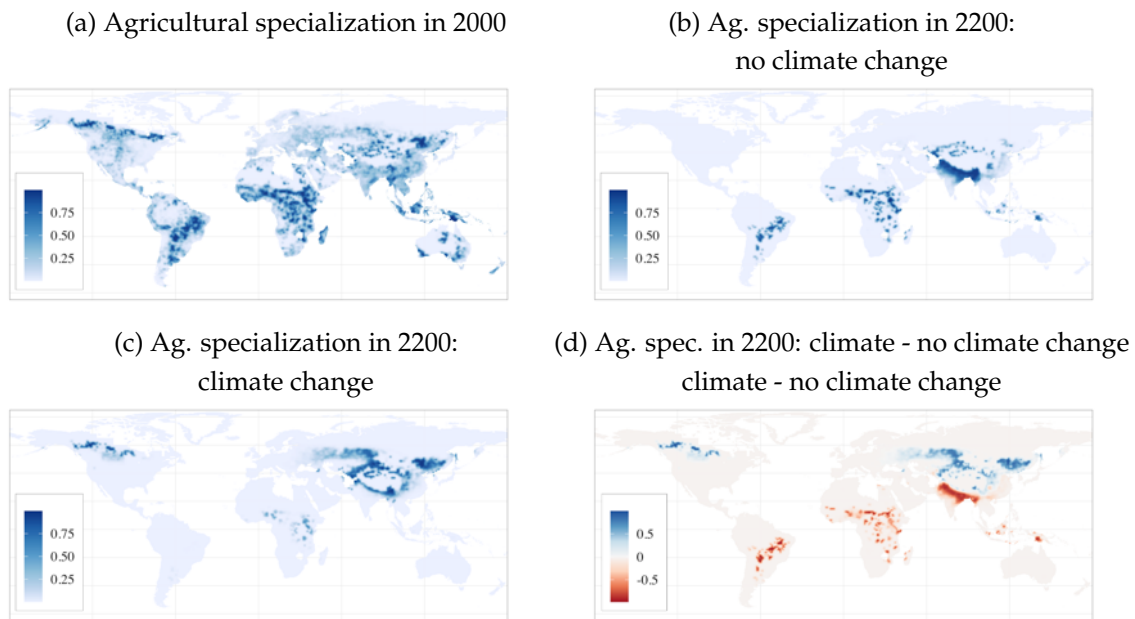
Note: Panel (a) displays share of labor employed in agriculture in period 1, Panel (b) displays the share of labor employed in agriculture in period 200 under no climate change, Panel (c) displays the share of labor employed in agriculture in period 200 under climate change, and Panel (d) displays the difference in the share of labor employed in agriculture with and without climate change in period 200.

FIGURE 3.11: Aggregate Real GDP per Capita and Utility: Growth Rates and Levels

(a) Growth rates with climate change

(b) Log difference: climate - no climate change
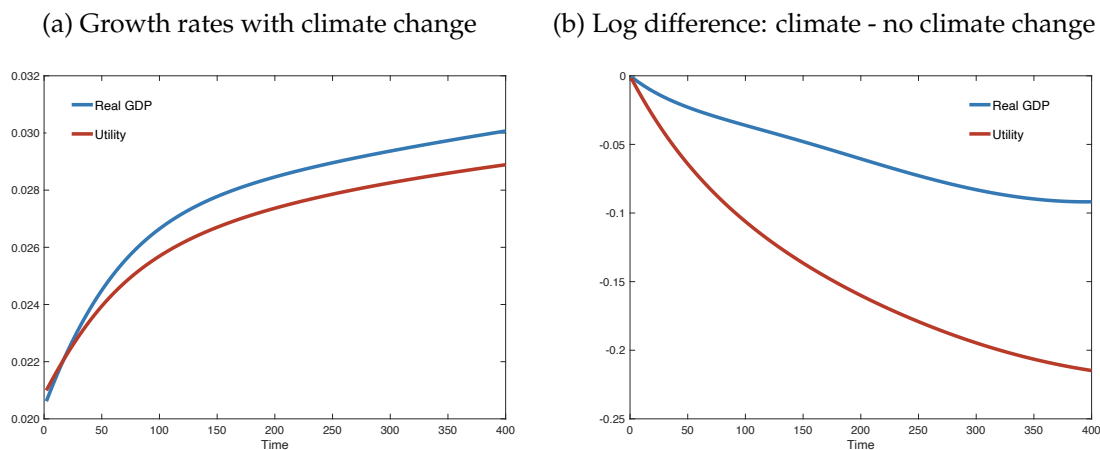
3.4.2 Trade Costs

We now explore how different levels of trade costs affect the world's economic geography. In particular, we compare a world with 50% higher trade costs to one with 50% lower trade costs.

FIGURE 3.12: Productivity Growth and Employment

(a) Productivity growth:
climate - no climate change

(b) Agricultural employment (billions)
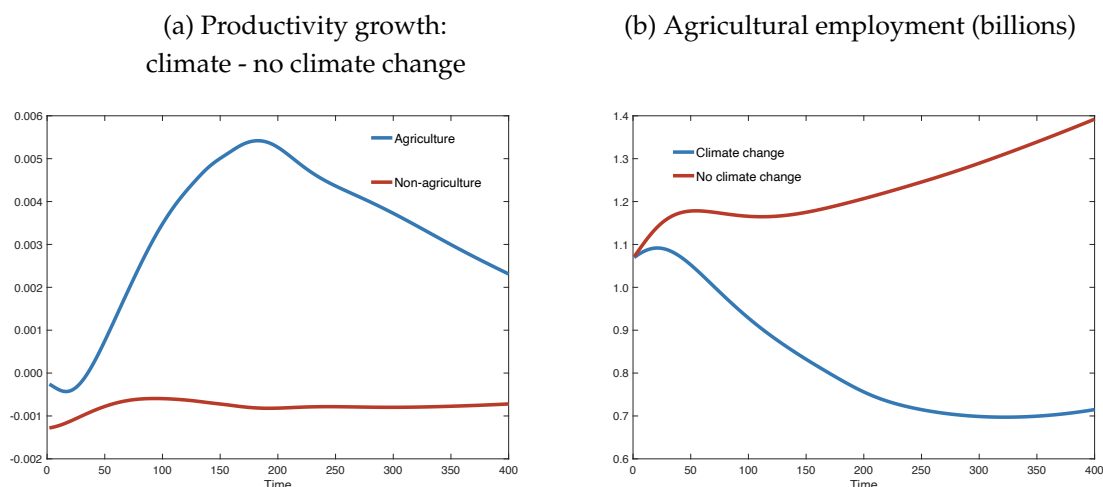
Spatial distribution of population and GDP per capita. Consider first the effect of trade costs on the spatial distribution of population in the year 2200 in a world with climate change. Figure 3.13 depicts the log difference in population when we increase trade costs by 50% relative to a scenario where we decrease them by 50%. As the figure shows, in a world with high transport costs, population is more concentrated in today's developed countries and regions, such as the U.S., Europe, and Japan. Living far from the main production centers becomes more costly, so population concentrates. This also explains why Africa, South America, and Australia all lose considerable fractions of their population in the high trade cost scenario.

Now consider the effect that trade costs have on the impact of climate change across the world. Figure 3.14 presents a difference-in-difference visualization of this effect. More specifically, it displays the difference between high and low trade costs in the climate-induced log difference in population in the year 2200. The figure shows that with high trade costs more people leave the areas that are estimated to suffer the most from global warming. That is, with higher trade costs we witness more relocation of people from regions closer to the Equator to areas closer to the poles. This suggests that trade and migration are substitutes. When faced with a climate-induced sectoral shock, higher trade costs limit the scope of locally adjusting by changing specialization. That makes adjusting through migrating relatively more attractive. The difference-in-difference graph for GDP per capita exhibits a very similar pattern, with production moving out of South America, Africa, and South Asia when trade costs are high, and concentrating in Canada and Siberia. We omit the map for brevity.

FIGURE 3.13: The Effect of Trade Costs on Population in 2200
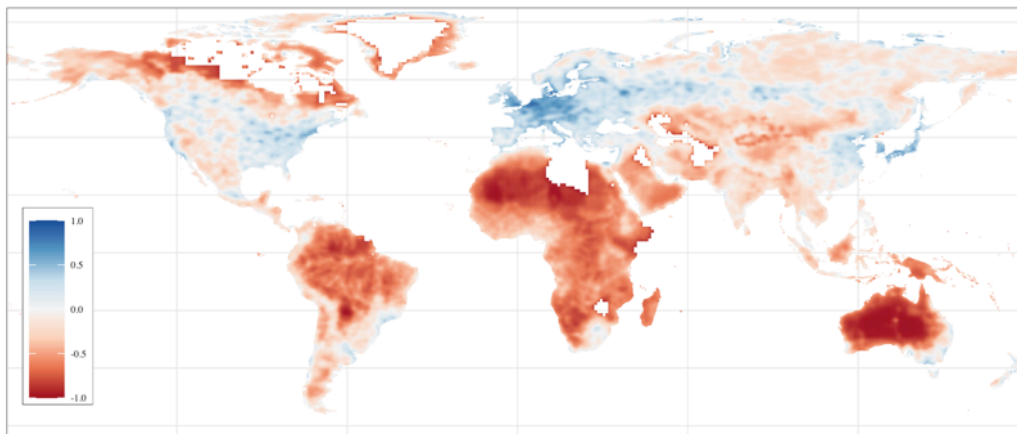
Note: Figure displays the difference in population with climate change in period 200, $\log(\bar{L}_{200}(r))$, with high (+50%) minus with low (-50%) trade costs.

FIGURE 3.14: The Impact of Trade Costs on the Effect of Climate Change on Population in 2200
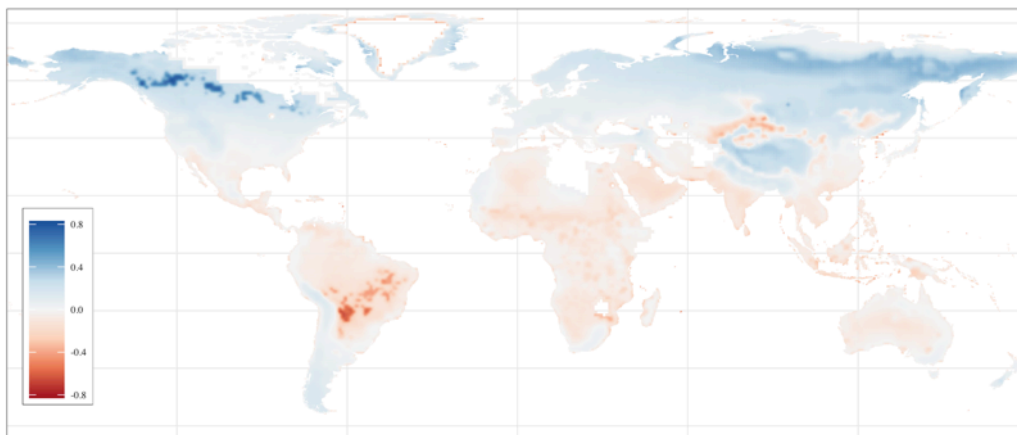
Note: Figure displays the difference with high (+50%) minus low (-50%) trade costs of the difference in $\log(\bar{L}_{200}(r))$ with minus without climate change

Sectoral specialization. Panels (a) and (b) of Figure 3.15 show that the predicted distribution of agricultural production in the year 2200 is more dispersed under high trade costs than under low trade costs, for the simple reason that people source goods from closer by. In particular, with high trade costs, Europe, North America, as well as parts of South America and sub-Saharan Africa, continue to be important agricultural producers. In addition, agriculture stretches into more northern latitudes of Siberia. When comparing climate change to no climate change in Panels (c) and (d), under low trade costs we see a resurgence of agriculture at moderate latitudes in Europe, Russia and North America. This resurgence is not present when trade

FIGURE 3.15: Agricultural Output and Trade Costs

(a) Agricultural Output: high trade costs

(b) Agricultural Output: low trade costs

(c) Effect of climate on ag. output:
high trade costs

(d) Effect of climate on ag. output:
low trade costs
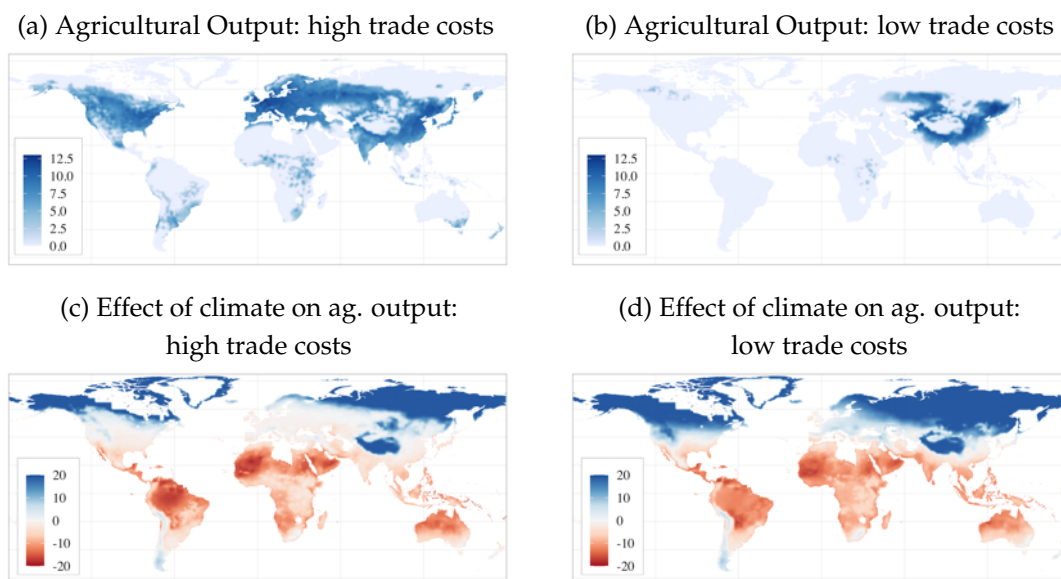
Note: Panel (a) displays log of agricultural output under climate change with +50% trade costs, Panel (b) displays log of agricultural output under climate change with -50% trade costs, Panel (c) displays log difference of agricultural output with and without climate change (+50% trade costs), Panel (d) displays log difference in agricultural output with and without climate change (-50% trade costs). In all panels agricultural output is normalized by average nominal wages in the world. All maps are for period 200.

costs are higher, because in that case these regions continue to be agricultural producers even in the absence of climate change.

When looking at the employment share in agriculture in the year 2200, Panels (a) and (b) of Figure 3.16 similarly display greater geographic dispersion under high trade costs. Rising temperatures lead to relocations that are also more spatially dispersed when trade costs are high. More specifically, in a world with high trade costs, agriculture relocates to many areas of East and Central Asia, as well as to more northern latitudes in Canada, whereas in a world with low trade costs, relocation occurs most prominently from northern India to parts of China and Central Asia. Note that the climate-induced resurgence of Europe and the US as agricultural producers if trade costs are low (Figure 3.15 Panel (d)) does not translate in a substantial increase in agricultural employment (Figure 3.16 Panel (d)), suggesting that these regions benefit from high-productivity agriculture that requires little labor.

When looking at non-agricultural output in Figure 3.17, higher temperatures lead to relocations to higher latitudes. There are some exceptions

FIGURE 3.16: Agricultural Specialization and Trade Costs
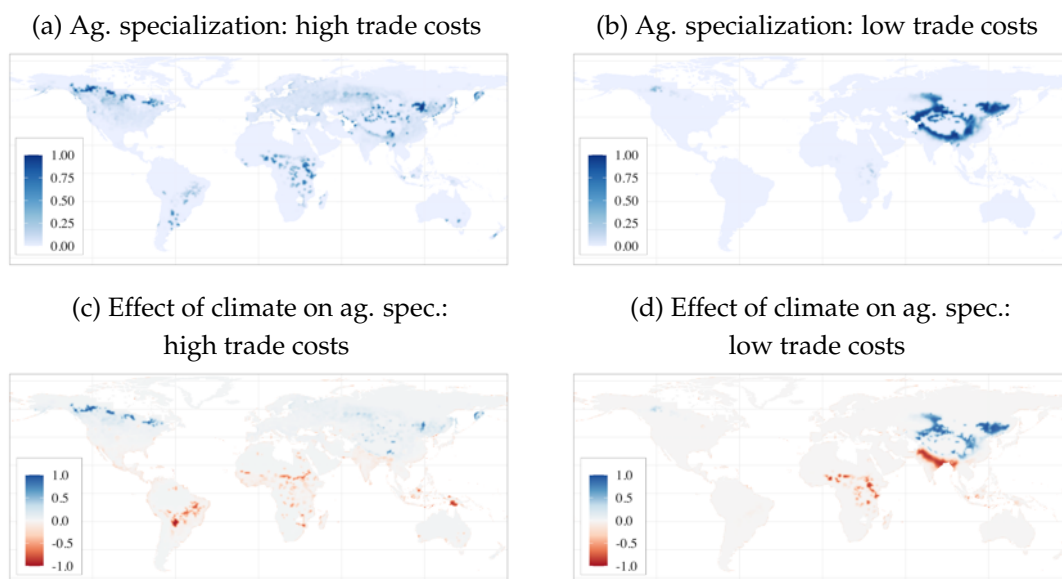
(a) Ag. specialization: high trade costs

(b) Ag. specialization: low trade costs

(c) Effect of climate on ag. spec.:
high trade costs

(d) Effect of climate on ag. spec.:
low trade costs

Note: Panel (a) displays share of agricultural employment under climate change with +50% trade costs, Panel (b) displays share of agricultural employment under climate change with -50% trade costs, Panel (c) displays difference in share of agricultural employment with and without climate change (+50% trade costs), Panel (d) displays difference in share of agricultural employment with and without climate change (minus $\log(\bar{L}_{200}(r))$ under no climate change with (-50% trade costs). All maps are for period 200.

FIGURE 3.17: Non-Agricultural Output and Trade Costs

(a) Effect of climate on non-ag. output:
high trade costs

(b) Effect of climate on non-ag. output:
low trade costs
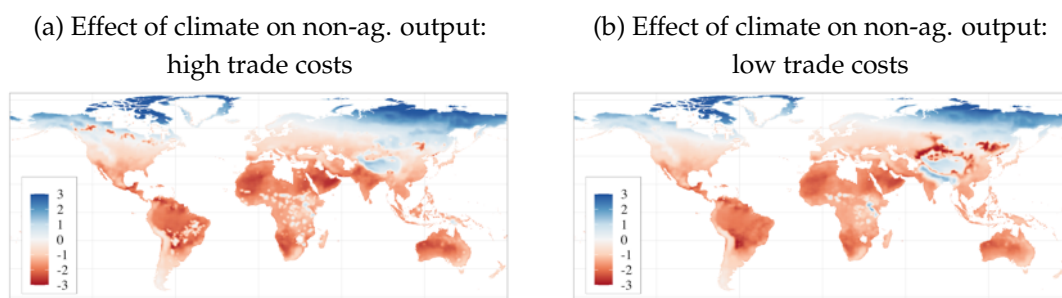
Note: Panel (a) displays log difference of non-agricultural output with and without climate change (+50% trade costs), Panel (b) displays log difference in non-agricultural output with and without climate change (-50% trade costs). In both panels non-agricultural output is normalized by average nominal wages in the world. Maps are for period 200.

though: under high trade costs, we see some areas in northern Canada losing non-agriculture, and a number of dispersed regions in Africa as well as the Tibetan Plateau gaining non-agriculture. These areas tend to be mirror images of the shifting specialization patterns observed in Figure 3.16

Panel (a). For example, northern Canada switches specialization, from non-agriculture to agriculture, whereas certain places in Africa experience the opposite, switching from agriculture to non-agriculture. The Tibetan Plateau is different: starting off with much lower temperatures, the rise in temperature increases its productivity, turning it into a region that experiences an important climate-induced increase in non-agricultural output. When comparing how climate-induced changes depend on trade costs, we observe a larger drop in non-agricultural output under low trade costs in the regions of China and Central Asia where world agricultural production becomes geographically concentrated.

Aggregate effects. By the year 2200 climate-induced losses in real GDP per capita are higher under low trade costs than under high trade costs, but this effect is reversed by the year 2400 (Figure 3.18 Panel (a)). On the one hand, with higher trade costs, there is less scope to respond to sector-specific climate shocks by changing specialization. This was evident from Figure 3.14 where we saw people adapt by migrating, rather than by shifting specialization, when trade costs are high. The lack of adaptation through trade makes a world with higher trade costs more vulnerable to climate change. On the other hand, with higher trade costs, Figure 3.13 showed that less people end up living in the warmest areas of the earth that suffer the most from temperature rises. This makes a world with higher trade costs less vulnerable to global warming. As Figure 3.18 Panel (a) shows, the second effect dominates for the first 300 years. Eventually, however, the concentration in agriculture

FIGURE 3.18: Aggregate Real GDP per Capita and Utility: Effect of Climate Change and Trade Costs

(a) Log real GDP per capita: climate - no climate change

(b) Log utility: climate - no climate change
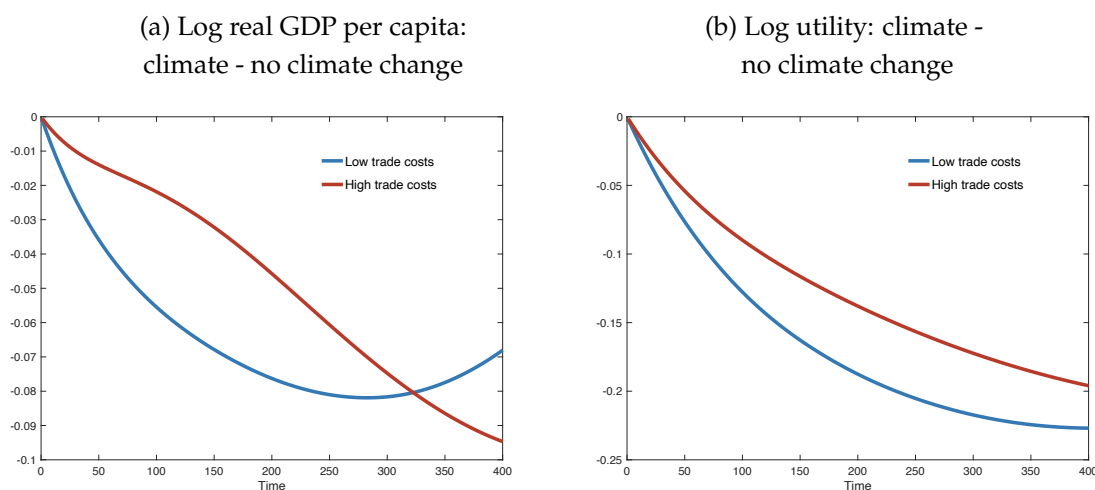
in northern latitudes makes lower trade costs a more important advantage.

When considering utility instead of real GDP per capita, as in Figure 3.18 Panel (b), the losses from climate change are smaller under high trade costs than under low trade costs throughout the 400 year period under investigation (though the difference between both narrows after 200 years). This points to a greater relocation of people and economic activity toward high-amenity locations under higher trade costs.

3.5 Conclusion

Global warming has heterogeneous effects across space, sectors, and time. Because climate shocks are location- and sector-specific, migration and trade are central to the economy's adjustment to rising temperatures. Convincingly assessing the local, sectoral, and aggregate economic effects of global warming therefore requires a multi-sector dynamic spatial model that incorporates migration and trade. This paper provides such a framework, and combines it with high-quality high-resolution data.

Under RCP 8.5, our results indicate that over a 200-year horizon rising temperatures push people and economic activity toward Siberia, Canada and Scandinavia. Because migration is costly, losses in real GDP per capita are geographically more widespread than losses in population. In a world without climate change, by the year 2200 clusters of agricultural specialization are found in Central Africa, Brazil, and India's Ganges Valley. Rising temperatures move these clusters toward Central Asia, northern Canada, and parts of China. Equatorial latitudes that suffer a relative decline in agricultural productivity fail to emerge as non-agricultural powerhouses. By the year 2200, predicted losses in real GDP and utility are, respectively, 6% and 15%. In spite of agriculture being more sensitive to temperature than non-agriculture, global warming increases agricultural productivity growth, while it decreases non-agricultural productivity growth. This unexpected result is due to rising temperatures shifting agriculture towards regions that become highly productive once the temperature increases enough.

Higher trade costs slow down the spatial concentration of agriculture. Because goods are sourced more locally, agriculture remains closer to the world's population centers. Trade and migration are substitutes. When faced with a climate shock, the scope to adjust through changing local specialization is smaller when trade costs are high, thus increasing the incentive to

move. Because migration tends to happen towards regions of relatively high productivity, higher trade costs generate smaller aggregate losses in real GDP than lower trade costs.

This paper can be extended in different directions. First, allowing for an elasticity of substitution between agriculture and non-agriculture of less than one would affect the world's vulnerability to climate change. For example, if agriculture experiences greater productivity gains than non-agriculture, it would lead to a shrinking share of employment in the sector that is most sensitive to global warming. Second, this paper has inevitably left many questions related to climate change unanswered. We have not investigated the impact of public policies, such as carbon taxes or innovation policies. Nor have we considered that climate change affects amenities. As the worlds warms, amenities in previously cold areas, such as Siberia, are bound to improve, whereas amenities in regions that already start out being very warm, will worsen. Another omission is having left out additional dimensions of climate change. Rising sea levels and more extreme weather phenomena, such as hurricanes, storm surges and droughts, are obvious examples. With adequate data, these aspects of climate change could be incorporated into the multi-sector dynamic spatial climate assessment model we have developed.

Appendix A

Appendix: Chapter 1

A.1 The Malian Context

TABLE A.1: Overview of Mali

	Most recent value	2004 value
Population (million)	19.08	12.37
Rural population (% of total population)	57.64	68.70
GDP per capita, PPP (constant 2011 USD)	2,056.00	1,710.11
Poverty headcount ratio at national poverty lines (% of population)	41.1	41.7
Life expectancy at birth (years)	67.48	51.22
Agriculture, forestry, and fishing, value added (% of GDP)	38.53	30.02

Data source: The World Bank country data. The most recent value for variables "Population", "Rural Population", "GDP per capita", "Life expectancy", "Agriculture, forestry, and fishing, value added" is year 2018. Since there is no available time series for variable "Poverty headcount ratio at national poverty lines", its most recent value is year 2009, while its 2004 value corresponds to year 2006.

FIGURE A.1: Desert locust breeding and invasion areas
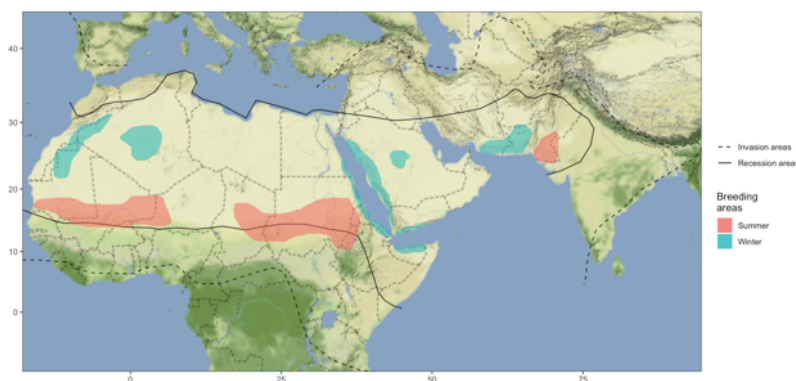
Note: Authors' calculation based on Cressman and Stefanski (2016)

FIGURE A.2: History of Locust Plagues
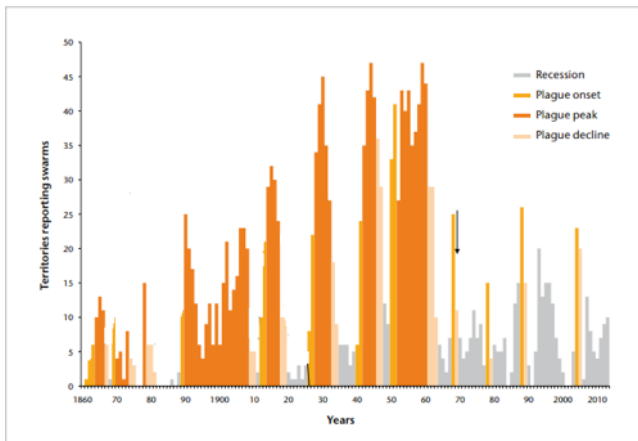
Source: Cressman and Stefanski (2016)

FIGURE A.3: Quarterly number of swarm events in Mali
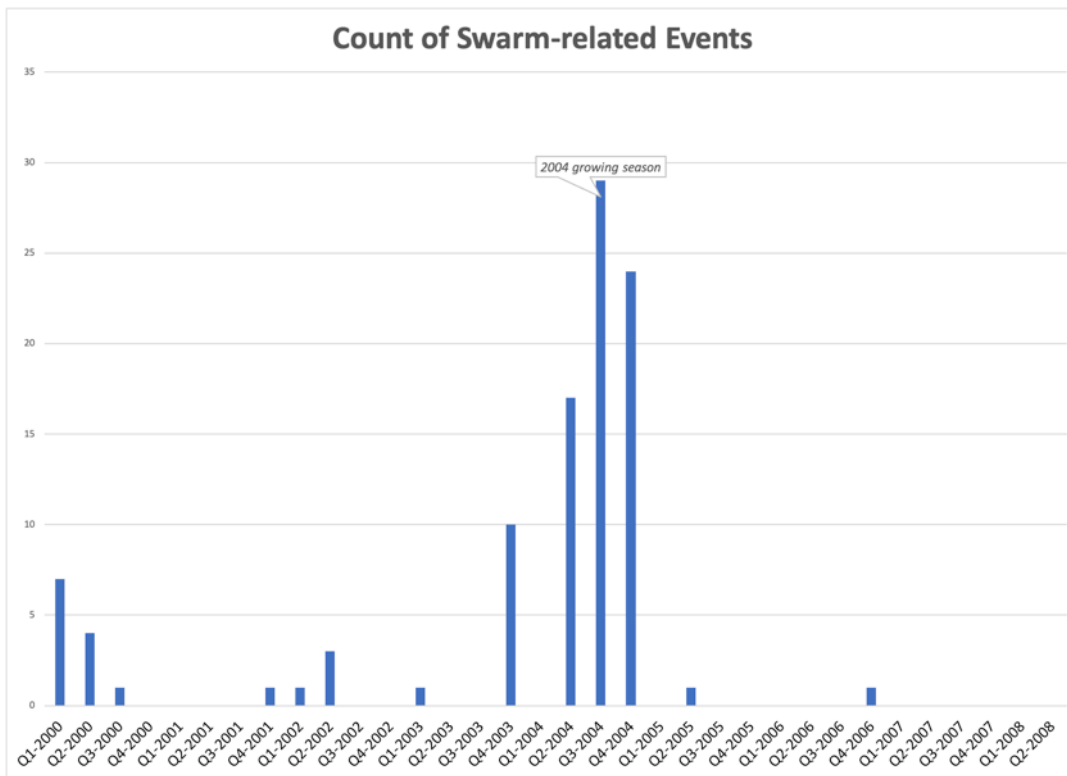
Source: SWARMS data base from FAO Desert Locust Information Service.

A.2   Climate Data

In order to account for potential weather-related omitted variables in our analysis, we collect data from the Standardized Precipitation Evapotranspiration Index (SPEI, see Vicente-Serrano et al., 2010). The SPEI is a multi scalar index that jointly maps rainfall, temperature and potential evaporation into a standardized index of drought. Importantly, it is measured in units of standard deviations from the long term average (1901 – 2015 in version 2.5), and has zero average by construction. It is available in a 0.5 x 0.5 grid, which is matched to the household coordinates available from the DHS surveys.

We want to control for exposure of individual pregnancies to food supply shocks due to weather conditions in our empirical specification. To do so we need to determine how weather affects each mother's nutritional intake during the 9 months in utero. We follow Kudamatsu et al. (2016) and focus on variations in SPEI index during the relevant growing seasons, as summarized by a simple index constructed as follows.

The relevant growing seasons of an individual birth depends on its timing relative to local harvest time. We weight the last 3 harvests before birth of cohort t (year-month) by the number of months that a pregnant woman will spend relying on each of them.

$$SPEI^{g,t} = \sum_{i=1}^{3} \omega_i S^{g,t}_{a(t)-i},$$

where $\sum_i \omega_i = 1$, $S^{g,t}_{a(t)}$ is average SPEI index in cell g during the growing season of the year in which children of cohort t are born. For example, children born in January of a given year a (conceived in April of previous year), spend 3 months relying on harvest from year $a - 1$ (October to December) and 6 months relying on the harvest of year $a - 2$ (April till September) so the weights are 0/9, 3/9 and 6/9 for $\omega_0, \omega_1, \omega_2$, respectively. The results are robust to using SPEI for the last 3 years as separate variables. They also do not change when we consider SPEI for the entire year.

A.3 Robustness of the Average Impact of Locust Plagues

In this Appendix, report the results of the robustness described in Section 1.6. We first test our definition of *treatment group*. We allow the threshold that defines a treated areas to vary between 20km to 70km, in steps of 2k; results are shown in Figure A.4. Moreover, we test the robustness of the results presented in Table 1.2 performing several robustness checks on alternative empirical specifications and data samples (described in Section 1.6). We present our results in Table A.2.

TABLE A.2: Heterogeneity: average impact of locust plague on child health

	(1) Years of residence	(2)	(3) Gender	(4)	(5) Place of residence	(6)
	2 + years	Always	Male	Female	Urban	Rural
In utero treatment	-0.405***	-0.504***	-0.536***	-0.337**	-0.331*	-0.473***
	(0.111)	(0.129)	(0.136)	(0.156)	(0.173)	(0.127)
Observations	8,811	4,995	4,654	4,519	2,694	6,479
R-squared	0.241	0.268	0.269	0.300	0.209	0.238
Cohort FE	YES	YES	YES	YES	YES	YES
Location FE	YES	YES	YES	YES	YES	YES
Child characteristics	YES	YES	YES	YES	YES	YES
Family characteristics	YES	YES	YES	YES	YES	YES
Mean dependent variable	-1.431	-1.449	-1.484	-1.364	-0.986	-1.607

Source: SWARMS data base from FAO Desert Locust Information Service and household survey data from 2006 DHS wave in Mali. Dependent variable is height-for-age Z-score. Full set of controls includes mother's height, education, gender and age of household head, household wealth index, SPEI index, birth order, time gap between conception and the previous and following pregnancies. Robust standard errors in parentheses are clustered at PRIO Cell grid level. *** p<0.01, ** p<0.05, * p<0.1. Column (1) and (2) report the results of the baseline specification (Column (3) of Table 1.2) restricting the sample to households that have reported living in the location where they were interview for at least 2 years, or since ever, respectively. Columns (3) restricts the sample to male children while column (4) uses only female ones. Columns (5) and (6) split the sample between urban and rural.

FIGURE A.4: Local impact of locust plague on child health
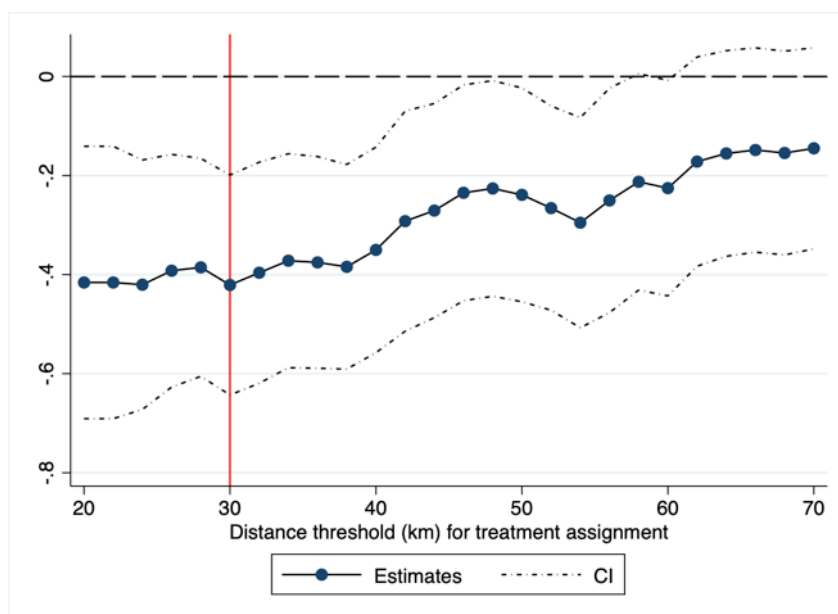
Source: SWARMS data base from FAO Desert Locust Information Service and DHS data, Mali wave 2006. The dependent variable in each specification is height-for-age Z-score. In each iteration we change the definition of treatment group: in the first specification an area treated if it is located at most 20 km from at least one swarm event; in the subsequent specifications we add progressively 2 km to the threshold that defines what is a treatment area, up to 70 km. For each of these specifications, we plot the estimates of the impact of locust plague on height-for-age Z-score (i.e., γ in Equation 1.1) together with their 95% confidence bands.

A.4 Additional Analyses

TABLE A.3: Additional analyses: impact of locust plague on child health

	(1)	(2)	(3)	(4)	(5)	(6)	(7)	(8)
Treatment with 30 km ring	-0.182**	-0.336***	-0.476***			-0.333***	-0.287***	
	(0.082)	(0.120)	(0.085)			(0.101)	(0.106)	
Treatment at municipality level				-0.327***				
				(0.117)				
Treatment including swarms beyond country borders					-0.392***			
					(0.113)			
Placebo treatment								0.150
								(0.195)
Observations	9,173	9,173	9,173	9,173	9,173	14,209	9,059	4,182
R-squared		0.247	0.2	0.238	0.239	0.226	0.257	0.346
Number of mother	6,953							
Cohort FE	YES	YES	YES	YES	YES	YES	YES	YES
Mother FE	YES							
Child characteristics	YES	YES	NO	YES	YES	YES	YES	YES
Location FE		YES	YES	YES	YES	YES	YES	YES
Family characteristics		YES	NO	YES	YES	YES	YES	YES
Mean dependent variable	-1.425	-1.425	-1.425	-1.426	-1.425	-1.284	-1.117	-1.276

Source: SWARMS data base from FAO Desert Locust Information Service and household survey data from 2006 DHS wave in Mali. The dependent variable in all regression are the children's height-for-age Z-scores. Robust standard errors in parentheses are clustered at enumeration area level. *** p<0.01, ** p<0.05, * p<0.1. Column (1) to (4) use data from the 2006 wave. Column (1) shows results for a specification with mother fixed-effects. Coulumn (2) is equivalent of our main specification in Column (3) Table 1.2, but using DHS survey sample weights. Column (3) shows baseline resutls with no controls allowing for spatial HAC standard errors as in Conley (1999). Column (4) defines treatment area at municipality level. Column (5) adds events that occurred beyond the borders of Mali to define treatment areas. Column (6) uses data from 2006 and 2012 DHS survey waves. Column (7) restrict the previous sample to children born after June 2004. Column (8) is a placebo specification that uses only data from the 2012 DHS survey wave and treated children are those born in locust affected areas after 2010 (in 2011 or 2012).

TABLE A.4: Impact of locust plague on neo-natal and infant mortality

	death < 1 month		death < 12 month	
	(1)	(2)	(3)	(4)
In utero treatment	0.007	0.007	-0.005	-0.003
	(0.010)	(0.010)	(0.019)	(0.018)
Observations	24,189	24,189	22,638	22,638
R-squared	0.073	0.074	0.112	0.113
Cohort FE	YES	YES	YES	YES
Location FE	YES	YES	YES	YES
Child characteristics	YES	YES	YES	YES
Family characteristics	YES	YES	YES	YES
Region specific time trend	N0	YES	N0	YES
Mean dependent variable	0.0499	0.0499	0.122	0.122

Source: SWARMS data base from FAO Desert Locust Information Service and household survey data from 2006 DHS wave in Mali. Dependent variable is dummy equal 1 for children who die within the first month for n'eo-natal mortality and within the first year for infant mortality. Full set of controls includes mother's height, education, gender and age of household head, household wealth index, SPEI index, birth order, time gap between conception and the previous and following pregnancies. Robust standard errors in parentheses are clustered at PRIO Cell grid level. *** $p<0.01$, ** $p<0.05$, * $p<0.1$.

A.5   Local Crop Price Evolution

We provide additional evidence of the occurrence of local inflation during the speculative effect period in locust affected areas. We run an alternative version of Equation (1.2) that splits the treatment variable by quarter around the year of the plague. Results are depict in Figure A.5 below.

FIGURE A.5: Local impact of the locust plague on crop prices by year–quarter.
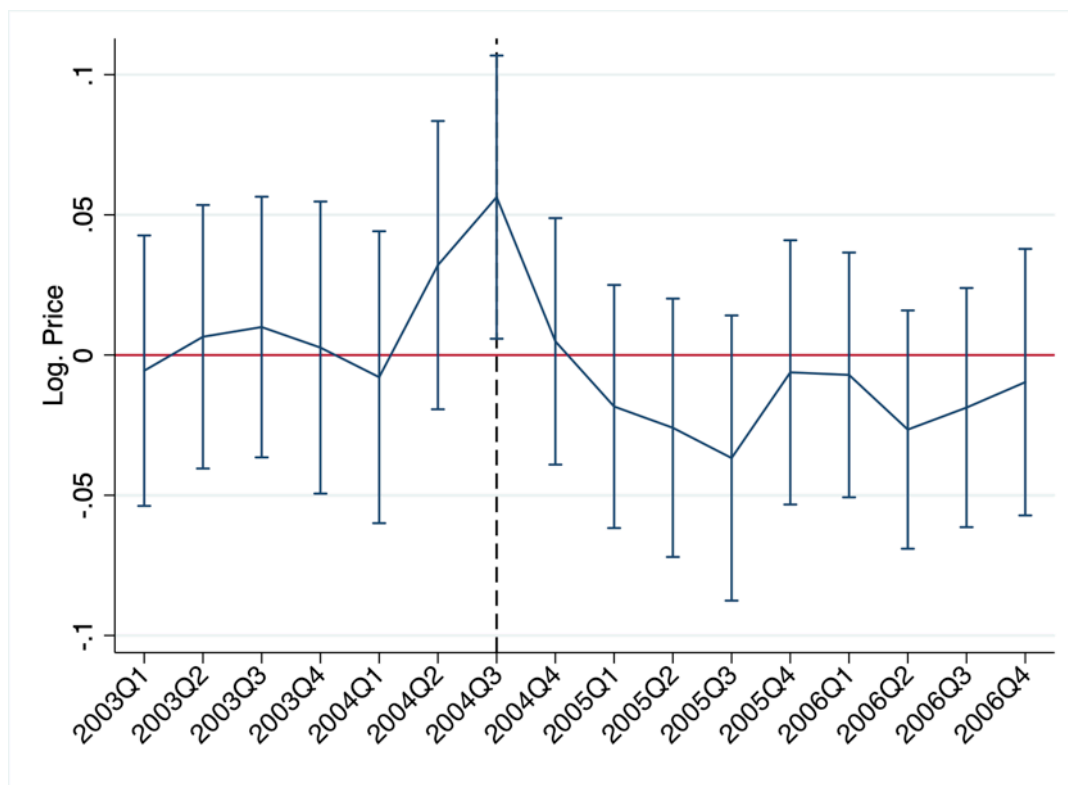
Source: OMA price data Mali and SWARMS data base from FAO Desert Locust Information Service. The dependent variable is monthly (log-) price of sorghum, millet, rice, and mais characterizing each local market m present in the OMA database. The regressors are interactions quarter dummies between 2000 and 2015 and a dummy that equals 1 if market m is located within a 30km radius from a locust invasion event. We plot coefficients related to years 2003-2006.

A.6 Exploring Further the Role of Market Access

In this Appendix, we use a binary definition of market access, based on the travel distance measure described in Section 1.6.5. In particular, we denote as isolated households located in DHS clusters belonging to the the top quartile of the travel distance distribution, i.e. above the 75th percentile, as shown in Figure 1.1, Panel B. We use this definition in Table A.5 to perform robustness checks of results reported in Table 1.5.

TABLE A.5: Impact of the locust plague on child health and market isolation

	Place of residence: urban areas			Place of residence: rural areas		
	(1)	(2)	(3)	(4)	(5)	(6)
		Lives in isolated areas			Lives in isolated areas	
		NO	YES		NO	YES
Teatment with speculative price effect	-0.568*	-0.453	-1.859***	-0.469**	-0.146	-1.159***
	(0.337)	(0.404)	(0.594)	(0.223)	(0.330)	(0.332)
Treatment with both	-0.291	-0.298	-0.462	-0.261*	-0.241	-0.592
	(0.213)	(0.254)	(0.464)	(0.142)	(0.153)	(0.360)
Treatment with crop failure effect	-0.267	-0.274	-0.153	-0.438***	-0.307*	-1.123***
	(0.259)	(0.282)	(0.767)	(0.148)	(0.167)	(0.325)
Treatment with speculative price effect × travel time	-0.282			-0.049		
	(0.334)			(0.081)		
Treatment with both × travel time	-0.126			-0.130***		
	(0.099)			(0.019)		
Treatment with crop failure effect × travel time	0.107			-0.174***		
	(0.296)			(0.028)		
Observations	2,694	2,203	491	6,479	4,316	2,163
R-squared	0.209	0.223	0.259	0.240	0.260	0.236
Cohort FE	YES	YES	YES	YES	YES	YES
Location FE	YES	YES	YES	YES	YES	YES
Child characteristics	YES	YES	YES	YES	YES	YES
Family characteristics	YES	YES	YES	YES	YES	YES

Source: SWARMS data base from FAO Desert Locust Information Service and household survey data from 2006 DHS wave in Mali. *** $p<0.01$, ** $p<0.05$, * $p<0.1$. The dependent variable in all regression are the children's height-for-age Z-scores. Full set of controls includes mother's height, education, gender and age of household head, household wealth index, SPEI index, birth order, time gap between conception and the previous and following pregnancies. Households are defined as isolated (green triangles) if in the bottom quartile of the distribution of market access of each of the measures.

Appendix B

Appendix: Chapter 2

This appendix contains additional material related to the main text. In particular, appendix B.1 documents theoretical derivations that support the main results of Section 2.4. Appendix B.2 provides more details about the data sources mentioned in Section 2.2 and other data sources not mentioned therein. Appendix B.3 contains additional figures and tables.

B.1 Theory appendix

B.1.1 Derivation of shipping prices

The representative firm in location i uses labor as the unique input of a linear production technology. Locations trade with one another; following the iceberg-like formulation of trade costs, the quantity of a good from sector k produced by the representative firm from i shipped to location j is

$$q_{ij}^k = \frac{b_i^k A_i^k L_i^k}{\tau_{ij}}.$$

Thus, the representative firm solves

$$\max_{L_i^k} p_{ij}^k \frac{b_i^k A_i^k L_i^k}{\tau_{ij}} - w_i L_i^k \quad \forall k.$$

As a constant returns to scale problem, the solution is straight-forward: at an interior optimum, shipping prices will equal marginal shipping costs, i.e.

$$p_{ij}^k = \left(\frac{w_i}{b_i^k A_i^k} \right) \tau_{ij} \quad \forall i, j, k. \tag{B.1}$$

B.1.2 Derivation of bilateral trade shares

When maximizing welfare with respect to consumption of varieties, worker v solves

$$\max_{\{q_{ji}^k\}_{j,k}} \left(\sum_{k \in \mathcal{K}} (C_i^k)^{(\eta-1/\eta)} \right)^{\eta/\eta-1} \varepsilon_i(v) \quad \text{s. to} \quad \sum_{j \in \mathcal{S}} \sum_{k \in \mathcal{K}} p_{ji}^k q_{ji}^k \leq w_i \quad \forall i,$$

where $C_i^k = \left(\sum_{j \in \mathcal{S}} (q_{ji}^k)^{\frac{\sigma-1}{\sigma}} \right)^{\frac{\sigma}{\sigma-1}}$. Suppose first workers choose sector composites; i.e. taking first order conditions with respect to C_i^k (μ stands for the Lagrange multiplier):

$$\frac{\eta}{\eta-1} w_i^{1/\eta-1} \frac{\eta-1}{\eta} (C_i^k)^{-1/\eta} - \mu P_i^k \leq 0 \quad \forall i,j, \quad = 0 \text{ for interior solution.} \rightarrow$$

$$(C_i^k)^{\frac{-1}{\eta}} = \mu P_i^k \times w_i^{1-\eta} \quad \forall i,j, \tag{B.2}$$

Then, one can write ratio of two sector consumptions as

$$\frac{C_i^k}{C_i^s} = \left(\frac{P_i^k}{P_i^s} \right)^{-\eta} \quad \rightarrow \quad C_i^k = \left(\frac{P_i^k}{P_i^s} \right)^{-\eta} \times C_i^s \quad \forall i,j,s. \tag{B.3}$$

Then, by defining μ_i^k as the share of i's spending in k-sector goods and making use of eq. (B.3),

$$\mu_i^k = \frac{P_i^k C_i^k}{\sum\limits_{k \in \mathcal{K}} P_i^s C_i^s} = \frac{P_i^k (P_i^k/P_i^s)^{-\eta} C_i^s}{\sum\limits_{k \in \mathcal{K}} P_i^j (P_i^j/P_i^s)^{-\eta} C_i^s} = \left(\frac{P_i^k}{P_i} \right)^{1-\eta} \quad \forall i,j,$$

where the last equation takes advantage of the definition of the price index from eq. (2.8). By proceeding analogously for the choice of crop varieties (q_{ji}^k), one finds that the share of spending on each location variety is defined as eq. (2.5).

B.1.3 Derivation of population shares

Take the definition of the welfare attained by a worker v living in i and moving to j as $W_i(v) = (w_i/P_i)\varepsilon_i(v)$, $\varepsilon_i \sim G_i(v) = e^{-v^{-\theta}u_i}$.[1] Following Eaton and Kortum (2002), one can obtain the distribution of the welfare from one

---

[1] For the sake of neatness, I omit the congestion forces present in the main model; i.e. I assume that $\alpha = 0$. The results are analogous if otherwise.

specific location i as

$$A_i(w) \equiv \mathbb{P}(W_i \le w) = G_j(w \times P_i/w_i) = e^{-(w \times P_i/w_i)^{-\theta}u_i}.$$

Thus, the joint distribution of welfare of all destinations from i can be derived as

$$A(w) = \prod_{i \in S} e^{-(w \times P_i/w_i)^{-\theta}u_i} = e^{-\Phi \times w^{-\theta}}, \quad \text{where } \Phi = \sum_{i \in S}(P_i/w_i)^{-\theta}u_i.$$

Now, recalling the share of workers living in i is equivalent to the probability that the welfare attained at i, w, is the highest among all other locations, one writes

$$\Pi_i(w) = \mathbb{P}\left(W_i(v) \equiv w \ge \max\{W_j(v)\}_{j \ne i}\right) = \prod_{j \ne i} \mathbb{P}(W_j \le w) = e^{-\Phi^{-i} \times w^{-\theta}}.$$

With that, it is possible to obtain the unconditional probability Π_i by integrating over all possible values of $w \in \mathbb{R}_+$, i.e.

$$\begin{aligned}
\Pi_i &= \int_0^\infty \Pi_i(w) \, d\mathbb{P}(W_i \le w) \, dw \\
&= \int_0^\infty e^{-\Phi^{-i} \times w^{-\theta}} \times \left(e^{(w \times P_i/w_i)^{-\theta}u_i}(-\theta)w^{-\theta-1}(P_i/w_i)^{-\theta}u_i\right) dw \\
&= u_i\left(\frac{P_i}{w_i}\right)^{-\theta} \times \int_0^\infty e^{-\Phi \times w^{-\theta}}(-\theta)w^{-\theta-1}dw; \quad \text{multiply/divide by } \Phi \\
&= u_i\left(\frac{P_i}{w_i}\right)^{-\theta}\frac{1}{\Phi} \times \underbrace{\int_0^\infty \overbrace{e^{-\Phi \times w^{-\theta}}\Phi(-\theta)w^{-\theta-1}}^{dA(w)} dw}_{=1} \\
&= \frac{(w_i/P_i)^\theta u_i}{\sum_{j \in S}(w_j/P_j)^\theta u_j},
\end{aligned}$$

which is the equivalent of eq. (2.13) without congestion forces.

B.1.4 Numerical algorithm for solving the model

To solve for the model's spatial equilibrium, I use a fixed-point approach starting from eq. (2.16). In particular, one can re-write it as

$$w_i L_i = \sum_{j \in S} \sum_{k \in \mathcal{K}} (P_j^k / P_j)^{1-\eta} \left(\frac{w_i \tau_{ji}}{b_i^k A_i^k P_j^k} \right)^{1-\sigma} w_j L_j$$

$$w_i^\sigma = L_i^{-1} \sum_{j \in S} \sum_{k \in \mathcal{K}} (P_j^k / P_j)^{1-\eta} \left(\frac{\tau_{ji}}{b_i^k A_i^k P_j^k} \right)^{1-\sigma} w_j L_j \rightarrow$$

$$w_i \equiv g_i(\mathbf{w}) = \left[L_i^{-1} \sum_{j \in S} \sum_{k \in \mathcal{K}} (P_j^k / P_j)^{1-\eta} \left(\frac{\tau_{ji}}{b_i^k A_i^k P_j^k} \right)^{1-\sigma} w_j L_j \right]^{1/\sigma}. \quad \text{(B.4)}$$

Noting that prices and labor are all explicit function of wages (eqs. (2.17) to (2.19)), starting from an initial guess of $\mathbf{w}$, eq. (B.4) provides an updated, model implied value of it. By iterating this procedure until the differences between steps are sufficient small, I solve for optimal wages up to a normalization. I then use the values found to solve for optimal prices and labor distributions in Equations (2.17) to (2.19).

B.1.5 Model inversion

I invert the spatial equilibrium of my model to back out the unobserved non-agricultural productivities, $\mathbf{A^K} \equiv \{A_i^K\}_i$, and productivity shifters for all sectors, $\mathbf{b^k} \equiv \{b_i^k\}_{i,k}$. First, to quantify $\mathbf{A^K}$, one can use eq. (2.16) to write

$$w_i L_i = \sum_{j \in S} \sum_{k \in \mathcal{K}} \left(\frac{P_j^k}{P_j} \right)^{1-\eta} \left(\frac{w_i \tau_{ij}}{b_i^k A_i^k P_j^k} \right)^{1-\sigma} w_j L_j$$

$$w_i L_i = \sum_{j \in S} \sum_{k \neq K} \left(\frac{P_j^k}{P_j} \right)^{1-\eta} \left(\frac{w_i \tau_{ij}}{b_i^k A_i^k P_j^k} \right)^{1-\sigma} w_j L_j + \sum_{j \in S} \left(\frac{P_j^K}{P_j} \right)^{1-\eta} \left(\frac{w_i \tau_{ij}}{b_i^K A_i^K P_j^K} \right)^{1-\sigma} w_j L_j \rightarrow$$

$$A_i^K \equiv g_i(\mathbf{A^K}) = \left[\frac{w_i L_i - \sum_{j \in S} \sum_{k \neq K} \left(P_j^k / P_j \right)^{1-\eta} \left(w_i \tau_{ij} / b_i^k A_i^k P_j^k \right)^{1-\sigma} w_j L_j}{\sum_{j \in S} \left(P_j^K / P_j \right)^{1-\eta} \left(w_i \tau_{ij} / b_i^K P_j^K \right)^{1-\sigma} w_j L_j} \right]^{1/\sigma-1},$$

$$\text{(B.5)}$$

i.e. an expression for A_i^K as a function of all exogenous parameters, endogenous variables $\{w_i, L_i\}_{i \in S}$, fundamental productivities, and producitivity shifters. Amenities are not accounted conditional on observing labor distribution. Therefore, for an initial guess for $\mathbf{A^K}$, eq. (B.5) provides updated, model implied optimal values for $\mathbf{A^K}$ itself.

Subsequently, one can analogously solve Equation (2.10) for $\mathbf{b^k}$ as follows:

$$X_i^k = \sum_{j \in S} \left(\frac{P_j^k}{P_j} \right)^{1-\eta} \left(\frac{w_i \tau_{ij}}{b_i^k A_i^k P_j^k} \right)^{1-\sigma} w_j L_j, \rightarrow$$

$$b_i^k \equiv f_i(\mathbf{b^k}) = \left[X_i^k / \sum_{j \in S} \left(\frac{P_j^k}{P_j} \right)^{1-\eta} \left(\frac{w_i \tau_{ij}}{A_i^k P_j^k} \right)^{1-\sigma} w_j L_j \right]^{1/\sigma - 1} \tag{B.6}$$

Equations (B.5) and (B.6) provide to fixed–point solutions for $\{\mathbf{A^K}, \mathbf{b^k}\}$, conditional on observing endogenous variables $\{w_i, L_i, X_i^k\}_{i,k}$. As they both depend on one another, my algorithm consists of solving them sequentially, starting from an initial guess, until they both hold (i.e. until the difference between left and right hand sides are sufficiently small in both equations).

Importantly, given my model structure, I cannot separately identify in my estimation b_i^K from A_i^K; i.e. the fundamental producitvity and shifter of the non–agricultural sector. Therefore, it requires me to normalize $b_i^K = 1 \; \forall i$, so that the parameter that I identify in Equation (B.5) stands for the product of them. Moreover, the shifters I quantify with Equation (B.6) have a relative interpretation, that is, with respect to the shifter of the non–agricultural sector whose level I cannot pin down.

B.2 Data appendix

Several sources of data were put together for the purpose of this project. Here I describe in some more detail some of the sources detailes in section 2.2, and provide information of auxiliar data not mention thereof. A summary of all data sources used and their temporal coverage is described in Table B.1.

TABLE B.1: Main data sources

Type of data	Coverage	Source
GDP and Population	2000	G-Econ Project v4.0 (Nordhaus et al., 2006a)
Population	1975, 2000	Global Human Settlements Project (Florczyk et al., 2019)
Population projections	2021 – 2100	United Nations and Social Affairs (2019)
Area Harvested/Crop	2000	GAEZ v3.0 (IIASA and FAO, 2012)
Agric. Productivities	1960–2000	GAEZ v3.0 (IIASA and FAO, 2012)
Climate Δ projections	2020, 2050, 2080	GAEZ v3.0 (IIASA and FAO, 2012)
Transportation data	2000	gROADS project (CIESIN, 2013)
Friction transportation surface	2000	Accessibility to Cities' project (Weiss et al., 2018)
Bilateral crop trade data	2000–2010	COMTRADE (COMTRADE, 2010)

B.2.1 GAEZ agro-climatic yields.

The GAEZ's database provides estiamtes of agricultural potential yields for several crops, in different time periods, and for different degrees of technology usage in agriculture. As my interest in subsistence agriculture setup of SSA, I aim at building a time varying dataset of potential yields over the entire subcontinent, for several crops, at low usage of modern inputs: with rainfed water access, labor intensive techniques, and no application of of nutrients, no use of chemicals for pest and disease control and minimum conservation measures.

A challenge, however, is that the time varying potential yields from GAEZ are available only for **high usage of modern inputs** (based on improved high yielding varieties, fully mechanized with low labor intensity techniques, and usage of optimum applications of nutrients and chemical pest, disease and weed control). The estimates for different input levels are only available for the long–run estimates (averages between 1960–1990).

Therefore, to obtain a time varying dataset of the agro–climatic yields at low input usage, I first use the long–run values to calculate the GAEZ–implied ratio between high inputs $(A_i^{k,h})$ / low inputs $(A_i^{k,l})$ yields for each crop. This procedures reveals how the gains from adopting higher input levels differ across locations and crops – Figure B.1 illustrates the results for two selected crops in deciles. I use the calculated ratios to scale down the time varying estimates for high inputs that I collect.

Armed with the location–crop technology scales, I collect the time varying estimates of agro–climatic yields for high input usage. For the estimates in the past, retrieve those for 1971–1975 and 1996–2000. I average out the 5 years' blocks so to avoid year-specific outliers. The reason is to capture long term changes, which could be contaminated if a certain year faces unusual climate conditions.

FIGURE B.1: Yield gains from adoption of high inputs in agriculture vis–à–vis low inputs for selected crops.

Panel A: Gains for adoption of high inputs for rice   Panel B: Gains for adoption of high inputs for sorghum
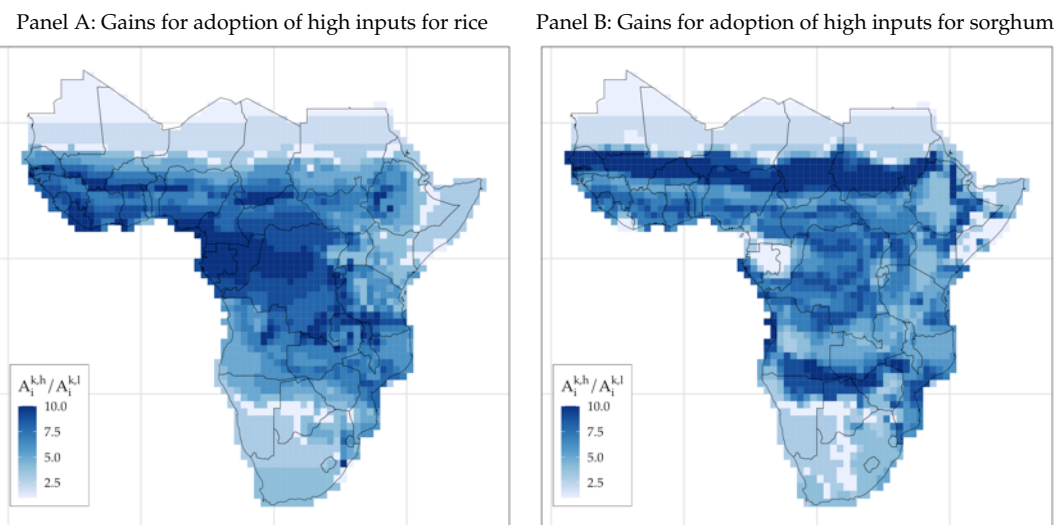
Notes: Panels A and B show the ratio of high/low input usage yields for growing two selected crops according to GAEZ long–run estimates. The values are shown in deciles; 1 (10) stands for the bottom (top) decile of each sample.

The yield estimates for future periods require another parametrical selection: the underlying scenario for which the data is produced and with which climatic (general circulation) model (GCM) the data is produced. As carefully discussed by Costinot et al. (2016a), the GAEZ v3.0 database provides such estimates produced with four main GCM, and for several future scenarios. The latter is of key importance: it contains the underlying assumption on how the global carbon emissions are going to evolve in the future so to produce the changes in the climate.

I choose the scenario A2 from the GAEZ database, which matches closely the current standard of severe evolution of the global climate for the future: the Representative Concentration Pathway (RCP) 8.5.[2] This scenario assumes a steady increase in carbon stocks in the atmosphere througout the 21st and 22nd centuries, becoming stable by mid–23rd century. A milder scenario that I use for my robustness checks is the B1, which is similar to the nowadays–standard RCP 4.5. It assumes that the global stock of carbon will peak by late 21st century, becoming stable thereafter. Figure B.2 illustrates the equivalence between the SRES and RCP scenarios.

---

[2]Unfortunatelly, the GAEZ v3.0 database contains data produced under old standards for future climate scenarios – those produced in the Special Report on Emission Scenarios (SRES; see IPCC, 2000). The SRES scenarios were later updated by IPCC as the RCP scenarios, which are now the standards in the climate community (IPCC, 2012).

Figure B.2: Equivalence between long and longer–run estimates of radiative forcing (proportional to carbon emissions) between SRES and RCP scenarios.
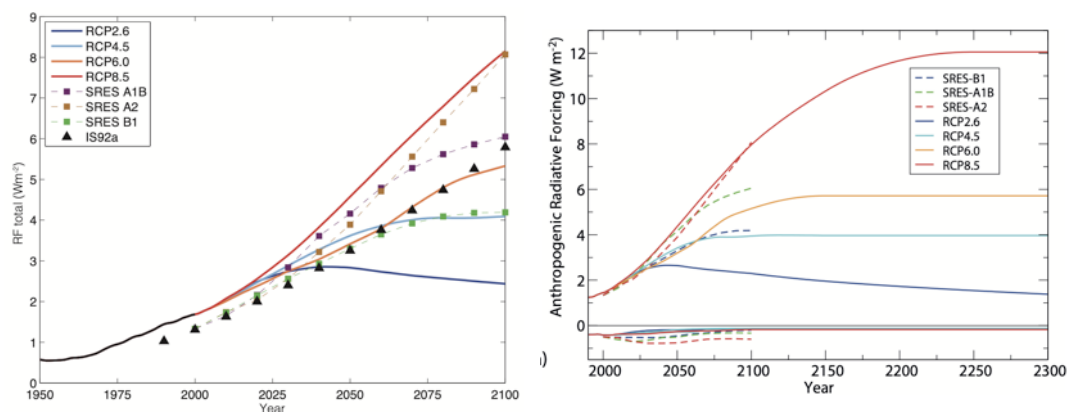
Source: IPCC (2012), chapter 1, Figure 1.15 (left) and Chapter 12, Figure 12.3 (right).

B.2.2   COMTRADE data.

The trade data used in this paper is obtained from the COMTRADE database (COMTRADE, 2010). I collect bilateral trade flows, in current US$, for all crops of my study, between all country–pairs of my empirical setup. To do that, I rely on the COMTRADE API system, which allows me to retrieve imports and exports trade flows between country at standard HS product codes.

Consistent with good practice with trade data, I collect import flows rather than exports. The reson for that is the usual discrepancy between total import and exports at the country–pair–product level. While import flows are registered between country of production and final country of shipment, export data usually register intermediate countries on the trade chain as final destination, biasing the trade flows (Veronese and Tyrman, 2009).

Finally, to transform the trade data to monetary unit of my study (US$ PPP from G–Econ), I proceed as follows. First, I calculate the share of trade flows, at the importer–exporter–crop–year levels, over the GDP of of the importing country in each year, in current values. Subsequently, I average out the shares over the 2000–2010 period, so to avoid outliers in the year of 2000. Finally, I multiply the shares at the importer–exporter–crop level by the importer GDP of G–Econ for the year of 2000.

B.2.3   Building the agricultural production data.

To build a dataset for agricultural production at the location–crop level for 2000, I combine the GAEZ data of production (in tonnes) with the FAOSTAT

agricultural production data (country–crop level) and World Bank country GDP data (both in current US$). First, I use the GAEZ data at the cell–crop level to calculate the share that each cell is observed to produce, of each crop, over its country's total production. Second, I obtain with the FAOSTAT and WB data the share of each country crop production for the years of 2000 to 2010. I average out such shares and multiply them by the country GDP implied by the G–Econ data, so that the unit is consistent with the monetary unit of the model (US$ PPP). Finally, I multiply the country–crop PPP values by the location–crop shares. For very liitle locations, however, the outcome can exceed the their total GDP. In these cases, I simply trim the value by 99.99% of its GDP.

B.2.4   Additional data sources

Main populated places. I collect the coordinaes of the main populated places of SSA from the Populated Places data set from Natural Earth. It consists of a geo-referenced dataset with the coordinates of about 90% of all cities, towns and settlements in the World. I use it to set coordinates for each of the cells of SSA. If a certain cell contains more than one location, I pick the one with the highest population. If another does not have any location to obtain the coordinates, I set them to be the cell's centroid. Finally, if any of the centroids are not located in the mainland (i.e. ocean, lakes), I set it to be the closest coordinate to the centroid that is on the mainland. See fig. B.6 for the result.

B.3 Additional figures and tables

TABLE B.2: Share of grain crop production (in tonnes)
over total production of the main staple and cash crops
in SSA.

Crop	Share of production
Grain crops:	
Cassava	56.65%
Maize	11.75%
Millet	4.59%
Rice	2.18%
Sorghum	6.15%
Wheat	1.13%
Total:	82.45%
Cash crops:	
Coffee	1.13%
Cotton	1.14%
Groundnut	2.72%
Palm oil	4.93%
Soybean	0.33%
Sugarcane	7.31%
Total:	17,55%

Source: GAEZ production data for 2000 aggregated in over
the 42 countries of my empirical setup. SSA includes all sub–
Saharan African countries but Somalia.

FIGURE B.3: Correlations between populations from G–Econ and GHSP
datasets for the year of 2000.
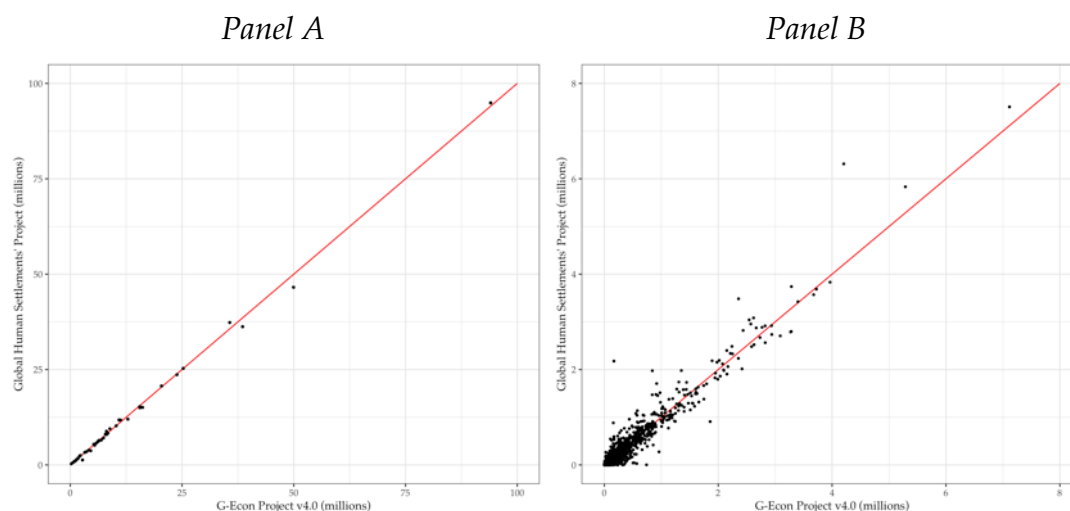
Notes: Panel A: Population counts in SSA from G–Econ (x axis) and GHSP (y axis) aggregate
at country level. Panel B: Population counts in SSA from G–Econ (x axis) and GHSP (y axis)
aggregate at 1 degree grid cells.

FIGURE B.4: Model implied agricultural output in 2080 under climate change for two selected crops.
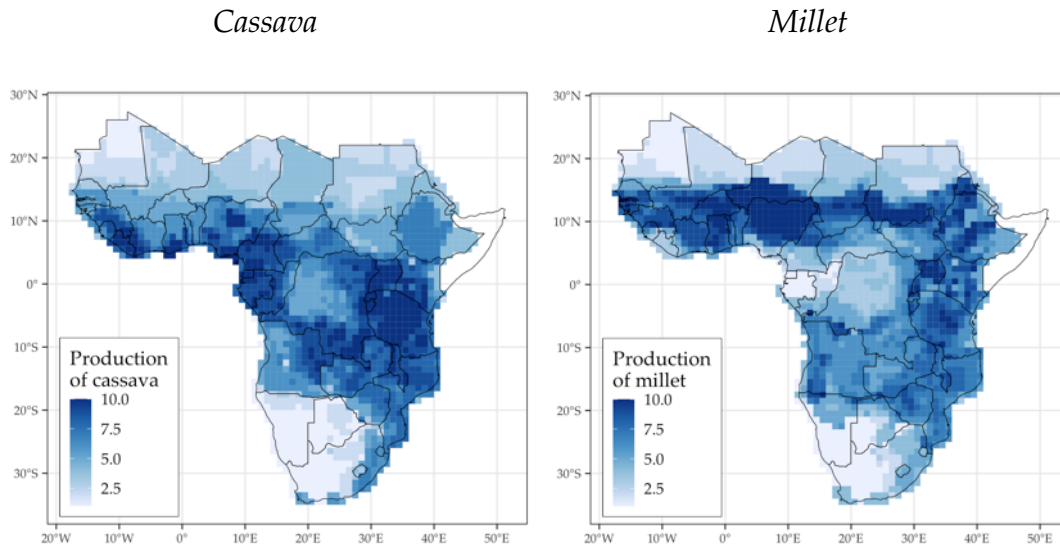
Cassava *Millet*

Notes: Total crop output from the benchmark counterfactual simulation for cassava and millet, shown in deciles of each sample. 1 (10) stands for the bottom (top) deciles.

FIGURE B.5: Kernel density estimates of most/least hit locations (in terms of population loss) with respect to fundamental amenities, non–agricultural productivities, and market access in 2000.

Amenities *Fundamental urban productivity* *Market access in 2000*
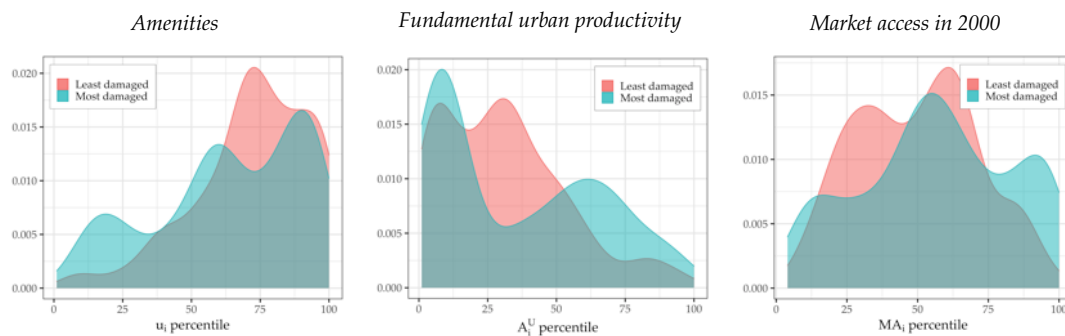
Notes: Densities with respect to the quantile of amenities, urban productivities and market access. The most hit locations stand for the bottom quintile of the subset of locations that are estimated to experience outflows of people, and account for about 17% of the total sample. The least hit locations stand for all of those expected to receive inflows of population, and represent about 20% of the sample.

FIGURE B.6: Coordinates for SSA grid cells (localities) for Western (left) and Eastern (right) Africa.
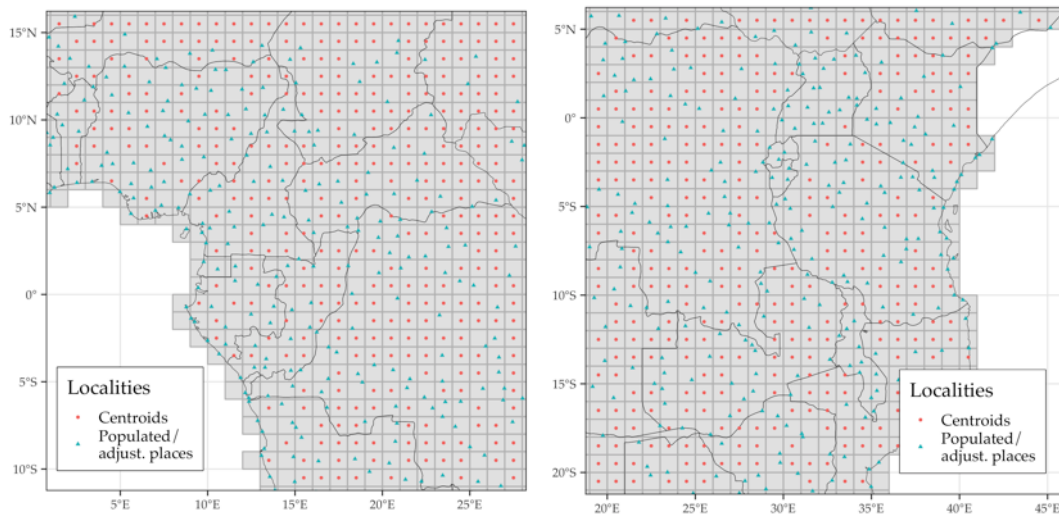
FIGURE B.7: Differences in differences results in terms of climate change–induced population changes between scenarios with different degrees of frictions and the benchmark results at the grid–cell level.
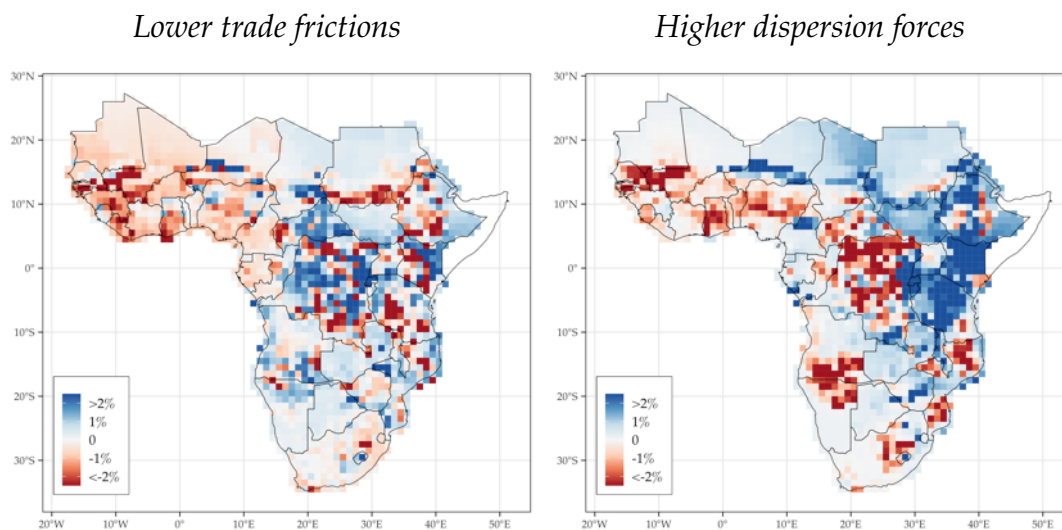
Notes: Both plots document the disaggregated effect of different degree of frictions (trade led by δ and dispersion forces by θ) on the estimated population changes induced by climate change. These are obtained as a differences in differences; i.e. the differences between the population changes in a scenario with lower trade frictions and those of the benchmark results (the same holds for the dispersion forces' plot).

B.4 Regression results for production and trade explained by comparative advantage

I explain here how I use the GAEZ data to investigate the relation between advantages to growing crops and the spatial patterns of agricultural production across and within countries of SSA and trade.

Comparative advantages and production. I combine three sources of GAEZ data: the agricultural production, in thousands of tonnes, the total harvested land, in thousands of hectares, and the average agro-climatic potential yields, for each crop. Formally, I define X_i^k as the dependent variable, standing for either total production/harvested land of crop k in grid cell i. Moreover, A_i^k is defined as the degree of suitability to grow k in cell i, in tonnes/hectares. I use it to estimate the following regression:[3]

$$\log\left(X_i^k\right) = \delta \log\left(A_i^k\right) + a_k + \varepsilon_i^k. \tag{B.7}$$

The parameter of interest, δ, estimates the average change in crop production (or harvested land), in percentual points, associated with a one percent increase in the crop suitability. Importantly, a_k stands for a set of crop fixed–effects (dummies); thus, the variation that identifies δ is within crops across geographical locations. Intuitively, δ shows the degree of association, throughout the entire SSA, of being more suitable to grow a certain crop and effectively producing it. That is, it provides evidence of an association between natural comparative advantage and specialization in agriculture at the crop level across SSA.

In order to understand whether such a relation holds at the country level, I replace a_k with a set of country–crop fixed effects. In that case, δ is identified with variation within country–crop , and its interpretation analogous. It identifies the intensity of the geographical clustering of agricultural activity on more suitable locations, according to GAEZ, within countries.

The results are documented in Table B.3. It provides strong evidence for the hypothesis in question. In particular, Panel A locations with potential yields one percent higher are found to produce, on average, 0.75% percent more if compared with all locations in SSA (column 1), and 0.62% if compared with locations from the same country (column 2). The results for

---

[3]If not otherwise specified, the regression models throughout the paper omit the constant as of neatness.

harvested land (Panel B) are qualitatively equivalent. Overall, it conveys a sound message: crop–specialization happens both across and within countries. To generate this pattern, my general equilibrium model will take the perspective of subnational units that specialize in crops based on comparative advantage.

Importantly, the resuls shown in Figure 2.3 stand for the residuals of X_i^k and A_i^k from a regression on location and crop–country fixed effects (the most demanding possible). The estimated line stands for the results of a semi–parametric (polynomial) regression of these two controlling for the same fixed effects.

TABLE B.3: Suggestive evidence for the relation between natural comparative advantage (relative potential yields) and crop-specialization (effective production) in sub-Saharan Africa.

	(1)	(2)	(3)	(4)
	Panel A: Crop production (in logs)		*Panel B: Harvest land (in logs)*	
Potential yields (logs)	0.753***	0.623***	0.694***	0.612***
	(0.057)	(0.071)	(0.053)	(0.068)
Observations	12,192	12,192	12,192	12,192
R^2	0.504	0.732	0.469	0.689
Crop FE	Yes	No	Yes	No
Country–crop FE	No	Yes	No	Yes

Notes: Estimation using GAEZ data (of year 2000) for agricultural production (thousands of tonnes), harvested land (hectares), and potential yields of agriculture (agro-climatic potential yields, in tonnes/hectare). Panel A uses crop production as the dependent variable; Panel B uses harvested land instead. *p<0.1; **p<0.05; ***p<0.01

Comparative advantage and trade. I provide further evidence of the importance of comparative advantage on economic outcomes in SSA by focusing on trade. In order to do that, I collect the average bilateral crop trade, in US$, between all country pairs of my empirical setup, from 2000 to 2010, from the UN Commodity Trade Statistics Database (COMTRADE, 2010).[4] By combining it with the GAEZ potential yields, I learn whether trade flows are somehow determined by the degree of comparative advantage between countries at the crop level.

I start by looking at aggregate flows. I sum up total exports at the country–crop level, defining X_c^k as the total exports of crop k from country c. Next, I average out the GAEZ yields at the country level, analogously defined as A_c^k, and use it to estimate the following regression:

$$\log\left(X_c^k\right) = \delta \log\left(A_c^k\right) + a_k + b_c + \varepsilon_c^k, \tag{B.8}$$

---

[4]Appendix B.2.2 describes carefully how I collect and aggregate the raw COMTRADE data for the following empirical exercise.

where a_k and b_c stand for crop and country set of fixed effects, respectively. Therefore, the parameter of interest δ is identified with variation at the country–crop level, net out of invariant country and crop characteristics.

Subsequently, I use the trade flows at the bilateral level to investigate further the relation of interest. I first define bilateral exports at the country pair–crop level as $X_{cc'}^k$, where c and c' stand for the exporting and importing countries, respectively. I proceed by calculating a bilateral measure of comparative advantage across countries, formally defined as $A_{cc'}^k = A_c^k / A_{c'}^k$,[5] and use it to estimate the following regression:

$$\log\left(X_{cc'}^k\right) = \delta \log\left(A_{cc'}^k\right) + a_k + b_c + d_{c'} + \varepsilon_c^k. \tag{B.9}$$

Equation (B.9) contains a set of crop, exporter and importer fixed effects, respectively a_k, b_c, and $d_{c'}$. Therefore, the correlation of interested, δ, is estimated with variation at the country pair–crop level, net out of the fixed effects. As of robustness, I add to Equation (B.9) a set of controls at the country pair level, such as distance between capitals, and dummies for geographical contiguity, common language, and ethnicity. Finally, I exploit the most of the variation in the data by adding country pair fixed effects, which net out all the variation in trade flows and comparative advantage at the bilateral level.

The results are documented in Table B.4. First, Panel A shows that the country's natural suitabilities are strong correlates of their exports: countries 1% more productive to grow a certain crop are observed to export about 0.5% more of that crop, on average. The same pattern holds at the bilateral level, shown in Panel B. The volume of crop exports from countries 1% more suitable, relative to the importing country, is about 0.4% higher, on average (column 2). The estimates become more precise with the inclusion of controls, as seen in column 3. Moreover, the magnitude of the estimates remains somehow stable even with the inclusion of more demanding (country pair) fixed effects, which absorb a substantial degree of the variation on relative suitabilities due to the high degree of spatial correlation between crop yields.

The results shown in Figure 2.3 stand for a semi–parametric regression (polynomial) of the specification of Table B.4, column 3. Moreover, the residuals plot are those of a regression of the dependent and independent variables on all fixed effects and controls.

---

[5]Defined as such, the data allows me to exploit the most of the trade flows, which contain exports between the same countries pairs in both directions.

TABLE B.4: Suggestive evidence for the relation between comparative advantages (relative potential yields) and crop exports in sub-Saharan Africa.

	(1)	(2)	(3)	(4)
	Panel A: Total	*Panel B: Total bilateral crop exports*		
	crop exports			
Country potential yields	0.473**			
(A_c^k, in logs)	(0.190)			
Bilateral relative yields		0.360**	0.490***	0.257
($A_{cc'}^k$, in logs)		(0.157)	(0.148)	(0.203)
Observations	198	924	924	924
R^2	0.645	0.350	0.415	0.677
Crop FE	Yes	Yes	Yes	Yes
Exporter FE	Yes	Yes	Yes	No
Importer FE	No	Yes	Yes	No
Bilateral controls	No	No	Yes	No
Exporter–Importer FE	No	No	No	Yes

Notes: The dependent variable in Panel A is average country crop exports, in US$, between 2000 and 2010, and bilateral crop exports (average flows between 2000 and 2010, in US$) in Panel B. The trade data is collected from COMTRADE, and the potential yields from GAEZ (as of year 2000). Refer to Appendix B.2 for details on the construction of the data. *p<0.1; **p<0.05; ***p<0.01

B.5 Model extensions

This appendix outlines two extensions of the baseline model of Section 2.4. It also discusses how the incorporation of these extensions would change, qualitatively and quantitatively, the main results of Sections 2.4.3, 2.5 and 2.6.

B.5.1 Model with bilateral migration frictions

Although the baseline model of Section 2.4 features frictions to the mobility of workers (driven by θ and α), it does not allow for these to be bilateral. In what follows, I develop and discuss a model that features bilateral migration frictions, the implications for the benchmark results, and the challenges for its implementation.

Environment. A continuum of agents are born in a location i; denote $\hat{L}_i$ the measure of agents born therein. The economy is thus initially populated by $\mathcal{L} = \{\hat{L}_i\}_{i \in S}$, which would choose which location j to live based on economic aspects and idiosyncratic preferences.

Technology and Market Structure. The production and trade structure of the economy is kept identical. Thus, the market for goods is disciplined by gravity trade equations.

Consumption Choice. As before, agents are homogeneous with respect to consumption preferences. Thus, total consumption would equal equilibrium local real wages in each location i.

Location Choice. The dimension along which agents differ is the location choice, which in this extension becomes a bilateral choice. In particular, workers choose where to migrate to (subject to frictions) so to maximize welfare. A v worker born in location i choosing location j to live enjoys

$$W_{ij}(v) = \left(w_j/P_j\right) \times \bar{m}_{ij}^{-1} \times \varepsilon_j(v). \tag{B.10}$$

$\bar{m}_{ij} = m_{ij} \times m_{c(j)}$ captures the utility cost associated to migrating from location i to j. It contains a location pair–specific parameter, m_{ij} (proportional to geographical distance), and a destination–specific shifter that varies at the country level, $m_{c(j)}$ ($c(j)$ stands for the country where location j belongs). As such, migration frictions also capture the fact that countries differ in the intensity of their borders for immigration. $\mathcal{M} \equiv \{m_{11}, m_{12}, ..., m_{NN}\}$ is the bilateral matrix of migration frictions.

Leaving the distributional assumptions on $\varepsilon_j(v)$ unchanged, one can obtain a closed form solution for the optimal location choice of individuals and the final population in each location j:

$$
\begin{aligned}
L_j &= \sum_{i \in S} \Pi_{ij} \times \hat{L}_i \\
&= \sum_{i \in S} \frac{\left(w_j/P_j\right)^\theta m_{ij}^{-\theta} m_{c(j)}^{-\theta} u_j L_j^{-\alpha}}{\sum_s \left(w_s/P_s\right)^\theta m_{is}^{-\theta} m_{c(s)}^{-\theta} u_s L_s^{-\alpha}} \hat{L}_i.
\end{aligned}
\tag{B.11}
$$

Its intuition follows: as choices are now made bilaterally, the total equilibrium population in location j is the sum of all individuals born in all origin locations i choosing to live in j, $\Pi_{ij} \times \hat{L}_i$.

Spatial Equilibrium. Given a geography $\mathcal{G}(S) = \{\mathcal{L}, \mathcal{A}, \mathcal{U}, \mathcal{M}, \mathcal{T}\}$, a spatial equilibrium is a set of factor prices and location choices $\{w_i, L_i\}_{i \in S}$ such that market for goods and labor clear. That would be require that eqs. (2.16) and (B.11) hold, and that price indexes are determined by eqs. (2.18) and (2.19).

Illustration of the spatial equilibrium. Analogously to Section 2.4.3, I illustrate the main mechanisms present in this extension by representing the geography as a line containing a discrete number of locations, divided into two countries (segments of the economy/line).

FIGURE B.8: Equilibrium values for $\{L_i\}_{i\in S}$ in the spatial model with bilateral migration represented on a line.
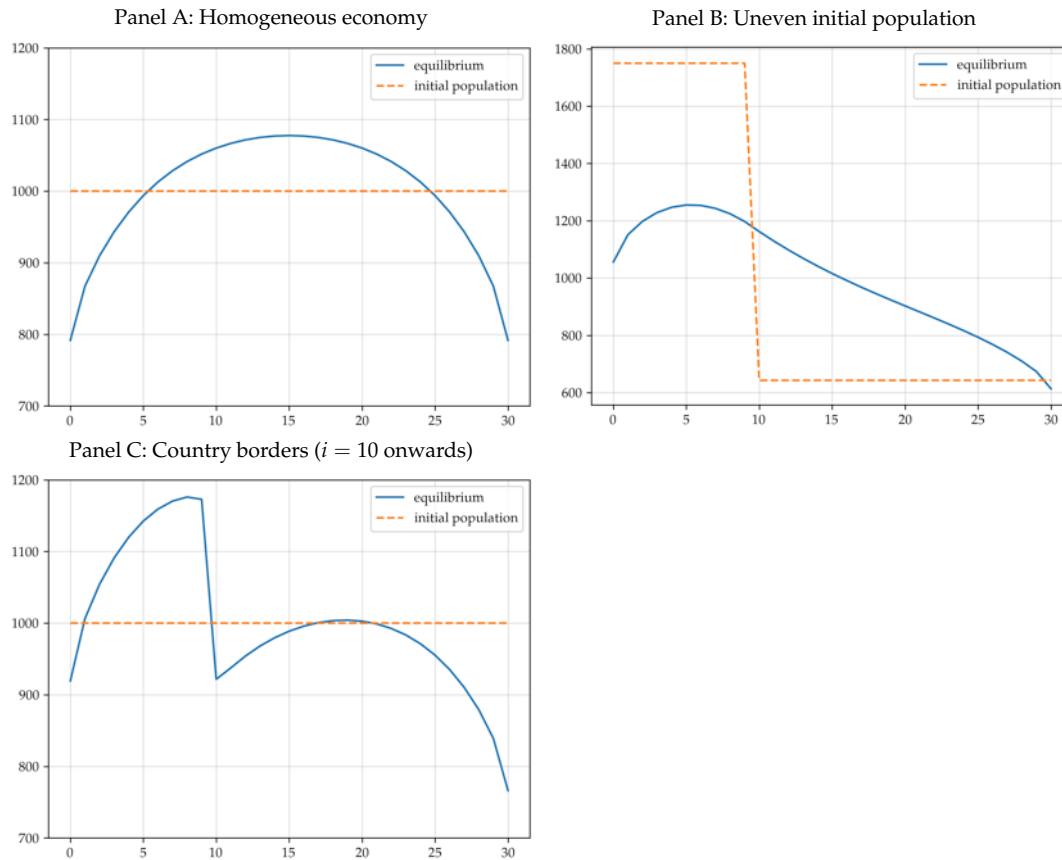
Panel A: Homogeneous economy

Panel B: Uneven initial population

Panel C: Country borders ($i = 10$ onwards)

Notes: Equilibrium labor allocations for a simplified version of the model as described in Appendix B.5.1. The economy (line) is divided in two countries (segments): country 1 ranges from location 0 to 10, and country 2 from 11 to 30. Panel A describes the allocation of workers of a fully homogeneous economy. Panel B plots how the equilibrium population changes if country 1 has a higher initial population. Panel C documents how that changes if there are also country barriers to migrate into country 2.

I assume that the economy is homogeneous with respect to fundamental initial populations, productivities, and amenities. I also set trade and bilateral migration frictions as proportional to distance, and no country migration barriers (e.g. $m_{c(j)} = 1 \; \forall j$). The result is documented in the Panel A of Figure B.8. It shows that the economy agglomerates at the more central locations, which can more easily supply all locations in the economy.

Panel B illustrates the role of the bilateral migration frictions in the resulting equilibrium. It assumes that each country has different initial populations. In the presence of these bilateral frictions, the equilibrium population in country 1 remains much higher than in country 2, as many individuals from the former cannot migrate all the way to the very distant locations in the latter. It shows clearly that, now, initial populations matter for the resulting equilibrium of the economy, an aspect not present in the baseline model.

Panel C illustrates how country barriers change results. It assumes homogeneous populations across locations and that country 2 has positive barriers for migration. The resulting changes in the equilibrium are stark. Many nationals from country 1 remain trapped there, as they cannot migrate to the larger country 2. Interestingly, they agglomerate closer to the border of these countries, because of trade frictions. Country 2, which is larger, has the gravity center of its population around its center.

Implications for main results. The current model extension would change drastically the concept of climate migration of the baseline model. As migration decisions become bilateral, it would be possible to distinguish explicit migration decisions from net displacement/flows of people to a certain location. Moreover, it would allow for the separation of population growth from migration. In the present setup, initial populations matter, so that introducing effects of climate change in the fertility rates heterogeneously across countries/locations would lead to substantial changes in the results. Moreover, an obvious policy experint with this extension would be to study how changes in the (country) migration frictions would affect the benchmark results.

Pilot model inversion. As of illustration, I bring the current version to the data in order to illustrate how the model inversion makes explicit the gains from the current extension of the model. In particular, I parametrize the bilateral component of migration frictions analogously to trade frictions, i.e.

$$\bar{m}_{ij} = \text{dist}(i,j)^{\phi} \times m_{c(j)}, \tag{B.12}$$

where ϕ is the elasticity of geographical migration frictions to distance. Under this formulation, the model inversion requires the additional calibration of this parameter as well as the set of country barriers.

For the sake of exposure, I assume an ad hoc value for $\phi = 0.335$.[6] By assuming so, I use bilateral migration data at the country level between all country pairs of SSA to calculate the total immigration into each country between 1990 and 2000, denoted as $\{L_c\}_{c=1}^{C}$ ($C = 42$ is the total number of countries). Powered with that, I can use the model structure to solve for the amenities and country barriers contemporaneously. That requires solving the

---

[6]The structural migration literature do provide some guidance for the values of ϕ. Values range from 0.05 (Pellegrina and Sotelo, 2021) to 0.147 (Bryan and Morten, 2019) to 4.43 (Monte et al., 2018)

simultaneous system of equations below:

$$[u_j]_{N \times 1} = L_j \times \left[\sum_i \frac{(w_j/P_j)^\theta \times m_{ij}^{-\theta} m_{c(j)}^{-\theta} L_j^{-\alpha}}{\sum_s (w_s/P_s)^\theta \times m_{is}^{-\theta} m_{c(s)}^{-\theta} u_s L_s^{-\alpha}} \hat{L}_i \right]^{-1} \tag{B.13}$$

$$[m_c]_{C \times 1} = \left[L_c^{-1} \times \sum_{i \notin c} \sum_{j \in c} \frac{(w_j/P_j)^\theta \times m_{ij}^{-\theta} u_j L_j^{-\alpha}}{\sum_s (w_s/P_s)^\theta \times m_{is}^{-\theta} m_{c(s)}^{-\theta} u_s L_s^{-\alpha}} \hat{L}_i \right]^{1/\theta} \tag{B.14}$$

The identification of the required parameters holds up–to–scale, as the migration barrier of one country needs to be normalized to one.

The results of this inversion is documented in Figure B.9. The distribution of the resulting amenities and country migration borders are shown in Panels D and E, respectively. For comparability, the distribution of the amenities u_i backed out using the baseline framework is also shown, in Panel B.

The most striking feature of the previous inversion results is somehow addressed with the current approach. In particular, Congo DRC and Ethiopia do not stand out as top amenity countries anymore. Their high population density is now rationalized by the model as if (part of) their population was incapable of leaving to somewhere else. By exploiting the variation in the immigration data, the model identifies that the nearby countries with higher incomes (e.g. Angola, Kenya) do not have as much immigration as they should and thus must have high migration barriers.

Another feature that stands out is the fact that northern–most locations in the Saharan desert are assigned to even lower amenities if compared to the baseline results. The reason for that is distance: now the model rationalizes that the reason for some people to be there is simply because migrating to locations with relative higher income is just too costly.

Overall, this extension of the baseline model provides great insights on how to allow for bilateral migration decisions in my framework and to separate migration border and fertility effects from the aggregate benchmark numbers of climate displaced individuals. A challenge stands on how to estimate ϕ fully incorporate this extension.

FIGURE B.9: Results of the model inversion and observed endogenous variables – comparison between baseline model and extension with bilateral migration frictions.
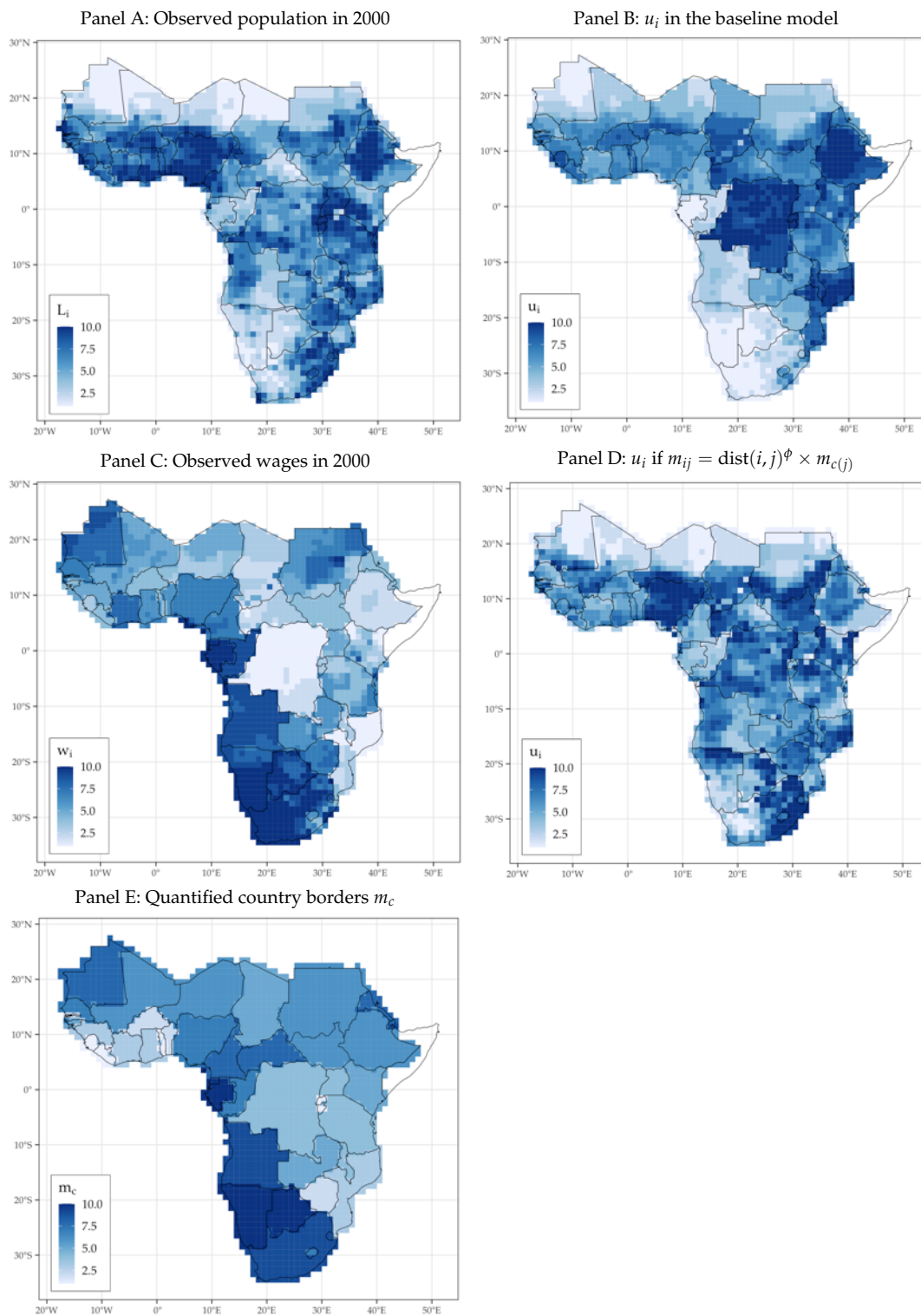
Notes: All results are shown in deciles, where 1 (10) stands for the bottom (top) decile of each sample.

B.5.2   Model with sectoral adjustment frictions

A key takeaway from the benchmark results is the fact that climate change can lead to an intense process of structural change in SSA, with factors moving out of agriculture to the non–agricultural sector. That movement, in the baseline model, happens frictionlessly, which might not be too realistic considering the context of SSA. In the following, I present a model that incorporate these frictions. I also discuss the implications of this additional layer for the benchmark results.

Environment. The economy is endowed with a continuum $\mathcal{L} = \sum_{i \in S} L_i$ of workers, each of which choosing where to live and which sector to work at (denoted by j or r) based on economic characteristics of each location–sector and idiosyncratic preferences.

Technology and Market Structure. The frictions to switch sectors would imply that real wages do not necessarily equalize across sectors within locations. Thus, nominal wages w_i^k are now location-sector–specific. Therefore, the market for goods, whose equilibrium would still be driven by gravity trade equations, would clear at the location–sector level as follows[7]

$$w_i^k L_i^k = \sum_r \sum_j \left(\frac{P_j^k}{P_j} \right)^{1-\eta} \left(\frac{w_i^k \tau_{ij}}{b_i^k A_i^k P_j^k} \right)^{1-\sigma} w_j^r L_j^r. \tag{B.15}$$

Consumption Choice. Preferences for consumption are kept identical, so that agents in location i would consume a basket of goods worth real wages w_i^k / P_i, which are now location–sector specific.

Location and Sector Choice. Agents now choose where to live and which sector to work simultaneously, and have heterogeneous preferences along this dimension. In particular, an agent v choosing to live in i and work in sector k enjoys

$$W_i^k(v) = \left(w_i^k / P_i \right) \times \varepsilon_i^k(v). \tag{B.16}$$

Note now that workers idiosyncratic preferences across location and sectors is disciplined by ε_i^k. Assuming $\varepsilon_i^k \sim G_i^k(z) = e^{-z^{-\theta} \times \left(u_i^k L_i^{-\alpha} \right)}$, one can obtain a

---

[7]Intuitively, in this framework, each location–sector would be equivalent to a location of the baseline model. However, location–sectors "located" at the same geographical location i would have no trade frictions between them, and so price indexes would be identical across these.

closed form solution for the optimal location–sector sorting as follows:

$$\Pi_i^k = P\left(W_i^k(v) \geq \max\{W_j^r(v)\}_{j,r}\right) = \frac{\left(w_i^k/P_i\right)^\theta u_i^k}{\sum_j \sum_r \left(w_j^r/P_j\right)^\theta u_j^r}. \tag{B.17}$$

Thus, equilibrium (sectoral) population are determined by, respectively

$$L_i^k = \Pi_i^k \times \mathcal{L} \tag{B.18}$$

$$L_i = \sum_k \Pi_i^k \times \mathcal{L}. \tag{B.19}$$

The parameter disciplining the "frictions" to switch sectors are the location–sector–specific amenities u_i^k. Now, each geographical location would provide diverse levels of utility for workers sorting into different sectors. Thus, this choice now would be also driven by this idiosyncratic characteristic rather than only by comparative advantages (the only force of sectoral specialization in the baseline model).

Spatial Equilibrium. Given a geography $\mathcal{G}(S) = \{\mathcal{L}, \mathcal{A}, \mathcal{U}, \mathcal{T}\}$, a spatial equilibrium is a set of sectoral factor prices and location choices $\{w_i^k, L_i^k\}_{i \in S, k \in \mathcal{K}}$ such that market for goods and labor clear. That would require that eqs. (B.15) and (B.18) hold, and that price indexes are determined by eqs. (2.18) and (2.19). Note that now the dimension of the model increases by the order of K sectors, as now there are $2 \times N \times K$ endogenous variables to be solved for.

Illustration of the spatial equilibrium. Again, I illustrate the main mechanisms present in this extension by representing the geography as a line containing a discrete number of locations. In particular, I first assume that the economy produces goods of two sectors, and is homogeneous with respect to fundamental productivities across locations (but make all locations more productive in sector 2) and sectoral amenities. I make again trade frictions proportional to distance; the equilibrium labor allocations are shown in Figure B.10, Panel A.

As expected, the economic activity and population concentrate at the most central locations due to comparative advantage (driven by trade frictions). There are higher employment shares in sector 2, the one the economy is most productive at. Being the amenities homogeneous across all locations and sectors, the only force driving specialization across space and sectors is comparative advantage.

FIGURE B.10: Simulation of the economy as a line with even and uneven sectoral amenities/shifters.
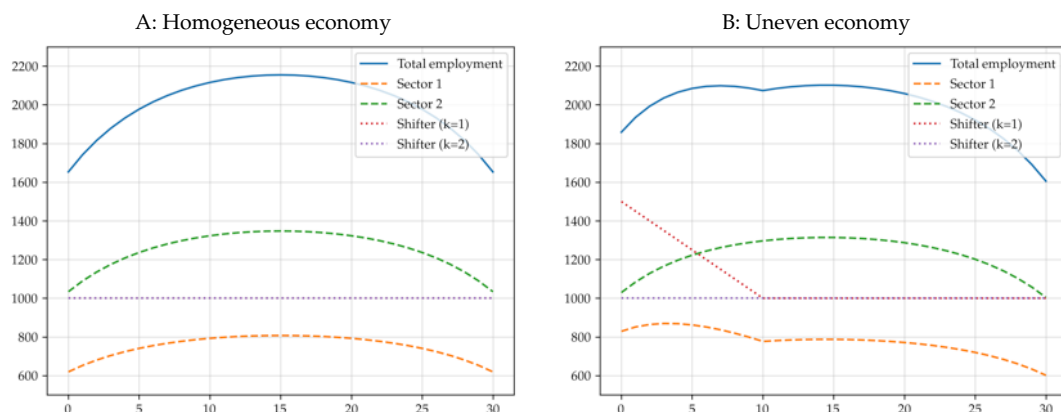
Notes: Equilibrium labor allocations for a simplified version of the model as described in Appendix B.5.2. Panel A describes the allocation of workers of a fully homogeneous economy. Panel B plots how the equilibrium population changes if some locations have higher amenities for sector 1.

Panel B shows how this changes if such sorting is also driven by idiosyncratic factors. In particular, I assume that the left–most locations of the economy provide higher utility for agents choosing to work in the least productive sector 1. Compared with Panel A, the allocation of labor is distorted: the left–most locations now concentrate a fair amount of labor in a rather unproductive sector, and real GDP shrinks vis–à–vis the equilibrium of Panel A.

Implications for main results. The formulation of sectoral sorting is capable of rationalizing the well–known empirical fact of substantial labor allocated in agriculture (a fairly unproductive sector) in SSA. In this setting, the stark reallocation of labor across sectors observed in the climate change counterfactuals of Section 2.6 would be attenuated. For instance, if countries like Nigeria, Mali, or Congo DRC were to have relatively higher forces keeping workers into agriculture, these would not be able to switch to the non–agricultural sector as shown in Figure 2.9, Panel B. Two resulting forces could arise: agents would either be trapped in agriculture in these locations, increasing the GDP losses by climate change, or move somewhere else, increasing climate migration.

Implementing this extension of the model is a fairly challenging task due to data restrictions. Performing a calibration analogously to Section 2.5 would now require observing sectoral wages and labor. The first step in this direction could be mimicking Peri and Sasahara (2019) and distinguish sectoral labor between non–/agricultural by population density, and retrieve

that from fine–grained gridded population data. To build location–sector wages, instead, a first step would be to verify whether one can back them out with sectoral production data, which is indeed observed and used in Section 2.3.

Appendix C

Appendix: Chapter 3

C.1 Solving the Model

We start by recovering the initial distributions of fundamental agricultural productivity, $\tau_{A0}(r)$, fundamental non-agricultural productivity, $\tau_{M0}(r)$, and fundamental amenities relative to utility, $\bar{a}(r)/u_0(r)$, that rationalize the data.

First, combine equations (3.33) and (3.32) to express location r's agricultural employment as

$$\bar{L}_{A0}(r) = \frac{\bar{L}_0(r)}{1 + \frac{\gamma_M + \mu_M}{\gamma_A + \mu_A}\left(\frac{Y_0(r)}{Y_{A0}(r)} - 1\right)} \tag{C.1}$$

where we use the fact that $\bar{L}_0(r) = \bar{L}_{A0}(r) + \bar{L}_{M0}(r)$. Next, combining equations (3.33) and (C.1) allows us to express wages in r as

$$w_0(r) = \left[\gamma_A + \mu_A + (\gamma_M + \mu_M)\left(\frac{Y_0(r)}{Y_{A0}(r)} - 1\right)\right]\frac{Y_{A0}(r)}{\bar{L}_0(r)} \tag{C.2}$$

where we apply the normalization $\int_S w_0(r)\,dr = 1$. Equation (3.17) then allows us to obtain land rents as

$$R_0(r) = \frac{w_0(r)}{H(r)}\left(\frac{1 - \gamma_A - \mu_A - \sigma_A}{\gamma_A + \mu_A}\bar{L}_{A0}(r) + \frac{1 - \gamma_M - \mu_M - \sigma_M}{\gamma_M + \mu_M}\bar{L}_{M0}(r)\right). \tag{C.3}$$

Two further notes are in order. First, Cobb–Douglas sectoral shares can be identified using

$$\frac{\chi_A}{\chi_M} = \frac{\int_S Y_{A0}(r)\,dr}{\int_S (Y_0(r) - Y_{A0}(r))\,dr}$$

and the fact that $\chi_A + \chi_M = 1$. Second, e_0 and Π_0 can be obtained from equations (3.29) and (3.30), respectively.

Recover fundamental productivities and ratio of amenities to utility. With these results in hand, we are ready to recover the distribution of fundamental productivities by sector. In the case of agriculture, equation (3.27) implies

$$P_{A0}(s)^{-\theta} = \kappa_A e_0^{-\sigma_A \theta}.$$
$$\int_S \hat{\tau}_{A0}(r)^\theta w_0(r)^{-(\alpha_A+\gamma_A+\mu_A)\theta} R_0(r)^{(\alpha_A+\gamma_A+\mu_A+\sigma_A-1)\theta} \varsigma(s,r)^{-\theta} dr,$$
(C.4)

where

$$\hat{\tau}_{A0}(r) = \tau_{A0}(r) g_A(T_0(r)),$$

while equation (3.28) implies

$$\hat{\tau}_{A0}(r)^{-\theta} = \chi_A \kappa_A e_0^{-\sigma_A \theta} w_0(r)^{-(\alpha_A+\gamma_A+\mu_A)\theta} R_0(r)^{(\alpha_A+\gamma_A+\mu_A+\sigma_A-1)\theta} Y_{A0}(r)^{-1} \cdot$$
$$\int_S P_{A0}(s)^\theta \left[(w_0(s) + \Pi_0/\bar{L}) \bar{L}_0(s) + R_0(s) H(s)\right] \varsigma(s,r)^{-\theta} ds.$$
(C.5)

In the case of non-agriculture, the same equations are

$$P_{M0}(s)^{-\theta} = \kappa_M e_0^{-\sigma_M \theta}.$$
$$\int_S \hat{\tau}_{M0}(r)^\theta w_0(r)^{-(\alpha_M+\gamma_M+\mu_M)\theta} R_0(r)^{(\alpha_M+\gamma_M+\mu_M+\sigma_M-1)\theta} \varsigma(s,r)^{-\theta} dr,$$
(C.6)

where

$$\hat{\tau}_{M0}(r) = \tau_{M0}(r) g_M(T_0(r)) \tag{C.7}$$

and

$$\hat{\tau}_{M0}(r)^{-\theta} = \chi_M \kappa_M e_0^{-\sigma_M \theta} w_0(r)^{-(\alpha_M+\gamma_M+\mu_M)\theta} R_0(r)^{(\alpha_M+\gamma_M+\mu_M+\sigma_M-1)\theta} Y_{M0}(r)^{-1} \cdot$$
$$\int_S P_{M0}(s)^\theta \left[(w_0(s) + \Pi_0/\bar{L}) \bar{L}_0(s) + R_0(s) H(s)\right] \varsigma(s,r)^{-\theta} ds.$$
(C.8)

Our aim is to solve the system (C.4) and (C.5) for $\hat{\tau}_{A0}(r)$ and $P_{A0}(r)$, and solve the system (C.6) and (C.8) for $\hat{\tau}_{M0}(r)$ and $P_{M0}(r)$. We can show the solution to each system exists and is unique:

Lemma 1 *The solution to (C.4) and (C.5) and the solution to (C.6) and (C.8) exist and both are unique to scale.*

Proof. The system of (C.4) and (C.5) constitutes a special case of the systems considered in Allen, Arkolakis and Li (2020):[1]

$$\prod_{h=1}^{H} x_h(r)^{\gamma_{kh}} = \int_S K_k(r,s) \prod_{h=1}^{H} x_k(r)^{\kappa_{kh}} x_h(s)^{\beta_{kh}} \qquad k = 1,2,...,H \qquad \text{(C.9)}$$

such that $H = 2$, $x_1(r) = P_{A0}(r)$, $x_2(r) = \hat{\tau}_{A0}(r)$,

$$K_1(r,s) = \kappa_A e_0^{-\sigma_A \theta} w_0(r)^{-(\alpha_A+\gamma_A+\mu_A)\theta} R_0(r)^{(\alpha_A+\gamma_A+\mu_A+\sigma_A-1)\theta} \varsigma(s,r)^{-\theta},$$

$$K_2(r,s) = \chi_A \kappa_A e_0^{-\sigma_A \theta} w_0(r)^{-(\alpha_A+\gamma_A+\mu_A)\theta} R_0(r)^{(\alpha_A+\gamma_A+\mu_A+\sigma_A-1)\theta} Y_{A0}(r)^{-1} \cdot$$
$$[(w_0(s) + \Pi_0/\bar{L}) \bar{L}_0(s) + R_0(s) H(s)] \varsigma(s,r)^{-\theta},$$

$\gamma_{11} = \gamma_{22} = -\theta$, $\gamma_{12} = \gamma_{21} = \kappa_{11} = \kappa_{12} = \kappa_{21} = \kappa_{22} = \beta_{11} = \beta_{22} = 0$, and $\beta_{12} = \beta_{21} = \theta$. Theorem 1 in Allen, Arkolakis and Li (2020) shows that the system (C.9) has a unique solution (to scale) if the largest eigenvalue of the matrix $|\left(\mathbf{B}(\mathbf{\Gamma} - \mathbf{K})^{-1}\right)_{kh}|$ is less than or equal to one, where $\mathbf{B}$ is the matrix whose (k,h) element is β_{kh}, $\mathbf{K}$ is the matrix whose (k,h) element is κ_{kh}, and $\mathbf{\Gamma}$ is the matrix whose (k,h) element is γ_{kh}. In our case, the largest eigenvalue of $|\left(\mathbf{B}(\mathbf{\Gamma} - \mathbf{K})^{-1}\right)_{kh}|$ equals one. The proof for the system of (C.6) and (C.8) is analogous. ∎

Allen et al. (2020) also show that the solution to (C.9) can be found by iteration if the largest eigenvalue of $|(\mathbf{B}\mathbf{\Gamma}^{-1})_{kh}|$ is strictly less than one. While this condition does not hold, we find that, in practice, iteration works on the system of (C.4) and (C.5). However, in the case of (C.6) and (C.8), iteration fails to find the solution. To address this issue, we follow the inversion procedure in Desmet et al. (2018) and approximate (C.6) by

$$P_{M0}(s)^{-\theta} = \kappa_M e_0^{-\sigma_M \theta} \cdot$$
$$\int_S \hat{\tau}_{M0}(r)^{\theta-\epsilon} w_0(r)^{-(\alpha_M+\gamma_M+\mu_M)\theta} R_0(r)^{(\alpha_M+\gamma_M+\mu_M+\sigma_M-1)\theta} \varsigma(s,r)^{-\theta} dr$$
$$\text{(C.10)}$$

where $\epsilon > 0$ is a constant. For any positive ϵ, the largest eigenvalue of the system of (C.8) and (C.10) is now strictly less than one, so that we can solve the system by iteration. We choose the value of ϵ sufficiently small such that the difference between equations (C.6) and (C.10) becomes negligible.

---

[1] See Remark 3 in Allen, Arkolakis and Li (2020) in particular.

Given that agricultural and non-agricultural productivities can only be identified up to a scale, we normalize their global averages to one:

$$\int_S \hat{\tau}_{A0}(r)\,dr = 1 \qquad \text{and} \qquad \int_S \hat{\tau}_{M0}(r)\,dr = 1$$

To separate fundamental productivity $\tau_{i0}(r)$ from $\hat{\tau}_{i0}(r)$, we use the sector-specific temperature discount factor $g_i(T_0(r))$. In the data section we explain how we get estimates of $g_i(T_0(r))$.

With $w_0(r)$, $R_0(r)$, $P_{A0}(r)$ and $P_{M0}(r)$ in hand, we can express amenities relative to utility from equations (3.2) and (3.4):

$$\frac{\bar{a}(r)}{u_0(r)} = \frac{P_{A0}(r)^{\chi_A} P_{M0}(r)^{\chi_M}}{w_0(r) + \Pi_0/\bar{L} + R_0(r)H(r)/\bar{L}_0(r)}\left(\frac{\bar{L}_0(r)}{H(r)}\right)^\lambda \qquad \text{(C.11)}$$

We have now finished solving for the initial distributions of fundamental productivities and amenities relative to utility. Since solving the system (C.6) and (C.8) required us to use an approximation, we want to ensure that this approximation is reasonable. To that end, we investigate whether the amenities and productivities backed out in the model inversion imply an equilibrium distribution of population that is sufficiently close to the one in the data. We do so by using the same algorithm as the one we use to solve the model forward.

Recovering fundamental amenities. To recover fundamental amenities $\bar{a}(r)$, we apply the same procedure as in Desmet et al. (2018). That is, we use subjective wellbeing data to measure $u_0(r)$ and obtain fundamental amenities as

$$\bar{a}(r) = \frac{\bar{a}(r)}{u_0(r)}u_0(r). \qquad \text{(C.12)}$$

We briefly discuss this in the data section.

Recovering moving costs. As in Desmet et al. (2018), we use location-level population data at time 1 to back out moving costs $m_2(r)$. Having total population at every location r at time 1, $\bar{L}_1(r)$, we guess a worldwide energy price e_1 as well as an agricultural employment level $\bar{L}_{A1}(r) \in (0, \bar{L}_1(r))$ and a wage $w_1(r)$ for every location.[2] In the first step, we compute

$$\Lambda_1(r) = \frac{1 - \gamma_M - \mu_M - \sigma_M}{\gamma_M + \mu_M}\bar{L}_1(r) + \left(\frac{1 - \gamma_A - \mu_A - \sigma_A}{\gamma_A + \mu_A} - \frac{1 - \gamma_M - \mu_M - \sigma_M}{\gamma_M + \mu_M}\right)\bar{L}_{A1}(r)$$

---

[2]In practice, we start with the guesses $e_1 = e_0$, $\bar{L}_{A1}(r) = \bar{L}_{A0}(r)$ and $w_1(r) = w_0(r)$.

and rewrite equation (3.17) as

$$R_1(r) = w_1(r) \Lambda_1(r) H(r)^{-1}.$$

Plugging this into equations (3.27) and (3.28), we obtain

$$P_{A1}(s)^{-\theta} = \kappa_A e_1^{-\sigma_A \theta} \int_S \tau_{A1}(r)^{\theta} g_A(T_1(r))^{\theta} \Lambda_1(r)^{(\alpha_A + \gamma_A + \mu_A + \sigma_A - 1)\theta} \cdot$$
$$H(r)^{-(\alpha_A + \gamma_A + \mu_A + \sigma_A - 1)\theta} w_1(r)^{-(1-\sigma_A)\theta} \varsigma(s,r)^{-\theta} dr \tag{C.13}$$

$$P_{M1}(s)^{-\theta} = \kappa_M e_1^{-\sigma_M \theta} \int_S \tau_{M1}(r)^{\theta} g_M(T_1(r))^{\theta} \Lambda_1(r)^{(\alpha_M + \gamma_M + \mu_M + \sigma_M - 1)\theta} \cdot$$
$$H(r)^{-(\alpha_M + \gamma_M + \mu_M + \sigma_M - 1)\theta} w_1(r)^{-(1-\sigma_M)\theta} \varsigma(s,r)^{-\theta} dr \tag{C.14}$$

$$\frac{w_1(r) \bar{L}_{A1}(r)}{\gamma_A + \mu_A} = \chi_A \kappa_A e_1^{-\sigma_A \theta} \tau_{A1}(r)^{\theta} g_A(T_1(r))^{\theta} \Lambda_1(r)^{(\alpha_A + \gamma_A + \mu_A + \sigma_A - 1)\theta} H(r)^{-(\alpha_A + \gamma_A + \mu_A + \sigma_A - 1)\theta} \cdot$$
$$w_1(r)^{-(1-\sigma_A)\theta} \int_S P_{A1}(s)^{\theta} \left[\left(w_1(s) + \frac{\Pi_1}{\bar{L}} \right) L_1(s) + w_1(s) \Lambda_1(s) \right] \varsigma(s,r)^{-\theta} ds \tag{C.15}$$

and

$$\frac{w_1(r) \bar{L}_{M1}(r)}{\gamma_M + \mu_M} = \chi_M \kappa_M e_1^{-\sigma_M \theta} \tau_{M1}(r)^{\theta} g_M(T_1(r))^{\theta} \Lambda_1(r)^{(\alpha_M + \gamma_M + \mu_M + \sigma_M - 1)\theta} H(r)^{-(\alpha_M + \gamma_M + \mu_M + \sigma_M - 1)\theta} \cdot$$
$$w_1(r)^{-(1-\sigma_M)\theta} \int_S P_{M1}(s)^{\theta} \left[\left(w_1(s) + \frac{\Pi_1}{\bar{L}} \right) L_1(s) + w_1(s) \Lambda_1(s) \right] \varsigma(s,r)^{-\theta} ds \tag{C.16}$$

where Π_1 can be obtained from equation (3.19). Combining (C.15) and (C.16) and rearranging yields

$$w_1(r)^{1+\theta} = \bar{L}_1(r)^{-1} \int_S \left[\chi_A(\gamma_A + \mu_A) \kappa_A e_1^{-\sigma_A \theta} \tau_{A1}(r)^{\theta} g_A(T_1(r))^{\theta} \Lambda_1(r)^{(\alpha_A + \gamma_A + \mu_A + \sigma_A - 1)\theta} \cdot \right.$$
$$H(r)^{-(\alpha_A + \gamma_A + \mu_A + \sigma_A - 1)\theta} w_1(r)^{\sigma_A \theta} P_{A1}(s)^{\theta} + \chi_M(\gamma_M + \mu_M) \kappa_M e_1^{-\sigma_M \theta} \cdot$$
$$\tau_{M1}(r)^{\theta} g_M(T_1(r))^{\theta} \Lambda_1(r)^{(\alpha_M + \gamma_M + \mu_M + \sigma_M - 1)\theta} H(r)^{-(\alpha_M + \gamma_M + \mu_M + \sigma_M - 1)\theta} \cdot$$
$$\left. w_1(r)^{\sigma_M \theta} P_{M1}(s)^{\theta} \right] \left[\left(w_1(s) + \frac{\Pi_1}{\bar{L}} \right) \bar{L}_1(s) + w_1(s) \Lambda_1(s) \right] \varsigma(s,r)^{-\theta} ds. \tag{C.17}$$

In the second step, we compute $P_{A1}(s)$ and $P_{M1}(s)$ using equations (C.13) and (C.14) and update $w_1(r)$ using equation (C.17). We proceed with this until $w_1(r)$ converges, where we also apply the normalization $\int_S w_1(r) dr =$

1. Next, we update $\bar{L}_{A1}(r)$ using

$$\bar{L}_{A1}(r) = \chi_A (\gamma_A + \mu_A) \kappa_A e_1^{-\sigma_A \theta} \tau_{A1}(r)^\theta g_A (T_1(r))^\theta \Lambda_1(r)^{(\alpha_A + \gamma_A + \mu_A + \sigma_A - 1)\theta} H(r)^{-(\alpha_A + \gamma_A + \mu_A + \sigma_A - 1)\theta} \cdot$$

$$w_1(r)^{-[1+(1-\sigma_A)\theta]} \int_S P_{A1}(s)^\theta \left[\left(w_1(s) + \frac{\Pi_1}{\bar{L}} \right) \bar{L}_1(s) + w_1(s) \Lambda_1(s) \right] \varsigma(s,r)^{-\theta} ds$$

$$(C.18)$$

which we obtained from rearranging equation (C.15), and we update e_1 using equation (3.29). After this, we return to the beginning of the first step. We proceed until convergence in $\bar{L}_{A1}(r)$.

Once we know $w_1(r)$, $P_{A1}(r)$, $P_{M1}(r)$ and $\Lambda_1(r)$, we can obtain the level of utility at any location from equations (3.2) and (3.4):

$$u_1(r) = \bar{a}(r) \left(\frac{\bar{L}_1(r)}{H(r)} \right)^{-\lambda} \frac{w_1(r) + \Pi_1/\bar{L} + w_1(r) \Lambda_1(r)/\bar{L}_1(r)}{P_{A1}(r)^{\chi_A} P_{M1}(r)^{\chi_M}} \qquad (C.19)$$

which allows us to obtain the level of moving costs (up to scale) from equation (3.3)

$$m_2(r) = \bar{m}_2 u_1(r) \bar{L}_1(r)^{-\Omega} \qquad (C.20)$$

where we choose the level shifter $\bar{m}_2$ such that $\min_{r \in S} m_2(r) = 1$, as in Desmet et al. (2018).

Solving for the equilibrium. We solve for the equilibrium of the model forward in time, similar to Desmet et al. (2018). As a first step, we recover the distribution of sectoral productivities in any period $t \geq 1$ by inserting the productivities and sectoral employment levels of period $t-1$ into equations (3.13) and (3.9). Next, we recover the distribution of temperature in period t by substituting the carbon emissions and temperature levels of period $t-1$ into equations (3.20) and (3.22). As a final step, we solve for sectoral employment levels, wages and prices in period t as a function of these productivities, so we can proceed with solving for the equilibrium of period $t+1$.

The final step of solving for the equilibrium consists of three loops embedded in each other. In the outermost loop, we guess a distribution of population $\bar{L}_t(r)$ and a worldwide energy price e_t, and proceed to the middle

loop.[3] In the middle loop, we guess a distribution of agricultural employ-ment $\bar{L}_{At}(r)$, compute

$$\Lambda_t(r) = \frac{1 - \gamma_A - \mu_A - \sigma_A}{\gamma_A + \mu_A}\bar{L}_{At}(r) + \frac{1 - \gamma_M - \mu_M - \sigma_M}{\gamma_M + \mu_M}\bar{L}_{Mt}(r)$$

and rewrite equation (3.17) as

$$R_t(r) = w_t(r)\,\Lambda_t(r)\,H(r)^{-1}.$$

Plugging this into equations (3.27) and (3.28), we obtain

$$P_{At}(s)^{-\theta} = \kappa_A e_t^{-\sigma_A\theta}\int_S \tau_{At}(r)^\theta\, g_A(T_t(r))^\theta\, \Lambda_t(r)^{(\alpha_A+\gamma_A+\mu_A+\sigma_A-1)\theta}\,.$$
$$H(r)^{-(\alpha_A+\gamma_A+\mu_A+\sigma_A-1)\theta}\,w_t(r)^{-(1-\sigma_A)\theta}\,\varsigma(s,r)^{-\theta}\,dr \tag{C.21}$$

$$P_{Mt}(s)^{-\theta} = \kappa_M e_t^{-\sigma_M\theta}\int_S \tau_{Mt}(r)^\theta\, g_M(T_t(r))^\theta\, \Lambda_t(r)^{(\alpha_M+\gamma_M+\mu_M+\sigma_M-1)\theta}\,.$$
$$H(r)^{-(\alpha_M+\gamma_M+\mu_M+\sigma_M-1)\theta}\,w_t(r)^{-(1-\sigma_M)\theta}\,\varsigma(s,r)^{-\theta}\,dr \tag{C.22}$$

$$\frac{w_t(r)\,\bar{L}_{At}(r)}{\gamma_A + \mu_A} = \chi_A\kappa_A e_t^{-\sigma_A\theta}\tau_{At}(r)^\theta\, g_A(T_t(r))^\theta\, \Lambda_t(r)^{(\alpha_A+\gamma_A+\mu_A+\sigma_A-1)\theta}\,H(r)^{-(\alpha_A+\gamma_A+\mu_A+\sigma_A-1)\theta}\,.$$
$$w_t(r)^{-(1-\sigma_A)\theta}\int_S P_{At}(s)^\theta\left[\left(w_t(s) + \frac{\Pi_t}{\bar{L}}\right)\bar{L}_t(s) + w_t(s)\,\Lambda_t(s)\right]\varsigma(s,r)^{-\theta}\,ds \tag{C.23}$$

and

$$\frac{w_t(r)\,\bar{L}_{Mt}(r)}{\gamma_M + \mu_M} = \chi_M\kappa_M e_t^{-\sigma_M\theta}\tau_{Mt}(r)^\theta\, g_M(T_t(r))^\theta\, \Lambda_t(r)^{(\alpha_M+\gamma_M+\mu_M+\sigma_M-1)\theta}\,H(r)^{-(\alpha_M+\gamma_M+\mu_M+\sigma_M-1)\theta}\,.$$
$$w_t(r)^{-(1-\sigma_M)\theta}\int_S P_{Mt}(s)^\theta\left[\left(w_t(s) + \frac{\Pi_t}{\bar{L}}\right)\bar{L}_t(s) + w_t(s)\,\Lambda_t(s)\right]\varsigma(s,r)^{-\theta}\,ds \tag{C.24}$$

where, naturally, $\bar{L}_{Mt}(r) = \bar{L}_t(r) - \bar{L}_{At}(r)$, and Π_t can be obtained from equation (3.19). Combining (C.23) and (C.24) and rearranging yields

$$w_t(r)^{1+\theta} = \bar{L}_t(r)^{-1}\int_S \Big[\chi_A(\gamma_A + \mu_A)\,\kappa_A e_t^{-\sigma_A\theta}\tau_{At}(r)^\theta\, g_A(T_t(r))^\theta\, \Lambda_t(r)^{(\alpha_A+\gamma_A+\mu_A+\sigma_A-1)\theta}\,.$$
$$H(r)^{-(\alpha_A+\gamma_A+\mu_A+\sigma_A-1)\theta}\,w_t(r)^{\sigma_A\theta}\,P_{At}(s)^\theta + \chi_M(\gamma_M + \mu_M)\,\kappa_M e_t^{-\sigma_M\theta}\,.$$
$$\tau_{Mt}(r)^\theta\, g_M(T_t(r))^\theta\, \Lambda_t(r)^{(\alpha_M+\gamma_M+\mu_M+\sigma_M-1)\theta}\,H(r)^{-(\alpha_M+\gamma_M+\mu_M+\sigma_M-1)\theta}\,.$$
$$w_t(r)^{\sigma_M\theta}\,P_{Mt}(s)^\theta\Big]\left[\left(w_t(s) + \frac{\Pi_t}{\bar{L}}\right)\bar{L}_t(s) + w_t(s)\,\Lambda_t(s)\right]\varsigma(s,r)^{-\theta}\,ds. \tag{C.25}$$

---

[3]In practice, we always start with guessing that the value of a given variable equals its value in period $t - 1$.

In the innermost loop, we guess a distribution of wages $w_t(r)$, and keep iterating on $w_t(r)$ using equation (C.25), also updating $P_{At}(s)$ and $P_{Mt}(s)$ using equations (C.21) and (C.22) in every iteration step. We proceed with this until convergence in $w_t(r)$, while we also apply the normalization $\int_S w_t(r)\,dr = 1$. This concludes the innermost loop.

In the middle loop, we update $\bar{L}_{At}(r)$ using

$$\bar{L}_{At}(r) = \chi_A(\gamma_A + \mu_A)\kappa_A e_t^{-\sigma_A\theta}\tau_{At}(r)^\theta g_A(T_t(r))^\theta \Lambda_t(r)^{(\alpha_A+\gamma_A+\mu_A+/\sigma_A-1)\theta} H(r)^{-(\alpha_A+\gamma_A+\mu_A+\sigma_A-1)\theta}.$$
$$w_t(r)^{-[1+(1-\sigma_A)\theta]}\int_S P_{At}(s)^\theta\left[\left(w_t(s)+\frac{\Pi_t}{\bar{L}}\right)\bar{L}_t(s)+w_t(s)\Lambda_t(s)\right]\varsigma(s,r)^{-\theta}\,ds$$

(C.26)

which we obtained from rearranging equation (C.23). We iterate on equation (C.26) until convergence in $\bar{L}_{At}(r)$. This concludes the middle loop.

In the outermost loop, we update $\bar{L}_t(r)$ using

$$\bar{L}_t(r) = \left[F_t\frac{(w_t(r)+\Pi_t/\bar{L})\bar{L}_t(r)+w_t(r)\Lambda_t(r)}{P_{At}(r)^{\chi_A}P_{Mt}(r)^{\chi_M}}\frac{\bar{a}(r)}{m_2(r)}H(r)^\lambda\right]^{\frac{1}{1+\lambda+\Omega}}$$

(C.27)

which comes from combining equations (3.2), (3.3) and (3.4). $F_t = \left(\frac{\bar{L}}{\int_S u_t(s)^{1/\Omega}m_2(s)^{-1/\Omega}\,ds}\right)^\Omega$ is a worldwide constant that drives the level of $\bar{L}_t(r)$. We do not need to explicitly solve for F_t as we can obtain the level of $\bar{L}_t(r)$ from the condition

$$\int_S \bar{L}_t(r)\,dr = \bar{L}.$$

We iterate on equation (C.27) until convergence in $\bar{L}_t(r)$. We also update e_t using equation (3.29) in every iteration step. This completes the outermost loop.

Bibliography

Acemoglu, Daron, Philippe Aghion, Leonardo Bursztyn, and David Hemous, "The Environment and Directed Technical Change," *American Economic Review*, 2012, *102* (1), 131–166.

_ , Ufuk Akcigit, Douglas Hanley, and William Kerr, "Transition to Clean Technology," *Journal of Political Economy*, 2016, *124* (1), 52–104.

Akbulut-Yuksel, Mevlude, "War during childhood: The long run effects of warfare on health," *Journal of Health economics*, 2017, *53*, 117–130.

Akresh, Richard, Leonardo Lucchetti, and Harsha Thirumurthy, "Wars and Child Health: Evidence from the Eritrean–Ethiopian Conflict," *Journal of Development Economics*, 2012, *99* (2), 330–340.

_ , Philip Verwimp, and Tom Bundervoet, "Civil war, crop failure, and child stunting in Rwanda," *Economic Development and Cultural Change*, 2011, *59* (4), 777–810.

_ , Sonia Bhalotra, Marinella Leone, and Una Okonkwo Osili, "War and Stature: Growing Up During the Nigerian Civil War," *The American Economic Review (Papers and Proceedings)*, 2012, *102* (3), 273–277.

Alderman, Harold, John Hoddinott, and Bill Kinsey, "Long term consequences of early childhood malnutrition," *Oxford economic papers*, 2006, *58* (3), 450–474.

Allen, Myles R., David J. Frame, Chris Huntingford, Chris D. Jones, Jason A. Lowe, Malte Meinshausen, and Nicolai Meinshausen, "Warming Caused by Cumulative Carbon Emissions towards the Trillionth Tonne," *Nature*, 2009, *458* (7242), 1163–1166.

Allen, Treb and Costas Arkolakis, "Trade and the Topography of the Spatial Economy," *The Quarterly Journal of Economics*, 2014, *129* (3), 1085–1140.

_ and Dave Donaldson, "Persistence and Path Dependence in the Spatial Economy," *Working Paper*, 2020.

__ , **Cauê de Castro Dobbin, and Melanie Morten**, "Border walls," Technical Report, National Bureau of Economic Research 2019.

__ , **Costas Arkolakis, and Xiangliang Li**, "On the Equilibrium Properties of Network Models with Heterogeneous Agents," Working Paper, Yale University 2020.

Almond, Douglas and Janet Currie, "Killing Me Softly: The Fetal Origins Hypothesis," *Journal of Economic Perspectives*, September 2011, *25* (3), 153–72.

__ , **Lena Edlund, Hongbin Li, and Junsen Zhang**, "Long-term effects of the 1959-1961 China famine: Mainland China and Hong Kong," Technical Report, National Bureau of Economic Research 2007.

Alvarez, José Luis Cruz and Esteban Rossi-Hansberg, "The Economic Geography of Global Warming," Working Paper 28466, National Bureau of Economic Research February 2021.

Baez, Javier, German Caruso, Valerie Mueller, and Chiyu Niu, "Heat Exposure and Youth Migration in Central America and the Caribbean," *American Economic Review*, 2017, *107* (5), 446–50.

Baker, Richard B, John Blanchette, and Katherine Eriksson, "Long-run impacts of agricultural shocks on educational attainment: Evidence from the boll weevil," *The Journal of Economic History*, 2020, *80* (1), 136–174.

Balboni, Clare, "In Harm's Way? Infrastructure Investments and the Persistence of Coastal Cities," Working Paper, MIT 2019.

Banerjee, Abhijit, Esther Duflo, Gilles Postel-Vinay, and Tim Watts, "Long Run Health Impacts of Income Shocks: Wine and Phylloxera in 19th Century France," *The Review of Economics and Statistics*, 2010, *92* (4), 714–728.

Barrios, Salvador, Luisito Bertinelli, and Eric Strobl, "Climatic change and rural-urban migration: The case of sub-Saharan Africa," 2006.

Baum-Snow, Nathaniel, J Vernon Henderson, Matthew A Turner, Qinghua Zhang, and Loren Brandt, "Does investment in national highways help or hurt hinterland city growth?," *Journal of Urban Economics*, 2020, *115*, 103124.

Behrman, Jere R and Mark R Rosenzweig, "Returns to Birthweight," *Review of Economics and Statistics*, 2004, *86* (2), 586–601.

Benveniste, Hélène, Michael Oppenheimer, and Marc Fleurbaey, "Effect of border policy on exposure and vulnerability to climate change," *Proceedings of the National Academy of Sciences*, 2020.

_ , _ , **and** _ , "Effect of Border Policy on Exposure and Vulnerability to Climate Change," *Proceedings of the National Academy of Sciences*, 2020, *117* (43), 26692–26702.

Berlemann, Michael and Max Friedrich Steinhardt, "Climate change, natural disasters, and migration—a survey of the empirical evidence," *CESifo Economic Studies*, 2017, *63* (4), 353–385.

Black, Sandra E, Paul J Devereux, and Kjell G Salvanes, "From the Cradle to the Labor Market? The Effect of Birth Weight on Adult Outcomes," *The Quarterly Journal of Economics*, 2007, *122* (1), 409–439.

Brader, L, H Djibo, FG Faye, S Ghaout, M Lazar, PN Luzietoso, and MA Ould Babah, "Towards a more effective response to desert locusts and their impacts on food security, livelihoods and poverty," *Multilateral evaluation of the 2003–05 Desert locust campaign. Food and Agriculture Organisation, Rome*, 2006.

Brenton, Paul, Alberto Portugal-Perez, and Julie Régolo, *Food prices, road infrastructure, and market integration in Central and Eastern Africa*, The World Bank, 2014.

Bryan, Gharad and Melanie Morten, "The aggregate productivity effects of internal migration: Evidence from Indonesia," *Journal of Political Economy*, 2019, *127* (5), 2229–2268.

Bundervoet, Tom, Philip Verwimp, and Richard Akresh, "Health and Civil War in Rural Burundi," *Journal of Human Resources*, 2009, *44* (2), 536–563.

Burgess, Robin and Dave Donaldson, "Can openness mitigate the effects of weather shocks? Evidence from India's famine era," *American Economic Review*, 2010, *100* (2), 449–53.

Burke, Marshall and Kyle Emerick, "Adaptation to climate change: Evidence from US agriculture," *American Economic Journal: Economic Policy*, 2016, *8* (3), 106–40.

_ , **Solomon M Hsiang, and Edward Miguel**, "Global non-linear effect of temperature on economic production," *Nature*, 2015, *527* (7577), 235.

Burzyński, Michał, Christoph Deuster, Frédéric Docquier, and Jaime De Melo, "Climate Change, Inequality, and Human Migration," 2019.

— **, Frédéric Docquier, and Hendrik Scheewel**, "The geography of climate migration," *Journal of Demographic Economics*, 2021, pp. 1–37.

Cai, Ruohong, Shuaizhang Feng, Michael Oppenheimer, and Mariola Pytlikova, "Climate variability and international migration: The importance of the agricultural linkage," *Journal of Environmental Economics and Management*, 2016, *79*, 135–151.

Caliendo, Lorenzo, Maximiliano Dvorkin, and Fernando Parro, "Trade and Labor Market Dynamics: General Equilibrium Analysis of the China Trade Shock," *Econometrica*, 2019, *87* (3), 741–835.

Cattaneo, Cristina, Michel Beine, Christiane J Fröhlich, Dominic Kniveton, Inmaculada Martinez-Zarzoso, Marina Mastrorillo, Katrin Millock, Etienne Piguet, and Benjamin Schraven, "Human migration in the era of climate change," *Review of Environmental Economics and Policy*, 2019, *13* (2), 189–206.

Ceccato, Pietro, Keith Cressman, Alessandra Giannini, and Sylwia Trzaska, "The desert locust upsurge in West Africa (2003–2005): Information on the desert locust early warning system and the prospects for seasonal climate forecasting," *International Journal of Pest Management*, 2007, *53* (1), 7–13.

CIESIN, "Global roads open access data set, version 1 (gROADSv1)," *Palisades, NY: NASA Socioeconomic Data and Applications Center (SEDAC)*, 2013.

Comin, Diego A., Mikhail Dmitriev, and Esteban Rossi-Hansberg, "The Spatial Diffusion of Technology," NBER Working Paper 18534 2012.

COMTRADE, UN, "United Nations commodity trade statistics database," *URL: http://comtrade. un. org*, 2010.

Conley, Timothy G, "GMM estimation with cross sectional dependence," *Journal of econometrics*, 1999, *92* (1), 1–45.

Conte, Bruno, "Climate Change and Migration: the case of Africa," *unpublished manuscript*, 2020.

— **, Klaus Desmet, Dávid Krisztián Nagy, and Esteban Rossi-Hansberg**, "Local Sectoral Specialization in a Warming World," Working Paper 28163, National Bureau of Economic Research December 2020.

Costinot, Arnaud, Dave Donaldson, and Cory Smith, "Evolving comparative advantage and the impact of climate change in agricultural markets: Evidence from 1.7 million fields around the world," *Journal of Political Economy*, 2016, *124* (1), 205–248.

_ , _ , **and** _ , "Evolving Comparative Advantage and the Impact of Climate Change in Agricultural Markets: Evidence from 1.7 Million Fields around the World," *Journal of Political Economy*, 2016, *124* (1), 205–248.

Cressman, K, "SWARMS: a geographic information system for desert locust forecasting," in "New Strategies in locust control," Springer, 1997, pp. 27–35.

Cressman, Keith and Robert Stefanski, "Weather and Desert Locusts," Technical Report, World Meteorological Organization and Food and Agriculture Organization of the United Nations 2016.

Dagnelie, Olivier, Giacomo De Luca, and Jean-François Maystadt, "Violence, Selection and Infant Mortality in Congo," *Journal of Health Economics*, 2018.

Dell, Melissa, Benjamin F Jones, and Benjamin A Olken, "Temperature and income: reconciling new cross-sectional and panel estimates," *American Economic Review*, 2009, *99* (2), 198–204.

_ , _ , **and** _ , "What do we learn from the weather? The new climate-economy literature," *Journal of Economic Literature*, 2014, *52* (3), 740–98.

Desmet, Klaus and Esteban Rossi-Hansberg, "Spatial Development," *American Economic Review*, 2014, *104* (4), 1211–1243.

_ **and** _ , "On the spatial economic impact of global warming," *Journal of Urban Economics*, 2015, *88*, 16–37.

_ , **Dávid Krisztián Nagy, and Esteban Rossi-Hansberg**, "The geography of development," *Journal of Political Economy*, 2018, *126* (3), 903–983.

_ , **Robert E. Kopp, Scott A. Kulp, Dávid Krisztián Nagy, Michael Oppenheimer, Esteban Rossi-Hansberg, and Benjamin H. Strauss**, "Evaluating the Economic Cost of Coastal Flooding," *American Economic Journal: Macroeconomics*, April 2021, *13* (2), 444–86.

Dethier, Jean-Jacques and Alexandra Effenberger, *Agriculture and development: A brief review of the literature*, The World Bank, 2011.

Donaldson, Dave, "Railroads of the Raj: Estimating the impact of transportation infrastructure," *American Economic Review*, 2018, *108* (4-5), 899–934.

_ **and Richard Hornbeck**, "Railroads and American economic growth: A "market access" approach," *The Quarterly Journal of Economics*, 2016, *131* (2), 799–858.

Duarte, Margarida and Diego Restuccia, "The Role of the Structural Transformation in Aggregate Productivity," *Quarterly Journal of Economics*, 2010, *125* (1), 129–173.

Ducruet, César, Réka Juhász, Dávid Krisztián Nagy, and Claudia Steinwender, "All aboard: The aggregate effects of port development," Technical Report, Working Paper 2021.

Eaton, Jonathan and Samuel Kortum, "Technology, geography, and trade," *Econometrica*, 2002, *70* (5), 1741–1779.

FAO, "Locust crisis to hit northwest Africa again - situation deteriorating in the Sahel (last visit 05.06.2018)," September 2004.

_ , "West African food crisis looming (last visit 05.06.2018)," June 2005.

_ , "Worsening food situation in parts of the Sahel (last visit 05.06.2018)," May 2005.

_ , "The Impact of Natural Hazards and Disasters on Agriculture and Food Security and Nutrition–A call for Action to Build Resilient Livelihoods," 2015.

FEWS-NET, "Senegal: monthly food security update," *FEWS NET monthly report*, 2005.

Florczyk, AJ, C Corbane, D Ehrlich, S Freire, T Kemper, L Maffenini, M Melchiorri, M Pesaresi, P Politis, M Schiavina et al., "GHSL Data Package 2019," *Luxembourg. EUR*, 2019, *29788.*

Golosov, Mikhail, John Hassler, Per Krusell, and Aleh Tsyvinski, "Optimal Taxes on Fossil Fuel in General Equilibrium," *Econometrica*, 2014, *82* (1), 41–88.

Gröger, André and Yanos Zylberberg, "Internal labor migration as a shock coping strategy: Evidence from a typhoon," *American Economic Journal: Applied Economics*, 2016, *8* (2), 123–53.

Hassler, J., P. Krusell, and A.A. Smith, "Environmental Macroeconomics," in J. B. Taylor and Harald Uhlig, eds., *Handbook of Macroeconomics*, Vol. 2B, Elsevier, 2016, chapter 24, pp. 1893–2008.

Hassler, John, Per Krusell, and Conny Olovsson, "The Consequences of Uncertainty: Climate Sensitivity and Economic Sensitivity to the Climate," *Annual Review of Economics*, 2018, *10* (1), 189–205.

Henderson, J Vernon, Adam Storeygard, and Uwe Deichmann, "Has climate change driven urbanization in Africa?," *Journal of development economics*, 2017, *124*, 60–82.

Herok, Claudia A, Stephan Krall et al., *Economics of Desert locust control.*, Deutsche Gesellschaft fur Technische Zusammenarbeit (GTZ) GmbH, 1995.

Herrendorf, Berthold, Richard Rogerson, and Ákos Valentinyi, "Growth and Structural Transformation," in Philippe Aghion and Steven N. Durlauf, eds., *Handbook of Economic Growth*, Vol. 2 of *Handbook of Economic Growth*, Elsevier, 2014, pp. 855 – 941.

IIASA and FAO, "Global Agro-Ecological Zones (GAEZ v3. 0)," 2012.

IPCC, "IPCC Special Report," 2000.

— , "Contribution of working group III to the fourth assessment report of the intergovernmental panel on climate change," *International Panel on Climate Change*, 2007.

— , *Managing the risks of extreme events and disasters to advance climate change adaptation: special report of the intergovernmental panel on climate change*, Cambridge University Press, 2012.

— , "Global warming of 1.5 C," *An IPCC Special Report on the impacts of global warming of 1.5 degrees*, 2018, *1*.

— , *Data Distribution Centre* 2020. Available at https://www.ipcc-data.org/.

Jones, Bryan and Brian C O'Neill, "Spatially explicit global population scenarios consistent with the Shared Socioeconomic Pathways," *Environmental Research Letters*, 2016, *11* (8), 084003.

Kudamatsu, Masayuki, "Has Democratization Reduced Infant Mortality in Sub-Saharan Africa? Evidence from Micro Data," *Journal of the European Economic Association*, 2012, *10* (6), 1294–1317.

__ , **Torsten Persson, and David Strömberg**, "Weather and Infant Mortality in Africa," Technical Report, CEPR Discussion Papers 9222 2012.

__ , __ , **and** __ , "Weather and Infant Mortality in Africa," 2016.

Lavy, Victor, Analia Schlosser, and Adi Shany, "Out of Africa: Human Capital Consequences of In Utero Conditions," Working Paper 21894, National Bureau of Economic Research January 2016.

Lustgarten, Abrahm, "The Great Climate Migration Has Begun," *The New York Times*, Jun 2020.

Maccini, Sharon and Dean Yang, "Under the Weather: Health, Schooling, and Economic Consequences of Early Life Rainfall," *American Economic Review*, 2009, *99* (3), 1006–26.

Maluccio, John A, John Hoddinott, Jere R Behrman, Reynaldo Martorell, Agnes R Quisumbing, and Aryeh D Stein, "The Impact of Improving Nutrition During Early Childhood on Education among Guatemalan Adults," *The Economic Journal*, 2009, *119* (537), 734–763.

Matthews, H. Damon, Nathan P. Gillett, Peter A. Stott, and Kirsten Zickfeld, "The Proportionality of Global Warming to Cumulative Carbon Emissions," *Nature*, 2009, *459* (7248), 829–832.

Moneke, Niclas, "Can Big Push Infrastructure Unlock Development? Evidence from Ethiopia," Technical Report, Working Paper 2020.

Monte, Ferdinando, Stephen J Redding, and Esteban Rossi-Hansberg, "Commuting, migration, and local employment elasticities," *American Economic Review*, 2018, *108* (12), 3855–90.

Morten, Melanie and Jaqueline Oliveira, "The effects of roads on trade and migration: Evidence from a planned capital city," *mimeo*, 2018.

Nagy, Dávid Krisztián, "Hinterlands, city formation and growth: evidence from the US westward expansion," Technical Report 2020.

Nath, Ishan B, "The Food Problem and the Aggregate Productivity Consequences of Climate Change," Technical Report, National Bureau of Economic Research 2020.

Nath, Ishan B., "The Food Problem and the Aggregate Productivity Consequences of Climate Change," NBER Working Papers 27297 2020.

Nordhaus, William, "An optimal transition path for controlling greenhouse gases," *Science*, 1992, *258* (5086), 1315–1319.

_ , "Rolling the 'DICE': An Optimal Transition Path for Controlling Greenhouse Gases," *Resource and Energy Economics*, 1993, *15* (1), 27–50.

_ , *A Question of Balance: Weighing the Options on Global Warming Policies*, Yale University Press, 2008.

_ , "Economic Aspects of Global Warming in a Post-Copenhagen Environment," *Proceedings of the National Academy of Sciences*, 2010, *107* (26), 11721–11726.

_ , "Integrated economic and climate modeling," in "Handbook of computable general equilibrium modeling," Vol. 1, Elsevier, 2013, pp. 1069–1131.

_ , "Projections and uncertainties about climate change in an era of minimal climate policies," *American Economic Journal: Economic Policy*, 2018, *10* (3), 333–60.

_ , "Climate change: The ultimate challenge for economics," *American Economic Review*, 2019, *109* (6), 1991–2014.

_ , **Qazi Azam, David Corderi, Kyle Hood, Nadejda Makarova Victor, Mukhtar Mohammed, Alexandra Miltner, and Jyldyz Weiss**, "The G-Econ database on gridded output: methods and data," *Yale University, New Haven*, 2006, *6.*

_ , _ , **David Corderi Novoa, Kyle Hood, Nadejda Victor, Mukhtar Mohammed, Alexandra Miltner, and Jyldyz Weiss**, "The G-Econ Database on Gridded Output: Methods and Data," Working Paper, Yale University 2006.

of Economic United Nations, Department and Population Division Social Affairs, "World Population Prospects 2019: Highlights," 2019.

Osborne, Theresa, "Imperfect competition in agricultural markets: evidence from Ethiopia," *Journal of Development Economics*, 2005, *76* (2), 405–428.

Pellegrina, Heitor S., "Trade, Productivity, and the Spatial Organization of Agriculture: Evidence from Brazil," *Working Paper*, 2020.

Pellegrina, Heitor S and Sebastian Sotelo, "Migration, Specialization, and Trade: Evidence from Brazil's March to the West," Working Paper 28421, National Bureau of Economic Research January 2021.

Peri, Giovanni and Akira Sasahara, "The impact of global warming on rural-Urban migrations: Evidence from global big data," Technical Report, National Bureau of Economic Research 2019.

Porteous, Obie, "High trade costs and their consequences: An estimated dynamic model of African agricultural storage and trade," *American Economic Journal: Applied Economics*, 2019, *11* (4), 327–66.

_ , "Trade and agricultural technology adoption: Evidence from Africa," *Journal of Development Economics*, 2020, *144*, 102440.

Redding, Stephen J, "Goods trade, factor mobility and welfare," *Journal of International Economics*, 2016, *101*, 148–167.

Redding, Stephen J. and Esteban Rossi-Hansberg, "Quantitative Spatial Economics," *Annual Review of Economics*, 2017, *9* (1), 21–58.

Restuccia, Diego, Dennis Tao Yang, and Xiaodong Zhu, "Agriculture and aggregate productivity: A quantitative cross-country analysis," *Journal of monetary economics*, 2008, *55* (2), 234–250.

Rigaud, KK, B Jones, J Bergmann, V Clement, K Ober, J Schewe, S Adamo, B McCusker, S Heuser, and A Midgley, "Groundswell: Preparing for Internal Climate Migration (Washington, DC: World Bank)," 2018.

Schlenker, Wolfram and David B Lobell, "Robust negative impacts of climate change on African agriculture," *Environmental Research Letters*, 2010, *5* (1), 014010.

_ , **W Michael Hanemann, and Anthony C Fisher**, "Will US agriculture really benefit from global warming? Accounting for irrigation in the hedonic approach," *American Economic Review*, 2005, *95* (1), 395–406.

Shayegh, Soheil, "Outward migration may alter population dynamics and income inequality," *Nature Climate Change*, 2017, *7* (11), 828–832.

Sheahan, Megan and Christopher B Barrett, "Ten striking facts about agricultural input use in Sub-Saharan Africa," *Food Policy*, 2017, *67*, 12–25.

Sotelo, Sebastian, "Domestic trade frictions and agriculture," *Journal of Political Economy*, 2020, *128* (7), 2690–2738.

Stein, Zena, Mervyn Susser, Gerhart Saenger, and Francis Marolla, *Famine and Human Development: The Dutch Hunger Winter of 1944-1945.*, Oxford University Press, 1975.

Stocker, Thomas F, Dahe Qin, Gian-Kasper Plattner, Melinda Tignor, Simon K Allen, Judith Boschung, Alexander Nauels, Yu Xia, Vincent Bex, and Pauline M Midgley, "Climate Change 2013: The Physical Science Basis," *Contribution of Working Group I to the Fifth Assessment Report of the Intergovernmental Panel on Climate Change*, 2013, *1535.*

Świecki, Tomasz, "Determinants of Structural Change," *Review of Economic Dynamics*, 2017, *24*, 95 – 131.

Symmons, PM, K Cressman, and HM Dobson, "Desert locust guidelines," 2001.

Tollefsen, Andreas Forø, Håvard Strand, and Halvard Buhaug, "PRIO-GRID: A Unified Spatial Sata Structure," *Journal of Peace Research*, 2012, *49* (2), 363–374.

Townsend, Robert M, "Consumption insurance: An evaluation of risk-bearing systems in low-income economies," *Journal of Economic perspectives*, 1995, *9* (3), 83–102.

Uchida, Hirotsugu and Andrew Nelson, *Agglomeration index: Towards a new measure of urban concentration* number 2010/29, WIDER Working Paper, 2010.

Uy, Timothy, Kei-Mu Yi, and Jing Zhang, "Structural Change in an Open Economy," *Journal of Monetary Economics*, 2013, *60* (6), 667 – 682.

Valente, Christine, "Civil Conflict, Gender-specific Fetal Loss, and Selection: A new Test of the Trivers–Willard hypothesis," *Journal of Health Economics*, 2015, *39*, 31–50.

van Vuuren, Detlef P., Jae Edmonds, Mikiko Kainuma, Keywan Riahi, Allison Thomson, Kathy Hibbard, George C. Hurtt, Tom Kram, Volker Krey, Jean-Francois Lamarque, Toshihiko Masui, Malte Meinshausen, Nebojsa Nakicenovic, Steven J. Smith, and Steven K. Rose, "The Representative Concentration Pathways: An Overview," *Climatic Change*, 2011, *109* (1), 5.

Veronese, N and H Tyrman, "MEDSTATII: Asymmetry in Foreign Trade Statistics in Mediterranean Partner Countries," Technical Report, Eurostat Methodologies Working Papers 2009.

Vicente-Serrano, Sergio M, Santiago Beguería, and Juan I López-Moreno, "A multiscalar drought index sensitive to global warming: the standardized precipitation evapotranspiration index," *Journal of Climate*, 2010, *23* (7), 1696–1718.

Vreyer, Philippe De, Nathalie Guilbert, and Sandrine Mesple-Somps, "Impact of natural disasters on education outcomes: evidence from the 1987–89 locust plague in Mali," *Journal of African Economies*, 2014, *24* (1), 57–100.

Weiss, D, A Nelson, HS Gibson, W Temperley, S Peedell, A Lieber, M Hancher, E Poyart, S Belchior, N Fullman et al., "A global map of travel time to cities to assess inequalities in accessibility in 2015," *Nature*, 2018, *553* (7688), 333.

World Bank, "The Locust Crisis: The World Bank's Response (last visit 22.08.2020)," July 2020.